CHALMERS

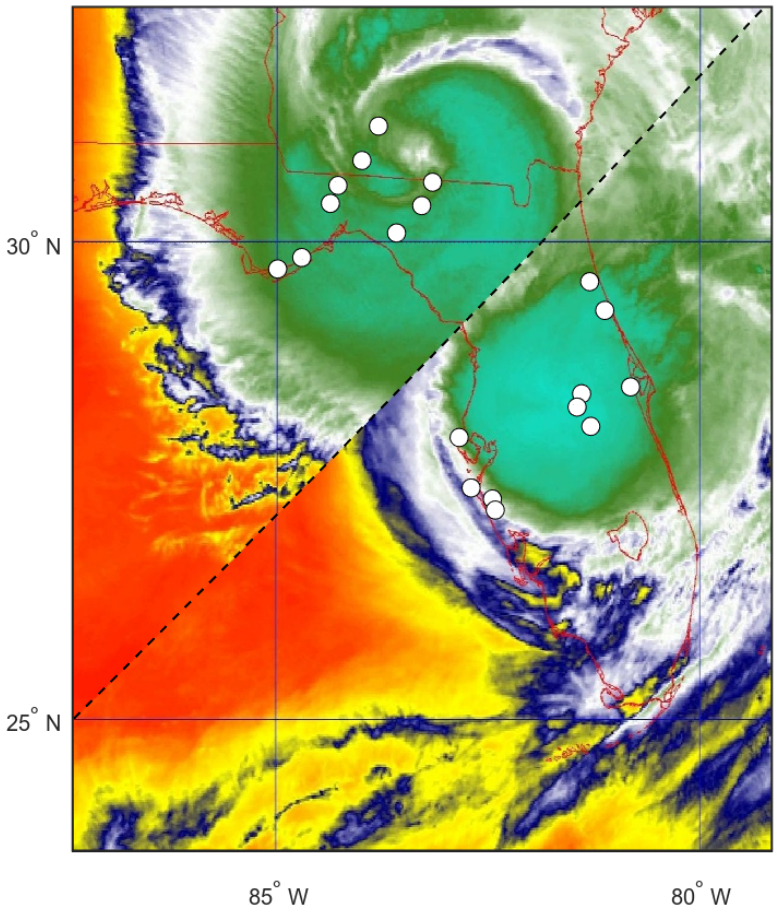

Investigating the tropical cyclones Helene and Milton – Utilizing GNSS data

Focusing on the use of Zenith Wet Delay and positioning of satellites for measuring speed, direction and land subsidence over Florida

Bachelor's thesis

Rawan Al Sheikh, Ada Haile, Benjamin Helin, Melissa Mujanovic

DEPARTMENT OF SPACE, EARTH AND ENVIRONMENT

CHALMERS UNIVERSITY OF TECHNOLOGY
Gothenburg, Sweden 2025
www.chalmers.se

Bachelor's thesis 2025

Investigating the tropical cyclones Helene and Milton – Utilizing GNSS data

Focusing on the use of Zenith Wet Delay and positioning of satellites for measuring speed, direction and land subsidence over Florida

Rawan Al Sheikh
Ada Haile
Benjamin Helin
Melissa Mujanovic

CHALMERS

Department of Space, Earth and Environment
Division of Onsala Space Observatory
Research Unit of Space Geodesy and Geodynamics
Chalmers University of Technology
Gothenburg, Sweden 2025

Investigating the tropical cyclones Helene and Milton – Utilizing GNSS data

Focusing on the use of Zenith Wet Delay and positioning of satellites for measuring speed, direction and land subsidence over Florida

Rawan Al Sheikh, Ada Haile, Benjamin Helin, Melissa Mujanovic

Supervisor: Professor Rüdiger Haas, *Department of Space, Earth and Environment*
Examiner: Adjunct Professor Jan Johansson, *Department of Space, Earth and Environment*

Bachelor's Thesis 2025
Department of Space, Earth and Environment
Division of Onsala Space Observatory
Research Unit of Space Geodesy and Geodynamics
Chalmers University of Technology
SE-412 96 Gothenburg
Telephone +46 31 772 1000

Cover: Satellite image depicting Hurricanes Milton (south) and Helene (north), along with locations of the permanent stations. Satellite images courtesy of NOAA / NESDIS Center for Satellite Applications and Research (NOAA, 2025a, 2025b).

Typeset in LaTeX
Printed by Chalmers Reproservice
Gothenburg, Sweden 2025

Investigating the tropical cyclones Helene and Milton – Utilizing GNSS data

Focusing on the use of Zenith Wet Delay and positioning of satellites for measuring speed, direction and land subsidence over Florida

Rawan Al Sheikh, Ada Haile, Benjamin Helin, Melissa Mujanovic

Department of Space, Earth and Environment
Chalmers University of Technology

Abstract

Each year, the North Atlantic experiences increasingly severe tropical storms. Recent studies suggest that both the frequency and intensity of these storms have risen, potentially as a consequence of climate change and global warming. In the fall of 2024, the state of Florida in the United States was struck by two major hurricanes – Helene and Milton.

This study investigates whether Zenith Wet Delay (ZWD) and height data derived from Global Navigation Satellite System (GNSS) can be used to monitor tropical storms speed, direction and impact on land subsidence. Data were collected from seventeen continuously operating GNSS permanent stations over a period ranging from thirteen to twenty-one days surrounding each storm event. The processing was conducted using the PRIDE's Precise Point Positioning with Ambiguity Resolution (PPP-AR) technique. Furthermore, data from two water gauge stations were used to validate and compare the GNSS-derived height variations.

This indicated that locating tropical storms with the help of ZWD is highly plausible, were the problem instead comes from locating the core's landfall. The height variation instead frequently shows significant variation at the core's landfall, making a combination of the two to be the most reliable method for identifying and tracking hurricanes. Analysing ZWD time series from different stations also seemed to prove that it is feasible to estimate velocities and trajectories, although the accuracy is largely impacted by uncertainties stemming from missing data and uneven station distribution.

Keywords: Global Navigation Satellite System (GNSS), Zenith Wet Delay (ZWD), Hurricane Milton, Hurricane Helene, Land subsidence.

Undersökning av de tropiska orkanerna Helene och Milton – Baserat på GNSS-data

Med fokus på användning av Zenith Wet Delay och positionering av satelliter för att mäta hastighet, riktning och landsänkning över Florida

Rawan Al Sheikh, Ada Haile, Benjamin Helin, Melissa Mujanovic

Institutionen för Rymd-, geo- och miljövetenskap
Chalmers Tekniska Högskola

Sammanfattning

Varje år drabbas Nordatlanten av allt kraftigare tropiska stormar. Nya studier tyder på att både frekvensen och intensiteten hos dessa stormar har ökat, vilket sannolikt är en följd av klimatförändringar och global uppvärmning. Under hösten 2024 drabbades delstaten Florida i USA av två kraftiga orkaner – Helene och Milton.

Denna studie undersöker huruvida Zenith Wet Delay (ZWD) och höjdinformation från Global Navigation Satellite System (GNSS) kan användas för att övervaka tropiska stormars hastighet, riktning och påverkan på landsänkningar. Data samlades in från sjutton kontinuerligt opererande permanenta GNSS-stationer under en period om tretton till tjugoen dagar kring respektive stormtillfälle. Bearbetningen genomfördes med hjälp av PRIDE:s Precise Point Positioning med Ambiguity Resolution (PPP-AR)-teknik. Därutöver användes data från två vattenståndsmätare för att validera och jämföra GNSS-härledda höjdvariationer.

Resultaten visade att det är fullt möjligt att lokalisera tropiska stormar med hjälp av ZWD, men att den största utmaningen ligger i att fastställa när stormens kärna når land. Höjdvariationer visade däremot ofta tydliga förändringar just vid kärnans kontakt med land, vilket gör en kombination mellan de två metoderna till det mest tillförlitliga sättet att identifiera och följa orkaner. Analys av ZWD-tidsserier från olika stationer indikerade även att det är genomförbart att uppskatta stormars hastighet och bana, även om noggrannheten påverkas av osäkerheter kopplade till bristfällig data och ojämn fördelning av mätstationer.

Nyckelord: Global Navigation Satellite System (GNSS), Zenith Wet Delay (ZWD), Orkanen Milton, Orkanen Helene, Landsänkning.

Acknowledgements

We would like to begin by expressing our sincere gratitude to our supervisor, Professor Rüdiger Haas for his continuous support, as well as for the many insightful discussions and valuable input throughout our work. His knowledge and time were deeply appreciated. We would also want to thank our examiner Adjunct Professor Jan Johansson, for taking his time to review our work and provide valuable feedback. Furthermore, we would also want to thank David Frisk, for providing a highly useful LaTeX template, which saved us many hours of formatting work. A huge thank you is also given to PRIDE Lab at Wuhan University for developing the software used to generate usable data from GNSS measurements. We are also deeply grateful for the information and data provided by the Florida Department of Transportation and the National Oceanic and Atmospheric Administration, without which this work would not have been possible.

Rawan Al Sheikh, Ada Haile, Benjamin Helin, Melissa Mujanovic

Gothenburg, May 2025

List of Acronyms

Below is the list of acronyms that have been used throughout this project, listed in alphabetical order:

AWE	NASA's Atmospheric Waves Experiment
BeiDou	"Northern Dipper", Chinese Global Navigation Satellite System
CWT	Continuous Wavelet Transform
FDOT	Florida Department of Transportation
FPRN	Florida Permanent Reference Network
Galileo	Europe's Global Positioning System
GLONASS	Global'naya Navigatsionnaya Sputnikovaya Sistema, Russian Global Navigation Satellite System
GNSS	Global Navigation Satellite System
GNSS-IR	Global Navigation Satellite System Interferometric Reflectometry
GPS	Global Positioning System, United States Global Navigation Satellite System
NESDIS	National Environmental Satellite, Data, and Information Service
NOAA	National Oceanic and Atmospheric Administration
PPP	Precise Point Positioning
PPP-AR	Precise Point Positioning with Ambiguity Resolution
PRN	Pseudorandom Noise (satellite identifier code)
PRIDE	Positioning Racers to Image & Decipher the Earth
PWC	Piece-Wise Constant
SNR	Signal-to-noise ratio
SST	Sea Surface Temperature
STO	Epoch-wise random walk, Stochastic model
UNDRR	United Nations Office for Disaster Risk Reduction
ZHD	Zenith Hydrostatic Delay
ZTD	Zenith Tropospheric Delay
ZWD	Zenith Wet Delay

List of Figures

List of Tables

Contents

1

Introduction

Each year, the North Atlantic experiences increasingly severe tropical storms. Recent evidence indicates that these storms have not only grown in number, but also in strength over the past few years – a trend which is possibly linked to climate change and global warming. In the fall of 2024, the state of Florida in the United States was struck by 2 major tropical storms – Helene and Milton, in the end of September and the beginning of October, respectively. Helene and Milton were tropical cyclones of category 4 and 5, which affected nearly the entirety of the peninsula, causing extensive floods and wind damage.

The state of Florida has a widespread net of Global Navigation Satellite System stations that spans the peninsula from coast to coast. The data from the stations is being collected continuously and can be analysed to for example determine precise station positions and so-called tropospheric products that reflects the amount of water vapour in the troposphere. The results of the analysis gives valuable insights into the load effects that are caused by floods, and the severe weather conditions. The advancements in technology, like the extensive GNSS network in Florida, are transforming the ability to collect and analyse weather-related data. These innovations are enhancing our capacities to track storms and general forecasting capabilities.

This is a vital topic to discuss and analyse due to the potential impact of tropical cyclones on the Florida Peninsula, demonstrated historically. Hurricanes are often at the top of lists of catastrophic natural disasters, which Florida has extensive experience with. There has been an estimate of over 450 billion dollars in damages, which goes to show the importance of examining earlier hurricanes and their patterns (Malmstadt et al., 2010).

Studying natural disasters is crucial for future risk assessment and the development of mitigation strategies, which emphasizing the need for proactive measure to protect vulnerable regions, such as the coasts of Florida. This research could also potentially touch on the role of government policy and urban planning to be able to manage future tropical storms.

1.1 Aim

The aim of this research is to use provided GNSS data to analyse the two tropical storms Helene and Milton and examine how the stations were affected due to flooding. The GNSS data can be used to determine the storm's progression and direction. The method involves using data analysis software to analyse the GNSS data and furthermore processing with custom-developed software.

In order to accomplish the aim of the research, the following research questions were formulated:

- **How do tropical storms impact land subsidence and how can this be researched with the use of GNSS data?**
  To see if there is visible land subsidence during tropical storms.

- **Can Zenith Wet Delay be used to observe tropical storms?**
  Looking for if the data provided for Zenith Wet Delay can be used to observe tropical storms.

- **Is it possible to use Zenith Wet Delay to find the speed and direction of tropical storms?**
  If data from Zenith Wet Delay can be used to detect tropical storms, is it also capable of tracking their speed and direction during their passage over Florida?

With the use of these research questions, the report is going to conclude a thorough study of how the behaviour of the tropical storms Milton and Helene affected Florida and what sort of conclusions can be drawn from the analysis.

1.2 Limitations

The project has several limitations. One key limitation is the number of stations from which GNSS data was extracted. For Hurricane Milton, specific stations were selected to cover the entire path of the storm. Three stations were chosen for the western, central, and eastern parts of Florida, respectively. By using three stations in each area, a diverse set of data is obtained, providing a more complete picture of how the storm affects different parts of the state. The selected stations were strategically placed to cover the entire storm path from west to east across the state.

For each geographical area (west, centre, and east), three stations were chosen at varying distances from the storm's path, with the central station being closest to the storm's core. This central station provides a direct indication of the storm's impact at the point where it passes. By comparing GNSS data from the other two stations, which are located to the north and south of the central station, any changes in GNSS signals can be observed, as well as how these changes diminish with increasing distance from the storm's centre. This allows for the study of variations in

velocity and other parameters along the storm's path and at different distances from its core, providing a better understanding of the storm's intensity and progression.

For Hurricane Helene, three stations were initially selected because they were well positioned along the storm's path, while nearby stations were poorly situated. As a result, data from Helene was primarily used to validate and compare the results obtained from Milton, particularly for assessing the accuracy of storm speed measurements. Meanwhile, data from Hurricane Milton was used to explore the feasibility of tracking storms using GNSS-derived parameters.

The data collection period has also been limited to the duration of the storm and a few days before and after its passage. This provides a good indication of the storm's impact on GNSS signals both before and after it has passed, allowing for the study of both the storm's progression and its effects on the area. It was also considered that some stations, although optimally located to measure the storms, had incomplete data during the observation period. As a result, these stations were replaced with the nearest available alternatives, potentially increasing uncertainty in the analysis.

Another limitation is that the report focuses on methods for studying tropical storms and their dynamics, without addressing the economic, social, and infrastructural implications. The primary purpose of the report is to present analyses of GNSS data from a scientific perspective.

2

Theory

2.1 Tropical Storms - An Overview

A tropical cyclone is a complex system that has a warm core in the centre of it, very steep pressure gradients, and strong winds near the Earth's surface that becomes nearly circular toward the centre. The tropical cyclones are divided into three categories, dependent on the maximum speed of the wind. They are; tropical depression whose maximum speed is less than 60 km/h, tropical cyclones whose maximum speed is greater than 110 km/h and tropical storms when the maximum speed is in between the interval of 60-110 km/h (Spiridonov & Ćurić, 2021).

Tropical storms, including hurricanes and cyclones, form over warm ocean waters and are primarily driven by convection – the powerful upward movement of warm, moist air. As this air rises and cools, water vapour condenses, releasing latent heat. This heat release fuels further convection and helps the storm intensify vertically. In the middle of a tropical cyclone, air is subsiding, resulting in dry conditions with few or no clouds and very light or no wind at ground level. This calm area is known as the eye of the storm and is surrounded by the eyewall – a ring of heavy rainfall and the system's most powerful winds. As the tropical storm approaches the coast, it draws in warm, humid air from surrounding areas, thereby increasing the water vapour content, particularly in coastal and inland regions. Once the storm's core moves over land, it begins to weaken due to the lack of moisture and heat that the ocean provides. After the storm passes, cooler and drier air often follows, driven by shifts in wind patterns and the weakening of convective processes, leading to a sharp decline in atmospheric moisture (Met Office, n.d. NOAA, 2023b, 2025c).

The difference between an extratropical storm and a tropical storm is that an extratropical storm undergoes an extratropical transition. An extratropical transition is a process where a regular tropical cyclone stops having its regular features and becomes more so called extratropical in nature. This usually occurs when a tropical cyclone is decaying and losing its speed, which can sometimes evolve into a much faster cyclone that in its turn, becomes extratropical. This transition can potentially become dangerous due to its unpredictability in nature. The transitions are difficult to predict and there is also a high level of uncertainty that occurs with predicting the intensity of the cyclone's speed (Jones et al., 2003).

The vital factors that initiates the formation of the different types of tropical cy-

clones are the sea surface temperature (SST) distribution, the geographical location, some pre-existing mesoscale atmospheric disturbance, prevailing winds, thermodynamic conditions, environmental instability parameters and vertical stratification of the atmosphere (Michener et al., 1997).

Understanding the relationship between tropical cyclones and climate change is vital. Although climate models are fairly reliable at projecting changes in the global mean climate driven by the enhanced greenhouse effect, their skill decreases when it particularly comes to forecasting regional climate variations or transient events like tropical cyclones. There remains substantial uncertainty at the regional level regarding whether the frequency of tropical cyclones will rise or fall, or whether areas where tropical storms typically occur will change. Similarly, while projections of cyclone intensity under climate change are still unsettled, current evidence points toward a modest increase in peak strengths (Walsh et al., 2016).

2.2 Hurricane Milton

One of the strongest storms of the 2024 Atlantic hurricane season, Hurricane Milton, provides a stark example of the interplay between atmospheric and ocean conditions with intense weather systems. The storm originated in the Bay of Campeche, where ocean temperatures and wind conditions facilitated quick intensification. Milton achieved Category 5 hurricane strength with winds of 285 km/h (180 mph), one of the most intense tropical cyclone classifications, within a matter of days. Unusually warm sea surface temperatures in the Gulf of Mexico were responsible for fuelling the storm's rapid development (Lang et al., 2024).

Climate change is believed to have contributed to these elevated sea temperatures, which got up to $30-31\,^{\circ}\mathrm{C}$. Global warming has seen violent storms like Milton become increasingly common (Thiem, 2024). While Milton weakened somewhat before making landfall along Florida's coast just west of Siesta Key on October 9, it nevertheless caused extensive damage. Millions of people were left without power, and homes and infrastructure were damaged by flooding, heavy rains and strong winds. To make matters worse, a record number of tornadoes were spawned across the state, amplifying the storm's already wide-reaching effects (NOAA, 2025b). Milton's destructive path highlights the urgent need to improve hurricane monitoring and forecasting systems. Due to complex ocean-atmosphere interactions, expanding our understanding of these dynamics is critical as storms continue to grow more intense and less predictable.

2.3 Hurricane Helene

Hurricane Helene was the strongest cyclonic event of the 2024 Atlantic hurricane season. The storm had begun as a low-level disturbance in the western Caribbean Sea on 23 September and intensified quickly in a highly conducive environment for its quick intensification. Unpredicted warm sea surface temperature in the Gulf

of Mexico above 30 °C provided abundant supply of latent heating, augmented by enhanced upper-tropospheric outflow as an added impetus towards quick intensification. Within 24 hours, Helene strengthened from a Category 1 to a Category 4 hurricane with maximum sustained winds of around 220 km/h (137 mph). Contrary to Hurricane Milton, Helene's track was dominated by variability in the Bermuda High and mid-latitude atmospheric steering regimes, resulting in an unpredictable and less consistent track. The hurricane struck south of Perry, Florida, on September 26 with one of the most climatologically and economically significant landfalls in Big Bend history (PO.DAAC, 2024).

Hurricane Helene's effects were extensive and disastrous, as the hurricane claimed at least 40 confirmed fatalities and caused utter destruction across Florida, Georgia, and the Carolinas. Rainfall of up to 760 mm in North Carolina regions contributed to catastrophic flooding that persisted well after the event. Further, Helene's convective complexes were associated with the generation of atmospheric gravity waves, monitored by NASA's Atmospheric Waves Experiment (AWE), and yielded new findings regarding the vertical propagation of energy during the occurrence of extreme weather events (Thomas, 2024). In conclusion, Hurricane Helene highlights the need for enhanced atmospheric observation networks and better model forecasts to accurately understand and contain the effects of increasingly unpredictable tropical cyclones.

2.4 Global Navigation Satellite System

Global Navigation Satellite System, referred to as GNSS, is a collective name for satellite navigation systems that broadcasts global positioning, navigation and timing services. There are four types of GNSS that are presently available: GPS (USA), Galileo (EU), GLONASS (Russia), BeiDou (China). These systems function by transmitting signals from space, delivering distance and time data to GNSS enabled receivers, which process the information to determine position (EUSPA, 2025). This section will outline the function and structure of GNSS, as well as explore its associated uncertainties.

2.4.1 Structure and Functionality

GNSS systems consist of a group of satellites circulating Earth, where each satellite has its fixed orbit at a specific altitude and functions by transmitting signals to a receiver on the ground. The receiver can for instance be a device to determine the location of a user, or permanent stations used for more precise measurements. The four primary constellations in orbit are GPS, Glonass, Galileo and BeiDou. Each of them is overseen by its respective country, except Galileo, which is overseen by the European Union. By measuring the distances to multiple satellites, the receiver can precisely determine its location. The GNSS signals also provide accurate time information, which is achieved by calculating the time delay between the transmission

and reception of the signals (NovAtel Inc, 2023).

GNSS signals are electromagnetic waves that travel through space at the speed of light, with frequencies between 1.2 and 1.6 GHz, which fall within the L-band. This allows for precise measurements and enables straightforward user devices. They also function reliably under typical weather conditions without significant weakening. Each GNSS signal has a wavelength in the range of 19-25 cm at the given frequencies. To compensate for ionospheric delays, GNSS transmits signals on at least two different frequencies, allowing for corrections based on the varying effects of the ionosphere on different wavelengths (Teunissen & Montenbruck, 2017).

As GNSS signals travel through the atmosphere, they are picked up and strengthened by the receiver's antenna. If the antenna can receive signals from several different satellite systems, the positioning becomes more accurate and reliable. With more satellites and signals, the receiver gets more information to work with, which helps it find the position more precisely, even in difficult environments (NovAtel Inc, 2023).

When it comes to determining the distance between a receiver and a satellite, there are several measurement techniques, with code-based (pseudorange) and carrier-phase positioning being the most common. In code-based positioning, the distance is calculated as the time it takes for the receiver to receive a signal from the satellite multiplied with the speed of light. GNSS satellites transmit a signal that contains a pseudorandom noise (PRN) code along with a precise timestamp of when the signal was sent. An identical code is generated at the GNSS receiver and will continuously be shifted in time until it aligns with the incoming signal. The amount of shift required to match the code will reveal how long the signal took to travel from the satellite to the receiver. The time-delay will then be multiplied with the speed of light. By measuring signals from three satellites at the same time, the GNSS receiver's position can roughly be calculated in three dimensions (X, Y, Z). Due to the fact that the receiver's clock is not as accurate as the satellite clocks, its time error also needs to be considered. Therefore, to accurately determine the GNSS receiver's position, signals from at least four satellites are required. This allows for solving the four unknowns: the three-dimensional coordinates (X, Y, Z) and the receiver's clock error. The uncertainty of pseudorange measurements depends on the signal resolution, which is approximately one percent of the signal wavelength. This results in position accuracies of a few meters (Lantmäteriet, n.d.-b; NovAtel Inc, 2023; Teunissen & Montenbruck, 2017).

For higher accuracies, carrier-phase measurements are used. In this technique, the receiver tracks the phase of the carrier that was transmitted by the satellite. By measuring the number of full wavelengths that fit between the receiver and the satellite, along with the fractional part of the wavelength, the distance can be retrieved. The frequency of the carrier wave is significantly higher than that of the PRN code, resulting in a wavelength of 19 cm. This gives an accuracy of approximately 2 millimeters, as the resolution of the signal is roughly one percent of the wavelength

(Lantmäteriet, n.d.-a; NovAtel Inc, 2023).

2.4.2 Uncertainties

There are various factors that can cause inaccuracies in GNSS measurements, including errors related to satellites, atmospheric conditions, and interference at the receiver. One potential source of error comes from the satellites themselves. Satellite clocks are incredibly precise but can still experience slight drifts. Even a timing error as small as 10 nanoseconds can result in a positioning error of about 3 meters. Another factor is the satellite's orbit. The receiver calculates its position based on the predicted locations of satellites, but these orbital predictions are not always perfectly accurate. If a satellite's actual position differs from its predicted position, the receiver may compute an incorrect location. Satellite timing and position drifts are continuously monitored and corrected by something known as GNSS ground control stations. To achieve higher accuracy and minimize these errors, more detailed information is required. This can be obtained through specialized services such as Precise Point Positioning (PPP) with Ambiguity Resolution, which provide enhanced corrections for more precise positioning by resolving the integer ambiguities in carrier-phase measurements, allowing for centimeter- to millimeter-level accuracy (Glaner & Weber, 2021; NovAtel Inc, 2023).

Another source of error arises from the atmosphere. GNSS signals can experience delays due to atmospheric conditions, which can result in inaccuracies when calculating the distance between the satellite and the receiver. The ionosphere, situated 60-300 km above Earth's surface, is filled with charged particles from the sun. These particles can delay the satellite signals as they travel, which can reduce the accuracy of the position data. Likewise, the troposphere, the layer nearest to Earth, can also cause errors. Variations in humidity, temperature, and atmospheric pressure can influence the GNSS signals, making it more challenging to determine precise locations (NOAA, 2023a; NovAtel Inc, 2023).

In addition to atmospheric delays, interference at the receiver can also impact GNSS signal quality and reduce positioning accuracy. One common type of interference is multipath, where signals bounce off nearby objects and take indirect paths to the receiver, causing measurement errors. Furthermore, unintentional interference can occur when nearby electronic devices emit radio frequencies, generating noise that disrupts the clarity of the signal and further degrades accuracy (NovAtel Inc, 2023).

2.5 Zenith Wet Delay

One of the key ways to analyse atmospheric moisture in GNSS-based meteorology is by looking at Zenith Wet Delay (ZWD). This delay happens when satellite signals get slowed down as they pass through moisture-rich layers of the troposphere. ZWD represents the variable part of the overall Zenith Tropospheric Delay (ZTD) that

depends on water vapour, while the more stable component, Zenith Hydrostatic Delay (ZHD), is linked to dry air. We can calculate ZHD fairly accurately using surface pressure data, however ZWD can vary quite a bit due to changes in humidity, temperature, and pressure. Because of this, we usually need real-time weather observations or empirical modelling methods to estimate ZWD accurately (Rocken et al., 1997).

Research over the past few decades has highlighted the importance of ZWD from GNSS data in tracking moisture dynamics in the troposphere. Its sensitivity to atmospheric water vapour makes it especially useful for spotting changes related to severe weather events. Many studies have shown that unusual ZWD patterns often occur before heavy rainfall and are closely tied to convective activity, particularly during the formation of tropical cyclones (Kermarrec et al., 2024). For instance, significant increases in ZWD were observed during Hurricanes Helene and Milton, indicating rapid rises in tropospheric humidity. These observations, supported by both GNSS time-series and satellite imagery, confirm that ZWD is a reliable indicator of storm intensity (NASA GPM Mission, 2024; PO.DAAC, 2024).

Lately, using ZWD data from GNSS networks has become a smart way to boost numerical weather prediction models through data assimilation techniques. This technology allows us to keep an eye on quickly changing moisture patterns in cyclone-prone areas, making ZWD an essential tool for predicting storm intensification, the start of rainfall, and the chances of coastal flooding. GNSS-based meteorological tools are thus improving early warning systems and reinforcing our strategies for climate resilience (PO.DAAC, 2024).

2.6 Land subsidence

Land subsidence is the incremental lowering of Earth's land surface. It is driven by a number of factors, either natural or anthropogenic, but it is often the result of solid or fluid mobilization. It is a very slow process which happens gradually over big time intervals which produces enormous loss of land elevation and can potentially span over big geographical areas. The progression of land subsidence can have lasting consequences - including damage of critical infrastructure, elevated risk of flooding and earth fissures (Herrera-García et al., 2021).

Rising evidence shows that land subsidence significantly worsens coastal inundation when tropical cyclones occur. Populations that live in low-lying coastal areas are especially susceptible to floods caused by tropical cyclones and even the most subtle land subsidence at low rates can markedly expand the effect of the flood. Due to climate change and the rising of sea levels, the historical 100-year flood level would rather occur every 1–30 years in the Gulf of Mexico regions in the late 21st century (Wang et al., 2024).

The typical causes of land subsidence in Florida are sediments compaction, soil

oxidation and sinkhole activity. Several populations that live by the coast in southeast Florida have been in several time periods, affected by flooding events which are caused by heavy rain, high tide and storm surges (Wdowinski et al., 2020).

3
Methods

This chapter describes the methods used to acquire and analyse the data that form the basis of the results presented in later sections. It covers the data acquisition process, the application of the PRIDE PPP-AR software, and the data analysis procedures carried out using MATLAB.

3.1 Data gathering

The selection of GNSS permanent stations relevant to this research was based on the graphical interface *Florida Permanent Reference Network (FPRN) Status*, accessed via the website provided by Florida Department of Transportation (FDOT) (Florida Department of Transportation, 2025a). With this tool, permanent stations in the proximity of the tropical storms could be located together with satellite images for Milton and Helene (NOAA, 2025a, 2025b). A condition for including these permanent stations were that sufficient data had to be available for at least a few days before, during, and after the storms. Stations that lacked data for an entire 24-hour period were excluded. To facilitate this process, a free student account was acquired to observe and download data from the website provided by FDOT (Florida Department of Transportation, 2025b). The stations used in this research for Milton and Helene can be seen in Table 3.1 and Table 3.2, respectively.

As seen in Figure 3.1, the stations chosen in each region follows a rough pattern from north to south, this was chosen deliberately so that the time of certain weather events would be closer to each other. This however could not be done as a fine line, seen especially in the western part of Figure 3.1, since the stations are not geographically located as north to south. Some of the best located stations also had to be swapped due to missing large amounts of data, where some even had several days missing, which is the reason for the large distances on the eastern stations.

For the stations regarding Helene, a different approach was needed due to an unfortunate location of the permanent stations. This resulted in that only three stations (FLPY, FLMD and FL75) would be used because of their ideal location with respect to the eye of Hurricane Helene, as seen from satellite images (NOAA, 2025a). Unfortunately the station FL75 had data faults at key points during the time of impact, so another segment consisting of five stations (FLCB, TALH, FLJL, GATE and GAME) also had to be included, as seen in Figure 3.2.

Table 3.1: *Permanent stations in Florida used for data collection during Hurricane Milton. The stations are listed in the order of the storm's progression through their respective regions. The last entry corresponds to the station used for water level measurements.*

Permanent Station	Region	Location
FLAI	Western	Bradenton Beach
FLSN	Western	North Sarasota
FLSC	Western	Central Sarasota
ORL1	Central	Orlando
FLKS	Central	Kissimmee
FLCC	Central	Central Osceola
FLBN	Eastern	Palm Coast
ORMD	Eastern	Ormond Beach
TTVL	Eastern	Titusville
WL: 8726724	Western	Clearwater Beach

Table 3.2: *Permanent stations in Florida used for data collection during Hurricane Helene. The stations are listed in the order of the storm's progression through their respective regions. The last entry corresponds to the station used for water level measurements.*

Permanent Station	Region	Location
FL75	Southern	Jennings
FLMD	Central	Madison
FLPY	Northern	Perry
FLCB	Southern	Carrabelle
TALH	South-Central	Tallahassee
FLJL	Central	Summerbrook
GATE	North-Central	Thomasville
GAME	North	Moultrie
WL: 8728690	Southern	Apalachicola

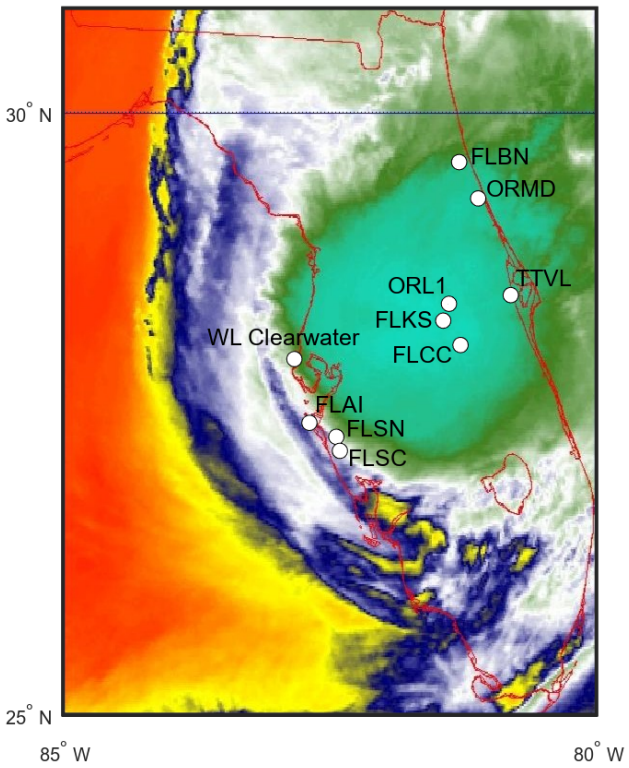

Figure 3.1: *Satellite image of Hurricane Milton, showing the locations of the permanent stations used in the analysis. Satellite image courtesy of NOAA / NESDIS Center for Satellite Applications and Research (NOAA, 2025b).*

The dates for Hurricane Milton were chosen from the 4th to the 24th of October 2024, which matched the storm's path as it swept over Florida. The official confirmation dates for tropical cyclone Milton were given between the 5th of October at approximately 15:00 UTC and the 10th of October at approximately 21:00 UTC by *National Weather Service*, which gave us one day before the formation and 14 days after to determine a baseline value (National Weather Service, 2025b). The reasoning behind the unequal lengths before and after the storm was that more days following the storm were considered sunny days while most days preceding it were cloudy and rainy, according to *World Weather* (World Weather, 2025). For Helene the dates 19th of September to 1st of October where chosen with the same reasoning in mind. Here, the *National Weather Service* provided the confirmation of tropical cyclone dates between 24th of September at approximately 15:00 UTC to 27th of September at approximately 21:00 UTC for the tropical storm (National Weather Service, 2025a).

For processing the raw data from the permanent stations, the free and open-source software PRIDE PPP-AR, developed by Wuhan University based *PRIDE Lab* was used (PRIDE Lab, 2018, 2025). As the data files from FDOT were provided in a daily format, each day's data had to be processed independently. The positioning was performed using the PPP-AR technique, which enhances the traditional Precise Point Positioning (PPP) method by resolving carrier-phase ambiguities as integer values. This significantly improves both positioning accuracy and convergence time.

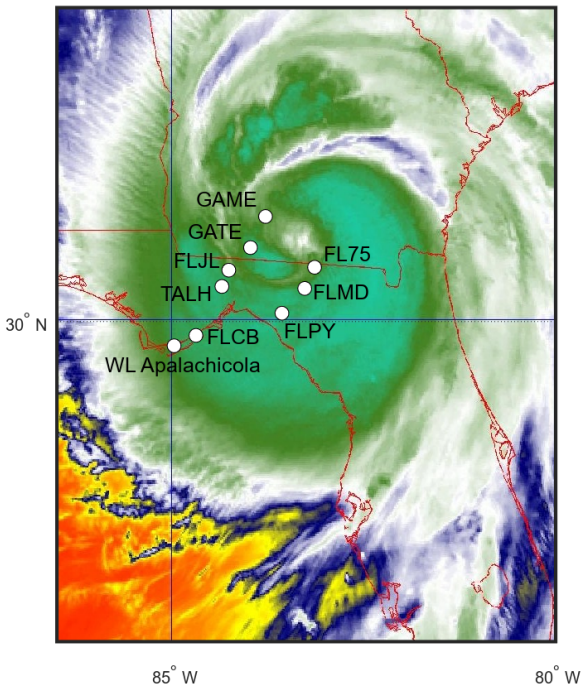

Figure 3.2: *Satellite image of Hurricane Helene, showing the locations of the permanent stations used in the analysis. The three stations to the east (right) correspond to the first segment, while the stations to the west (left) represent the second segment. Satellite image courtesy of NOAA / NESDIS Center for Satellite Applications and Research (NOAA, 2025b).*

PPP-AR achieves high-precision positioning through accurate modelling of satellite orbits, clock errors, and atmospheric signal delays.

Each daily processing session, using data sampled at 30-second intervals, required approximately 10 to 15 minutes to complete. Once the processing was finished, the output was organised into folders containing various types of data files. For the purposes of this study, focus was placed on the files containing ZWD and kinematic position estimates. These daily ZWD and kinematic files were compiled into two separate *.dat* files to ensure compatibility with MATLAB. This step provided clearer time series visualization, easier comparison between different tropical storms, and more robust statistical analysis.

3.2 Data analysis of Zenith Wet Delay

The analysis of ZWD was carried out using MATLAB due to its advanced built-in toolboxes for data processing and visualization.

ZWD data were retrieved from the PRIDE PPP-AR software, which provided modelled atmospheric delays caused by water vapour at selected GNSS-stations in Florida. The initial focus of the analysis was on identifying variations in ZWD values during periods associated with known tropical storm activity. Particular attention was

given to the station FLSN, which was selected as it was the first station in the dataset without significant data loss. Time series plots were generated to visualize temporal changes in ZWD, and specific time intervals, such as October 5th to 10th, were selected for closer examination due to their relevance to the passage of the tropical storms. These plots allowed for the identification of potential anomalies or spikes in ZWD data, which were subsequently compared to meteorological data and storm tracking information. The results and interpretation of these observations are presented in Section 4.

Based on this, a refined plot was generated using a moving mean function. For each data point, the mean was calculated using the 30 preceding and 29 following data points, effectively yielding a 30-minute moving average. This smoothing was primarily applied to reduce the influence of potential data anomalies. As shown in Figure 3.3, the transformation did not significantly alter the data; only when zooming in on certain peaks could the original values be seen as slightly higher.

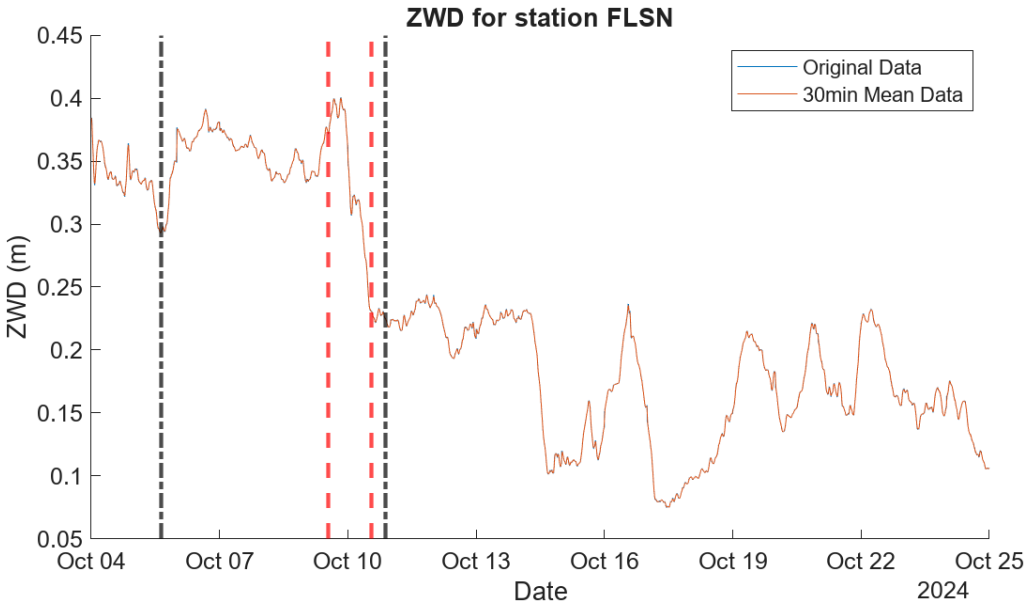

Figure 3.3: *Data of ZWD original and 30 minute mean for permanent station FLSN, where the red lines show when the storm's core entered and exited Florida and the black lines show approximate days of when the storm was active over Florida.*

Since the dataset used in this study was extensive – spanning multiple days of data from 17 different permanent GNSS stations – a sampling interval of 30 seconds was chosen as a first approximation. This reduced both processing time and computational load.

Due to the large volume of data, the initial data modelling from PRIDE PPP-AR was performed using piece-wise constant (PWC) model with 5-minute intervals, rather than an epoch-wise stochastic (STO) model. This PWC 5-minute interval sampling method was selected for comparison because it applied a constant ZWD correction (ZWDcorr) within each 5-minute interval. Although the original data had

a 30-second resolution, only one correction value was used per 5-minute window, instead of STO which calculated a separate ZWDcorr for each individual 30-second epoch. To assess whether the STO sampling method offered significant improvement over PWC 5 min, a preliminary comparison was conducted using data from permanent station FLSN. The intention was to apply STO for certain periods were more accurate data was needed. The preliminary results are presented in Figure 3.4.

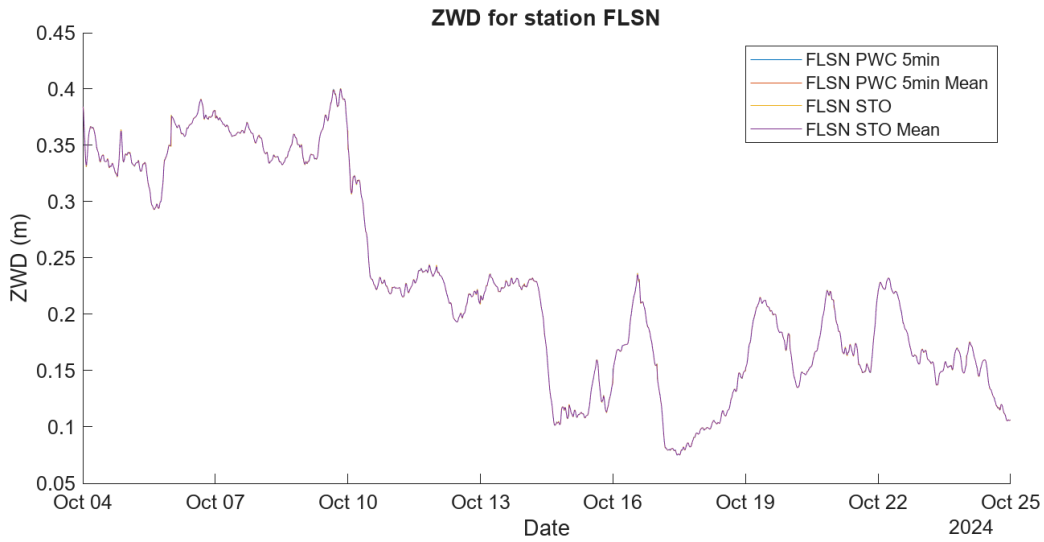

Figure 3.4: *Comparison of ZWD correction results using the PWC 5 min and STO sampling methods, along with their 30-minute means, illustrating differences in PRIDE PPP-AR output across the dataset.*

From this, a more extensive evaluation was conducted, where the focus was placed on one of the peaks, and the x-axis interval was effectively reduced from 21 days to approximately 1 hour, as shown in Figure 3.5. Up until this point, almost no difference could be observed. However, at this zoom level, a slight difference between the models became evident.

Based on this, a comparison of the deviations between the STO mean and PWC 5-minute mean was performed in MATLAB using the equation

$$\left| \frac{STO_{Mean} - PWC_{5minMean}}{PWC_{5minMean}} \right| \cdot 100 \tag{3.1}$$

which calculates the relative deviation between each corresponding data point, expressed as a percentage. The analysis resulted in a maximum deviation of 1.446 mm or 0.456 %. Based on this, a more normalized deviation test was performed by computing the mean of all deviations, which resulted in a significantly lower deviation of 18.523 ppm or 0.009 %.

Afterwards, a calculation was performed to assess whether the deviation was statistically insignificant, using a 99 % confidence interval. The 99 % confidence interval

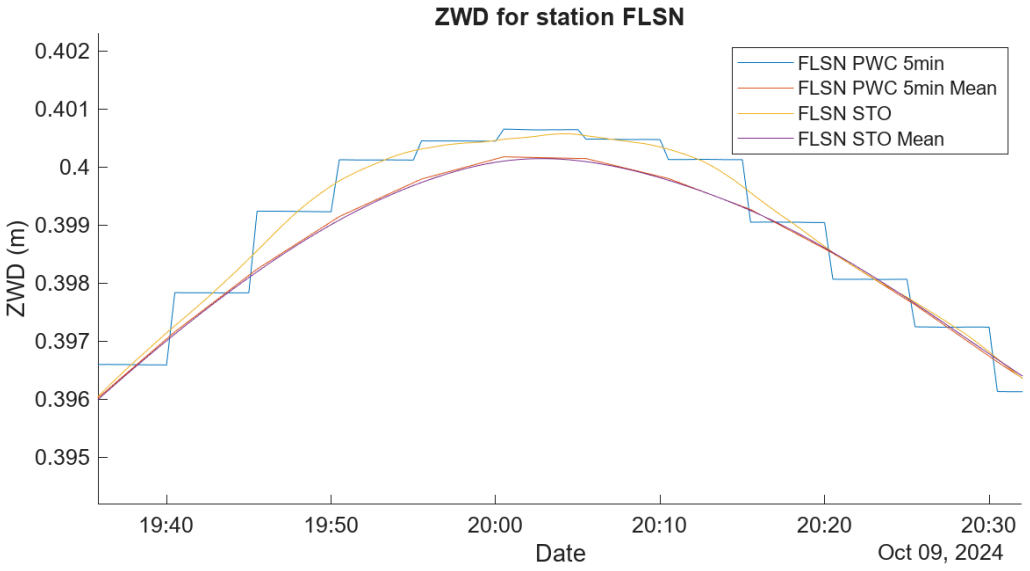

Figure 3.5: *Zoomed-in comparison of the PWC 5 min and STO sampling methods and their 30-minute means, highlighting differences in PRIDE PPP-AR corrections on a subset of the dataset.*

was then calculated using the Student's t-distribution with the equation

$$M_n(X) \pm t_{1-\alpha/2,(n-1)} \frac{S_n(X)}{\sqrt{n}} \tag{3.2}$$

where $M_n(X)$ is the sample mean, $t_{1-\alpha/2,(n-1)}$ is the critical value of the Student's t-distribution (calculated using MATLAB's *tinv*), n is the sample size, and $S_n(X)$ is the sample standard deviation. This resulted in a confidence interval width of about 1.919 mm, corresponding to ± 0.960 mm. Since the largest deviation exceeded this 0.960 mm half-interval, a test to see how many data points exceeded the deviation was created. This resulted in 78 data points above 0.960 mm, which only represented 0.129 % of the dataset. These data points were also sequential, corresponding to data points 17 404–17 481 (10th of October at approximately 00:00 UTC), during which the ZWD exhibited the most significant change as the storm passed.

Student's t-distribution provides a good approximation when the sample size is small or when there is insufficient information about the overall population, such as variance. However, since the data for this analysis was quite large (approximately 40 000 – 60 000 data points), the normal distribution is expected to yield similar results, in accordance with the law of large numbers. Therefore, a confidence interval based on the normal distribution was constructed using the equation

$$M_n(X) \pm Z_{\alpha/2} \frac{S_n(X)}{\sqrt{n}} \tag{3.3}$$

where $M_n(X)$ represents the sample mean, n is the sample size, $S_n(X)$ is the sample standard deviation, and $Z_{\alpha/2}$ was chosen as 2.576, corresponding to a 99 % confidence interval. This resulted in a confidence interval of 1.920 mm, indicating a slight

difference compared to the value obtained using the Student's t-distribution. Since the deviations were found to be statistically insignificant (with the 99 % confidence interval being wider), and only the largest deviations exceeded the confidence interval – occurring sequentially during the most drastic changes in ZWD – they are unlikely to significantly impact the overall uncertainty of the storms' data. Therefore, a change to STO for the more critical data points was deemed unnecessary.

Based on these mean-filtered data points, MATLAB's *Wavelet Transform* – specifically the *Continuous Wavelet Transform* (CWT) – was applied due to its suitability for analysing transient behaviour, rapidly changing frequencies, and slowly varying patterns (MathWorks, 2025). For a clearer analysis of when ZWD became irregular, a threshold from the median of the dataset was calculated to sort out small irregularities as can be seen in Section 4.

3.3 Data analysis of land subsidence

For the data analysis of land subsidence, MATLAB was once again chosen due to its advanced built-in toolboxes for data processing and visualization. For this, an initial plot of the modelled data from PRIDE PPP-AR was created to gain a preliminary understanding of the land subsidence both during and after the tropical storms impact on Florida. After this plot, MATLAB's CWT was once again used to analyse changes during the storm. For a clearer analysis of when land subsidence became irregular, a threshold from the median of the dataset was calculated to sort out small irregularities as can be seen in Section 4.

To assess the plausibility of the observed land subsidence values, water level data from nearby tide gauge stations were collected and compared to height changes measured by permanent GNSS stations. Due to the limited number of suitable stations in the vicinity of the storm's path, the station at Clearwater was selected for comparison, as it was the closest available station not located inside a bay. Data from Clearwater was compared with the height variations recorded at the FLSN station. Both time series were normalized relative to their respective medians to enable visual comparison. The resulting figure can be seen in Section 4.

3.4 The tropical storms speed and direction

To estimate the storms speed and direction MATLAB's *xcorr* function was used to perform cross-correlation between time series from different permanent GNSS stations. This technique allowed for identification of the time delay between similar patterns in the data, which corresponds to the time taken for the storm to move between the two locations. The delay was calculated in samples, and converted to time using the sampling interval of 30 seconds. This analysis was repeated for multiple station pairs, where the results from this method are presented in Section 4.

To get an approximated speed for this, the coordinates of the permanent stations

were implemented in MATLAB via the speed equation

$$s = \frac{d}{t} \tag{3.4}$$

where s is the speed, d is the distance and t is the time delay. Here, the distance was calculated from the coordinates thanks to MATLAB's *distance* and *deg2km* functions. The speeds can be seen in Section 4.

For the direction of the tropical storms, a different approach was used. This consisted of finding the stations with the highest ZWD for each segment for the stations regarding Milton, as shown in Figures 4.4, 4.5, and 4.6 which presented the ZWD data for each region. This thought process came from the theory and the visualization from satellite images (NOAA, 2025b), which showed that the most wet part was located close to the centre of the storm.

A search for a possible drastic decrease in ZWD were also conducted, since the eye of the storm usually creates this phenomena. This was however hypothesized to a low probability since these 'eyes' are usually relatively small and the amount of stations covering Florida may be large, but not nearly enough for this to be a general phenomenon.

4
Results

This chapter presents the results of the study and is divided into three main parts. First, the impact of tropical storms on land subsidence in Florida is examined, based on data from the selected permanent stations. Second, changes in ZWD before, during, and after the storms are analysed, to see if they are related to storm activity. Finally, the possibility of using ZWD data to estimate the speed and direction of the storms is explored, as a way to track their movement.

4.1 How do tropical storms impact land subsidence and how can this be researched with the use of GNSS data?

From the permanent station FLSN, Figure 4.1 illustrates the temporal evolution of land subsidence. As the storm's core made landfall, a clear indication of the storm can be seen in both the Wavelet scalogram and the Anomaly Detection results.

The permanent station FLCB shows a sharp rise in height shortly after Helene becomes active, a pattern that is clearly reflected in both the Wavelet scalogram and the anomaly detection results, as shown in Figure 4.2. During the passage of the storm, a few peaks can be observed. However, the Wavelet scalogram does not indicate as strong irregularities during the storm's core.

Figure 4.3 presents land subsidence alongside water level data and clearly indicates anomalies associated with the passage of the storm's core through Florida.

The results indicate that tropical storms have an impact on land subsidence and that GNSS can be used to demonstrate this correlation. At the selected stations, there are clear anomalies during the storm, coinciding with both the wavelet scalogram and the anomaly detection results. However, for the station FLCB it is not as clearly during the passage of the storm's core. Milton recorded most significant impact during the passage of the storm's core, whereas Helene recorded the strongest anomalies during the early stages of the storm.

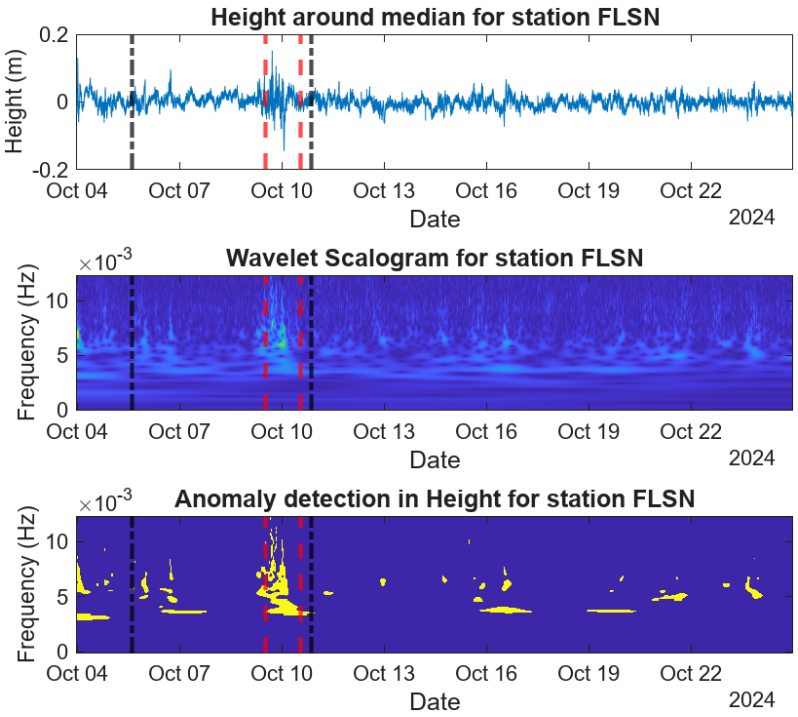

Figure 4.1: *Height relative to the median, Wavelet Scalogram, and anomaly detection results for station FLSN during Hurricane Milton. The red lines show when Milton's core entered and exited Florida and the black lines show approximate days of when the storm was active over Florida.*

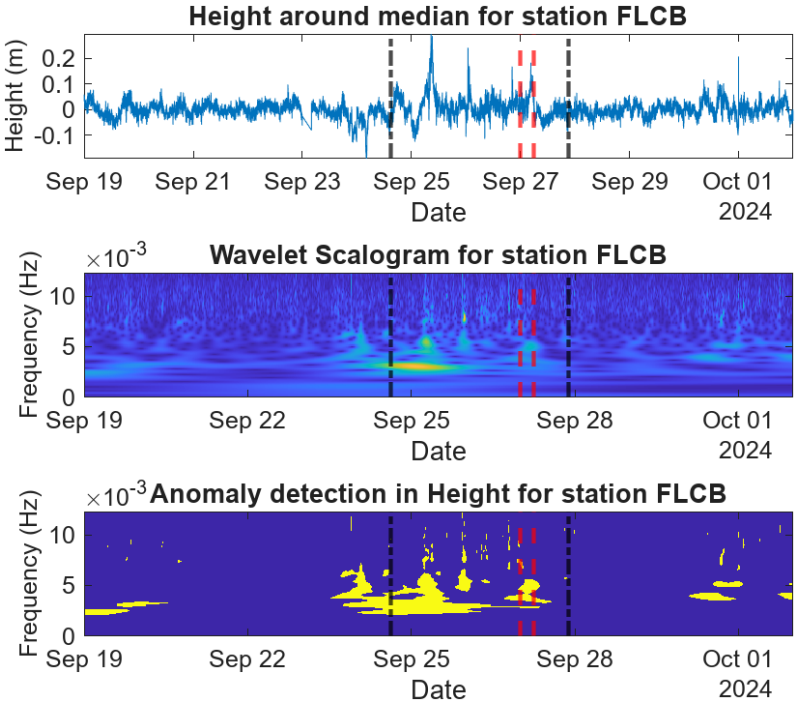

Figure 4.2: *Height relative to the median, Wavelet Scalogram, and anomaly detection results for station FLCB during Hurricane Helene. The red lines show when Milton's core entered and exited Florida and the black lines show approximate days of when the storm was active over Florida.*

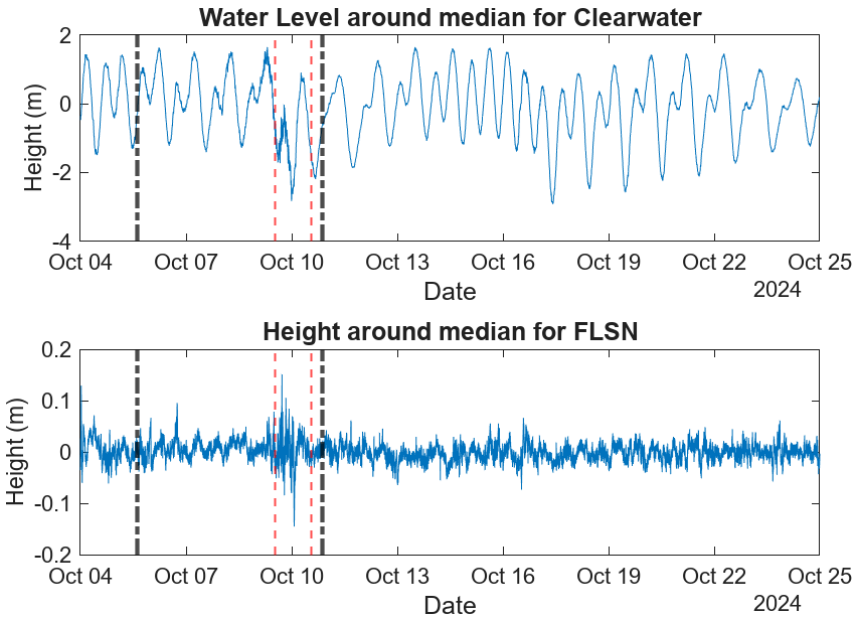

Figure 4.3: *Water Level relative to the median at Clearwater Beach and the Height relative to the median at FLSN during Hurricane Milton. The red lines show when Milton's core entered and exited Florida and the black lines show approximate days of when the storm was active over Florida.*

4.2 Can Zenith Wet Delay be used to observe tropical storms?

The variation in Zenith Wet Delay (ZWD) for the western, central, and eastern permanent stations in Florida during and after Hurricane Milton is shown in Figures 4.4, 4.5, and 4.6. They include red vertical lines indicating the estimated time when the core of the storm entered and exited Florida, and black lines marking the approximate duration of the storm's activity over the state.

Across all regions, a consistent pattern emerges. ZWD values can be seen to increase significantly during the storm's active period (October 5 – 10), reaching peaks of approximately 0.40 meters, followed by a significant drop in the following days, where values stabilize below 0.25 meters. An increase in ZWD is also visible in the days leading up to the storm's landfall.

For the western permanent stations (Figure 4.4), the ZWD values before the storm are fairly high, and slowly decreases from about 0.38 meters to below 0.30 meters. The ZWD thereafter starts to increase notably between October 5 – 9th, with a drop right in the middle of the storm. The ZWD peaks at approximately 0.41 meters and starts to decline significantly a short bit after the storms core enters. The drop continues for a short period, before stabilizing at lower levels with an ZWD of 0.21 meters shortly after the eye of the storm exits Florida. The values for the following days after the storm (October 11 – 25th), stay relatively stable, hovering between values of around 0.06 meters and 0.24 meters. The peaks thus remain minor and

none of them reach the peak levels observed during the storm.

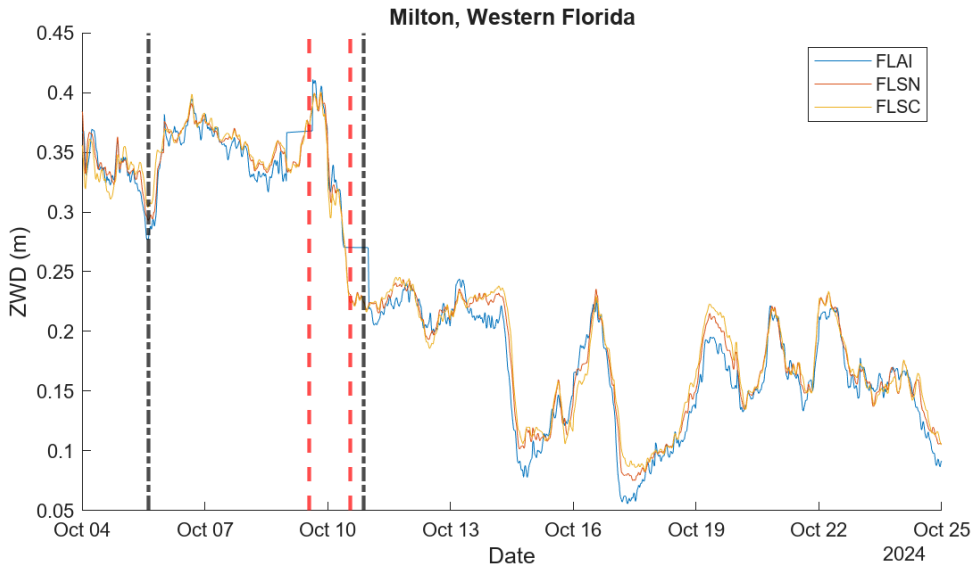

Figure 4.4: *ZWD for the three western permanent stations during Hurricane Milton.*

Central Florida, see Figure 4.5, shows a similar trend. The ZWD values before the storm are nearly as high as those in the western region, starting around 0.34 meters and declines to approximately 0.27 meters just before the storm's arrival. A rapid increase in ZWD occurs shortly thereafter, followed by a drop in the middle of the storm. It then continues to rise, reaching its peak of 0.40 meters in the early hours of October 10th, coinciding with the storm core's presence. A steep decline in ZWD occurs immediately afterward, dropping to approximately 0.22 meters shortly after the storm's core passes and right before the storm fully disappears. Post-storm values remain consistent with those in the western region, fluctuating around 0.08 to 0.25 meters.

In eastern Florida, see Figure 4.6, the pattern continues similarly. ZWD increases significantly as the storm approaches and enters the region, followed by a decrease in the middle of the storm and then continues to rise. Permanent stations FLBN and ORMD reach their peaks of around 0.36 meters just as the core of the storm arrives, while TTVL peaks slightly later at 0.39 meters, almost in the middle of the core. A steep decline follows the peak, and continues until the whole storm has exited the region, reaching ZWD values down to about 0.15 meters. The post-storm period shows relatively suppressed values, fluctuating between approximately 0.07 to 0.26 meters.

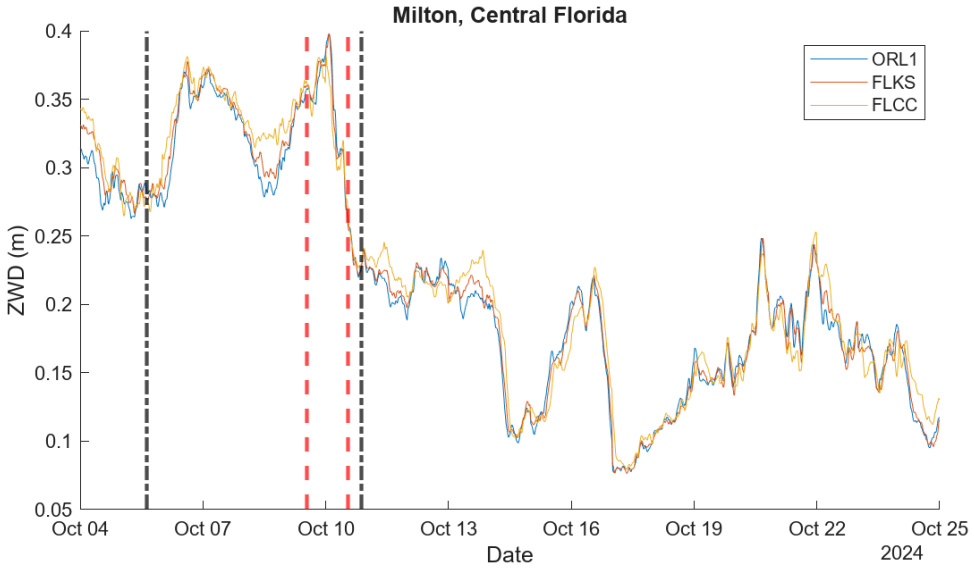

Figure 4.5: *ZWD for the three central permanent stations during Hurricane Milton.*

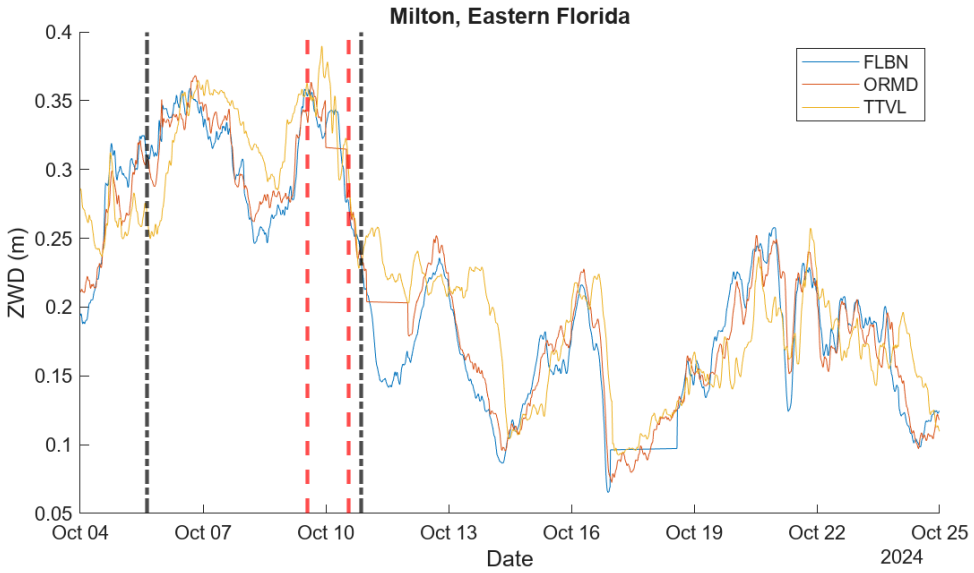

Figure 4.6: *ZWD for the three eastern permanent stations during Hurricane Milton.*

4.3 Is it possible to use Zenith Wet Delay to find the speed and direction of tropical storms?

The method used to estimate the speed of Hurricanes Milton and Helene is presented in Table 4.1 and Table 4.2, respectively. The speeds were calculated using Equation 3.4, which estimates the relative speed of the storm between permanent GNSS stations based on time lag between correlated ZWD time series and the geographic coordinates of stations. These results provide valuable insight into the speed of the storms across different station paths and support the feasibility of using ZWD data for tropical storm tracking.

The potential of using ZWD to determine the direction of tropical storms can be shown in Figure 4.6. Here, an indication for the storm's centre can be shown for the permanent station TTVL, where the ZWD is significantly higher than at FLBN and ORMD during Milton's descent over Florida.

Table 4.1: *Estimated storm speeds between permanent GNSS stations along three unaffected paths and two segments affected by data faults during Hurricane Milton. For each segment, the first row shows the speed between the first and last stations, while the remaining rows detail the speed across the entire path. An asterisk (*) shown in the table indicates that the corresponding permanent station is affected by significant data faults.*

Segment	Permanent Station 1	Permanent Station 2	Speed [m/s]	Speed [km/h]
Segment 1	FLSC	TTVL	17.827	64.176
	FLSC	FLKS	16.207	58.346
	FLKS	TTVL	25.648	92.334
Segment 2	FLSN	TTVL	21.615	77.813
	FLSN	FLCC	26.525	95.491
	FLCC	TTVL	14.624	52.645
Segment 3	FLSN	TTVL	21.615	77.813
	FLSN	ORL1	15.328	55.181
	ORL1	TTVL	56.034	201.721
Segment 4	FLAI*	TTVL	2.585	9.305
	FLAI*	ORL1	2.048	7.371
	ORL1	TTVL	56.034	201.721
Segment 5	FLSN	FLBN*	6.534	23.521
	FLSN	FLKS	16.775	60.390
	FLKS	FLBN*	3.815	13.734

Table 4.2: *Estimated storm speeds between permanent GNSS stations during Hurricane Helene. For each segment, the first row indicates the speed between the first and last stations, while the remaining rows present the speeds across the entire path. An asterisk (*) in the table indicates that the corresponding permanent station is affected by significant data faults.*

Segment	**Permanent Station 1**	**Permanent Station 2**	**Speed [m/s]**	**Speed [km/h]**
Segment 1	FLPY	FL75*	2.901	10.443
	FLPY	FLMD	30.607	110.184
	FLMD	FL75*	1.113	4.007
Segment 2	FLCB	GAME	6.527	23.497
	FLCB	TALH	3.473	12.503
	TALH	FLJL	14.735	53.047
	FLJL	GATE	31.824	114.565
	GATE	GAME	22.764	81.950

5

Discussion

This chapter presents a discussion based on the GNSS-based analysis of Tropical Storms Milton and Helene. The focus is placed on two primary components: land subsidence and variations in atmospheric water vapour as measured by ZWD. In addition, the limitations of the study and potential areas for improvement are addressed. These findings contribute to a deeper understanding of the geophysical processes associated with tropical storm activity and highlight the potential of GNSS technology as a versatile tool for monitoring both atmospheric conditions and surface deformation.

5.1 Land Subsidence During Tropical Storms

The figures in 4.1 did not clearly reveal the tropical storm's impact on land subsidence. However, for both Milton and Helene, the wavelet scalogram and the anomaly detection results clearly indicates that the stations height is being affected. This is evident during the passage of the storm's core for Milton, and similarly, clear effects are observed for Helene during that period. However, a large number of anomalies during the initial phase of the storm unfortunately overshadow these results.

The figure depicting water level together with station FLSN revealed, as initially thought, that water level and height would show clear correlation. However, another initial thought was that as the storm made landfall it would drag seawater inland, and then causing land subsidence due to the weight of it. This could unfortunately not be seen altogether. There is a slight indication of this in Figure 4.3, but since we also have to take in account the spacial distance between them, we can not with certainty prove this. The figure in Appendix B, showing the water level in Apalachicola and station FLCB also seem to disprove this theory.

This leads to our analysis falling a bit short of the clarity that we initially had sought out after and also hints at an unidentified bias or error margin in our measurements. The two storms also resulted in markedly different subsidence patterns, which further reduces confidence in the reliability findings. These results goes to show that this approach cannot be relied upon on its own.

One thing that both figures for height data did illuminate was that the irregularities – shown in the second and last plot in each respective figure – occurred mostly during the passage of the storm's core, but smaller irregularities also occurred both

before and after.

5.2 Zenith Wet Delay

As seen in Section 4.2, ZWD measurements from the permanent GNSS stations in the western, central, and eastern regions during Hurricane Milton exhibit a clear and consistent trend in atmospheric moisture related to the storm's progression. In all three areas (Figures 4.4, 4.5, and 4.6), ZWD values rose significantly in the days prior to the storm's landfall, reached their highest levels during the passage of the storm's centre, and then dropped sharply once the storm moved away. These patterns highlight ZWD's sensitivity to variations in tropospheric water vapour and support its potential use as a tool for observing tropical storms.

A notable increase in ZWD was observed several days before Milton's core made landfall. This pre-storm increase is likely linked to the inflow of warm, humid air drawn into the cyclone's circulation which is a typical characteristic of tropical systems. As the storm intensifies over oceanic regions, they carry significant amounts of moisture inland, which raises the atmospheric water vapour content and thus the ZWD. This is evident in all three regions, where ZWD values rose steadily, even before the core of Milton officially entered Florida.

Although ZWD is effective at capturing the build-up of atmospheric moisture ahead of approaching storms, it is not as precise for determining the exact moment of landfall. In all regions, ZWD values tend to peak either just before or during the passage of the storm's core, but the timing varies between stations. For example, in the eastern region (Figure 4.6), stations FLBN and ORMD peak just as the core arrives, while TTVL peaks slightly later. This variation highlights an important limitation of relying solely on ZWD since it measures total atmospheric moisture above a station which can vary due to storm structure, shifting wind patterns, and local geography. As a result, the peak in ZWD doesn't always match the exact moment the storm makes landfall, even though it still provides a strong signal of the storm's presence and strength.

Immediately following Milton's peak, all regions experienced a steep decline in ZWD. This is likely due to the storm gradually moving away, bringing in drier air, which is common in hurricanes and tropical storms. As the storm weakens, less moisture is pulled up into the storm, and the moist air is replaced by drier air, leading to a sharp decrease in ZWD. In western Florida, ZWD fell from over 0.40 m to 0.21 m within a day (Figure 4.4). A similar pattern is observed in central and eastern Florida, where values fell rapidly and stabilized at much lower levels (typically below 0.25 m) in the days following the storm.

As seen in Section 4.3, there is evidence pointing at measuring the speed of tropical storms is highly possible via ZWD. This however is not perfect. Both data losses and the general uncertainty of weather play a big role in the accuracy of the storm's speed. The amount of permanent stations also play a large role here, where more

stations would mean better accuracy and less impact on data faults. The same applies to determining the direction of the storm: if more stations were available, the centre could have been located with greater precision, possibly even identifying the storm's eye, which would provide more valuable data for future analyses.

5.3 Limitations and Uncertainties

As previously mentioned, there were several challenges in selecting the permanent stations. Some of the best-located stations suffered from significant data gaps, with missing data spanning the entire day or even multiple days during the periods when the storms were active in their regions. This unfortunately created a negative impact of the placement of the remaining stations, which created the large gaps seen in Figure 3.1 and the reason for the added segment in Figure 3.2. Even though these stations were excluded, there were still significant data losses that affected the study. Additionally, a few extreme outliers were flagged as uncertain by PRIDE PPP-AR and subsequently removed. As a result, MATLAB's *xcorr* function was unable to identify a reasonable correlation for some of the stations.

Selecting permanent stations used for measuring water levels also presented several challenges. One such challenge was that stations located near the western side of Florida, in proximity to the GNSS stations, were situated in a bay. This made them particularly sensitive during tropical storms, as these environments can produce swells and water movements which are difficult to predict and may not correspond to the storms initial landfall. As a result, these stations were unlikely to reveal a possible correlation between water level variations and land subsidence. Consequently, for Hurricane Milton, a time delay had to be considered between the water level measurements and the GNSS-based stations.

The movement of Hurricane Helene, combined with sparse distribution of surrounding permanent stations, meant that the stations were not densely clustered enough to form groups, as it were for Hurricane Milton. This limited the ability to determine whether ZWD data could be used to locate the storm's centre in case of Helene, and it reduced the reliability of using ZWD data alone to identify the centre of a tropical storm.

To estimate the speed at which the tropical storms passed over Florida, the *xcorr* function in MATLAB was used. While this method appeared effective for calculating storm speed, interpreting the results was more challenging. Since *xcorr* identifies the time shift that produces the highest correlation between two signals, it does not indicate the exact location or feature within the signal that caused the match. As a result, it was assumed that the correlation most likely corresponded to the storms' centre during landfall and passage. To verify this assumption, comparisons with satellite imagery were necessary.

One vital factor of uncertainty lies in the way we – and any reader for that matter – interpret the graphics presented throughout this report. Visualizing data can expose

trends and relationships better than simple values but they also introduce a level of subjectivity. They can be as insignificant as subtle differences in scale, but can lead to varying conclusions about the same dataset. This methodological approach increases the risk of human error at multiple stages. By relying heavily on our own judgements, we therefore have to consider that it could potentially be inconsistent comparisons and confirmation bias – all of which can compromise our findings in the end.

5.4 Improvements

A potential enhancement involves broadening the application of GNSS data through the implementation of GNSS-Interferometric Reflectometry (GNSS-IR) techniques for monitoring sea levels and flooding. The integration of GNSS-IR with sophisticated signal decomposition techniques can yield highly precise sea level height measurements with cm-level accuracy. The research conducted at the Onsala Space Observatory emphasises how GNSS utilization have developed from navigation and timing tasks to wider environmental observations, including soil moisture detection and sea level tracking. Moreover, it had been revealed that by precisely assessing the fluctuations in the GNSS signal-to-noise ratio (SNR) data, it is feasible to track surface water. Incorporating a GNSS-IR based approach into hurricane monitoring systems could facilitate the concurrent observation of both atmospheric water vapour as well as land subsidence during storms, thereby providing a more comprehensive understanding of storm effects. This dual functionality could validate particularly relevant for early warning and disaster response efforts in coastal areas (Haas et al., 2021).

6
Conclusion

The results of this study suggest that combining both ZWD data and GNSS-derived height data provides the most reliable method for identifying and tracking tropical storms. ZWD has proven to be highly effective in detecting the early development of a storm, often registering abnormally high values only hours after official reports from the National Weather Service. However, the results also indicate that ZWD is less effective at capturing the moment when the storm core makes landfall. In contrast, GNSS-derived height data appears to be a more reliable indicator during landfall, as it frequently shows significant variations at that time.

Additionally, by analysing ZWD time series from different stations, it was feasible to estimate the velocities and trajectories of the storms, although the accuracy was impacted by uncertainties stemming from missing data and uneven station distribution.

The results also suggests that, although many GNSS permanent stations are already installed, it would be beneficial to increase their number further. In particular, prioritizing stations equipped with GNSS-IR capabilities could enhance the integration of height data and water level measurements. This would help minimizing the time delay caused by the spatial separation between tide gauges and GNSS stations, thereby improving the temporal resolution and the accuracy of the observations.

Expanding the GNSS network in this way would contribute to more resilient geophysical monitoring infrastructure, with direct applications in climate adaptation strategies and early warning systems for coastal hazards.

Bibliography

EUSPA. (2025). *What is gnss*. European Union Agency for the Space Programme. Retrieved April 20, 2025, from https://www.euspa.europa.eu/eu-space-programme/galileo/what-gnss

Florida Department of Transportation. (2025a). *FPRN Status*. Retrieved February 16, 2025, from https://www.myfloridagps.com/DMap/

Florida Department of Transportation. (2025b). *Spider Business Center - SNC Login*. Retrieved February 16, 2025, from https://www.myfloridagps.com/sbc/spider-business-center

Glaner, M., & Weber, R. (2021). PPP with integer ambiguity resolution for gps and galileo using satellite products from diferent analysis centers. *GPS Solutions*, *25*(102). https://doi.org/10.1007/s10291-021-01140-z

Haas, R., Hu, Y., Yuan, X., Liu, W., Wickert, J., & Jiang, Z. a. (2021). Gnss-ir model of sea level height estimation combining variational mode decomposition. *IEEE Journal of Selected Topics in Applied Earth Observations and Remote Sensing*, *PP*, 1–1. https://doi.org/10.1109/JSTARS.2021.3118398

Herrera-García, G., Ezquerro, P., Tomás, R., Béjar-Pizarro, M., López-Vinielles, J., Rossi, M., Mateos, R. M., Carreón-Freyre, D., Lambert, J., Teatini, P., Cabral-Cano, E., Erkens, G., Galloway, D., Hung, W.-C., Kakar, N., Sneed, M., Tosi, L., Wang, H., & Ye, S. (2021). Mapping the global threat of land subsidence. *Science*, *371*(6524), 34–36. https://doi.org/10.1126/science.abb8549

Jones, S. C., Harr, P. A., Abraham, J., Bosart, L. F., Bowyer, P. J., Evans, J. L., Hanley, D. E., Hanstrum, B. N., Hart, R. E., Lalaurette, F., Sinclair, M. R., Smith, R. K., & Thorncroft, C. (2003). The extratropical transition of tropical cyclones: Forecast challenges, current understanding, and future directions. *Weather and Forecasting*.

Kermarrec, G., Calbet, X., Deng, Z., & Carbajal Henken, C. (2024). Can zenith wet delay from gnss "see" atmospheric turbulence? insights from case studies across diverse climate zones. *EGUsphere*. https://doi.org/10.5194/egusphere-2024-2680

Lang, S., Huffman, G., & Reed, J. (2024, October 9). *Extremely powerful hurricane milton forms in the gulf of mexico* [Visualizations by Alex Kekesi and NASA SVS. Updated: 2024-10-10. Accessed: 2025-03-27]. NASA Global Precipitation Measurement (GPM). https://gpm.nasa.gov/applications/weather/news/extremely-powerful-hurricane-milton-forms-gulf-mexico

Lantmäteriet. (n.d.-a). *Avståndsmätning med bärvåg*. Retrieved March 17, 2025, from https://www.lantmateriet.se/sv/geodata/gps-geodesi-och-swepos/GPS-och-satellitpositionering/Metoder-for-GNSS-matning/Avstandsmatning-med-barvag/

Lantmäteriet. (n.d.-b). *Avståndsmätning med kod*. Retrieved March 17, 2025, from https://www.lantmateriet.se/sv/geodata/gps-geodesi-och-swepos/GPS-och-satellitpositionering/Metoder-for-GNSS-matning/Avstandsmatning-med-kod/

Malmstadt, J. C., Elsner, J. B., & Jagger, T. H. (2010). Frequency and intensity of hurricanes within florida's threat zone. In J. B. Elsner, R. E. Hodges, J. C. Malmstadt, & K. N. Scheitlin (Eds.), *Hurricanes and climate change: Volume 2* (pp. 191–203). Springer Netherlands. https://doi.org/10.1007/978-90-481-9510-7_11

MathWorks. (2025). *Wavelet Transforms in MATLAB - MATLAB & Simulink*. https://se.mathworks.com/discovery/wavelet-transforms.html

Met Office. (n.d.). *Tropical cyclone facts*. Retrieved May 10, 2025, from https://www.metoffice.gov.uk/research/weather/tropical-cyclones/facts#How%20do%20TCs%20form

Michener, W. K., Blood, E. R., Bildstein, K. L., Brinson, M. M., & Gardner, L. R. (1997). Climate change, hurricanes and tropical storms, and rising sea level in coastal wetlands. *Ecological Applications*. https://esajournals.onlinelibrary.wiley.com/doi/abs/10.1890/1051-0761%281997%29007%5B0770%3ACCHATS%5D2.0.CO%3B2

NASA GPM Mission. (2024, October 9). *Extremely powerful hurricane milton forms in the gulf of mexico* [Accessed: 2025-03-30]. NASA. https://gpm.nasa.gov/applications/weather/news/extremely-powerful-hurricane-milton-forms-gulf-mexico

National Weather Service. (2025a). *Hurricane HELENE Advisory Archive*. https://www.nhc.noaa.gov/archive/2024/HELENE.shtml?

National Weather Service. (2025b). *Hurricane MILTON Advisory Archive*. https://www.nhc.noaa.gov/archive/2024/MILTON.shtml?

NOAA. (2023a). *Jetstream max: The ionosphere*. https://www.noaa.gov/jetstream/ionosphere-max

NOAA. (2023b). *Tropical cyclone structure*. National Weather Service. https://www.noaa.gov/jetstream/tropical/tropical-cyclone-introduction/tropical-cyclone-structure

NOAA. (2025a). *Post-tropical Cyclone Helene - Band 10 at 36.6°N - 87.4°W*. https://www.star.nesdis.noaa.gov/GOES/floater_band.php?stormid=AL092024&band=10&length=240&dim=0

NOAA. (2025b). *Post-tropical Cyclone Milton - Band 10 at 29.5°N - 76.3°W*. https://www.star.nesdis.noaa.gov/goes/floater_band.php?stormid=AL142024&band=10&length=240&dim=1

NOAA. (2025c). *Tropical cyclone introduction*. NOAA. https://www.noaa.gov/jetstream/tropical/tropical-cyclone-introduction

NovAtel Inc. (2023). *An introduction to GNSS: A primer in using Global Navigation Satellite Systems for positioning and autonomy* (3rd edition). Hexagon.

PO.DAAC. (2024, October). *Data in action: The warm waters in the gulf of mexico helped 'fuel' hurricane helene* [Accessed: 2025-03-28]. NASA Jet Propulsion Laboratory. https://podaac.jpl.nasa.gov/DataAction-2024-10-03-The-warm-waters-in-the-Gulf-of-Mexico-helped-fuel-Hurricane-Helene

PRIDE Lab. (2018). *Contact*. http://pride.whu.edu.cn/newsDetails.shtml?newskindid=20180202104938686UK1IciPqastDp

PRIDE Lab. (2025). *Introduction • PrideLab/PRIDE-PPPAR Wiki • GitHub*. Retrieved February 18, 2025, from https://github.com/PrideLab/PRIDE-PPPAR/wiki/Introduction

Rocken, C., Ware, R., Van Hove, T., & Solheim, F. (1997). Sensing atmospheric water vapor with the global positioning system. *Geophysical Research Letters*, *24*(24), 3221–3224.

Spiridonov, V., & Ćurić, M. (2021). Tropical storms. In *Fundamentals of meteorology* (pp. 275–288). Springer International Publishing. https://doi.org/10.1007/978-3-030-52655-9_18

Teunissen, P. J. G., & Montenbruck, O. (2017). *Springer handbook of Global Navigation Satellite Systems* (1st ed.). Springer. https://doi.org/10.1007/978-3-319-42928-1

Thiem, H. (2024, October 8). *Hurricane milton rapidly intensifies into category 5 hurricane, becoming the gulf's strongest late-season storm on record* [Accessed: 2025-03-27]. NOAA Climate.gov. https://www.climate.gov/news-features/event-tracker/hurricane-milton-rapidly-intensifies-category-5-hurricane-becoming

Thomas, V. (2024, November 7). *Hurricane helene's gravity waves revealed by nasa's awe* [Accessed: 2025-03-25]. NASA. https://science.nasa.gov/centers-and-facilities/goddard/hurricane-helenes-gravity-waves-revealed-by-nasas-awe/

Walsh, K. J., McBride, J. L., Klotzbach, P. J., Balachandran, S., Camargo, S. J., Holland, G., Knutson, T. R., Kossin, J. P., Lee, T.-c., Sobel, A., & Sugi, M. (2016). Tropical cyclones and climate change. *WIREs Climate Change*, *7*(1), 65–89. https://doi.org/https://doi.org/10.1002/wcc.371

Wang, K., Chen, J., Valseth, E., Wells, G., Bettadpur, S., Jones, C. E., & Dawson, C. (2024). Subtle land subsidence elevates future storm surge risks along the gulf coast of the united states [e2024JF007858 2024JF007858]. *Journal of Geophysical Research: Earth Surface*, *129*(9), e2024JF007858. https://doi.org/https://doi.org/10.1029/2024JF007858

Wdowinski, S., Oliver-Cabrera, T., & Fiaschi, S. (2020). Land subsidence contribution to coastal flooding hazard in southeast florida. *Proceedings of the International Association of Hydrological Sciences*, *382*, 207–211. https://doi.org/10.5194/piahs-382-207-2020

World Weather. (2025). *Weather in Sarasota in October 2024 (Florida) - Detailed Weather Forecast for a Month*. https://world-weather.info/forecast/usa/sarasota/october-2024/

A

Zenith Wet Delay Figures

This appendix presents detailed time series of the Zenith Wet Delay (ZWD), wavelet scalogram, and anomaly detection results for the scalogram, measured at different stations during Tropical Storms Milton and Helene. The figures show the complete station datasets used in this study, which were excluded from the main report due to space limitations, but which provide valuable information supporting the certainty of several conclusions made.

Each figure follows the same format, with ZWD data, the corresponding wavelet scalogram, and the anomaly detection results. Red lines indicate when the storm's core entered and exited Florida, while the black lines show the storm's active period. An asterisk (*) displayed after the station name indicates that the corresponding permanent station is affected by significant data faults.

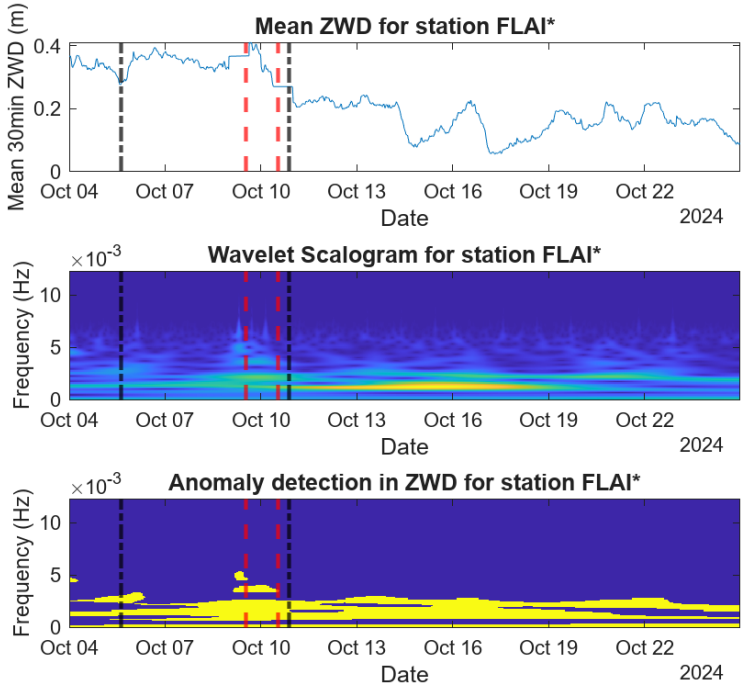

Figure A.1: *ZWD, Wavelet Scalogram, and anomaly detection results for station FLAI during Hurricane Milton.*

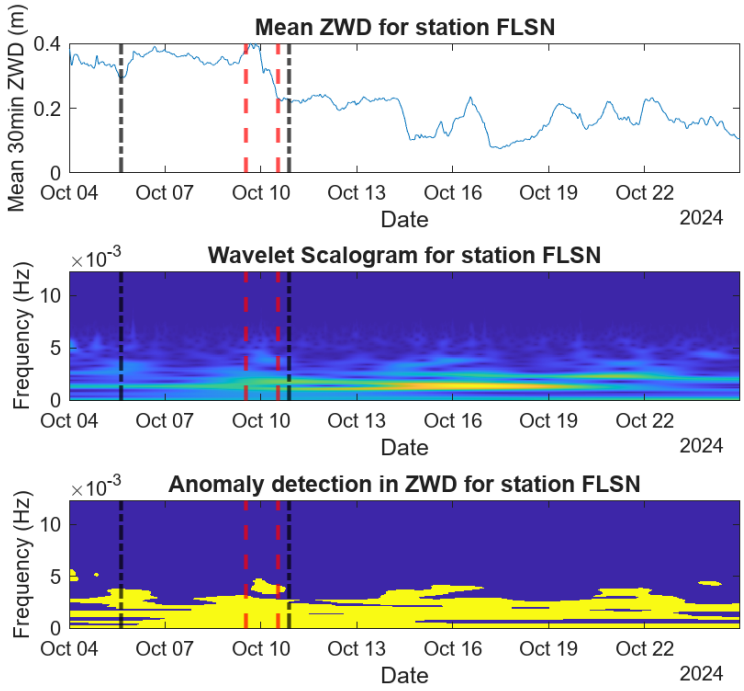

Figure A.2: *ZWD, Wavelet Scalogram, and anomaly detection results for station FLSN during Hurricane Milton.*

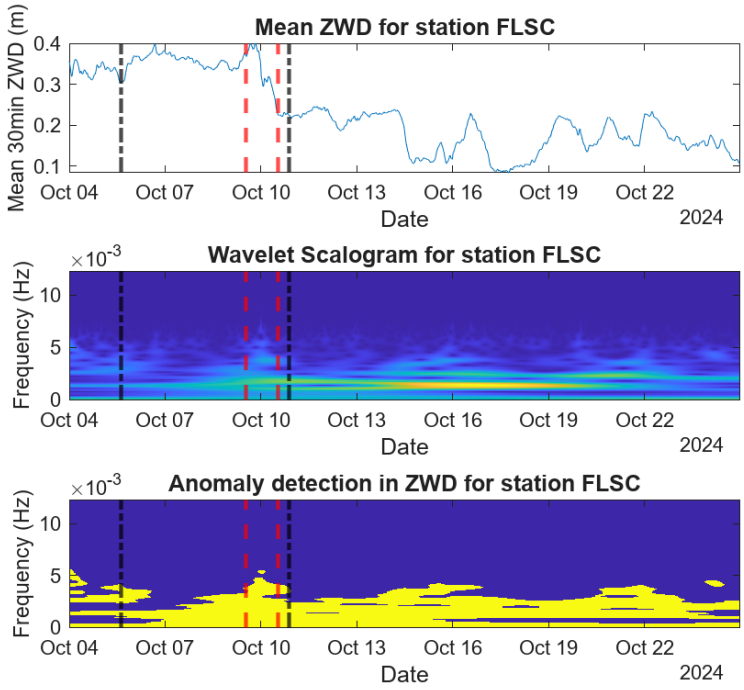

Figure A.3: *ZWD, Wavelet Scalogram, and anomaly detection results for station FLSC during Hurricane Milton.*

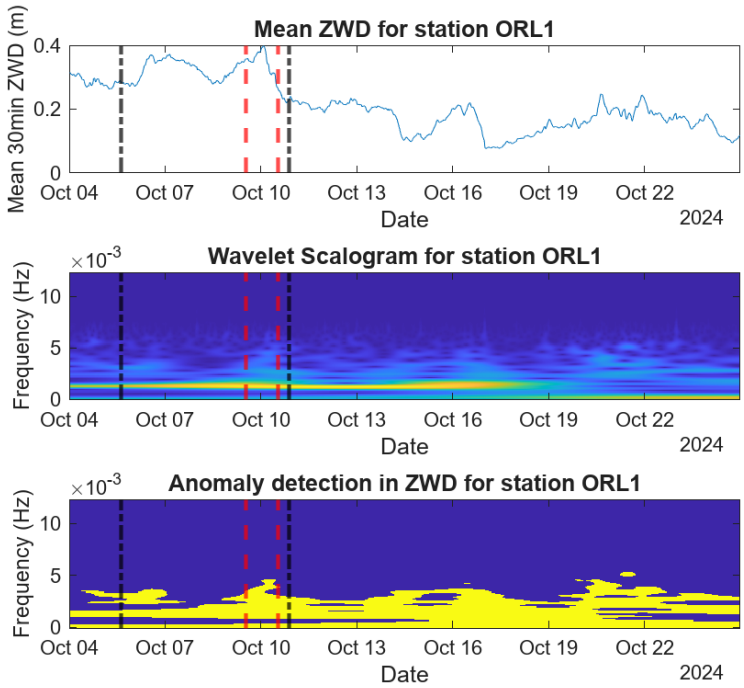

Figure A.4: *ZWD, Wavelet Scalogram, and anomaly detection results for station ORL1 during Hurricane Milton.*

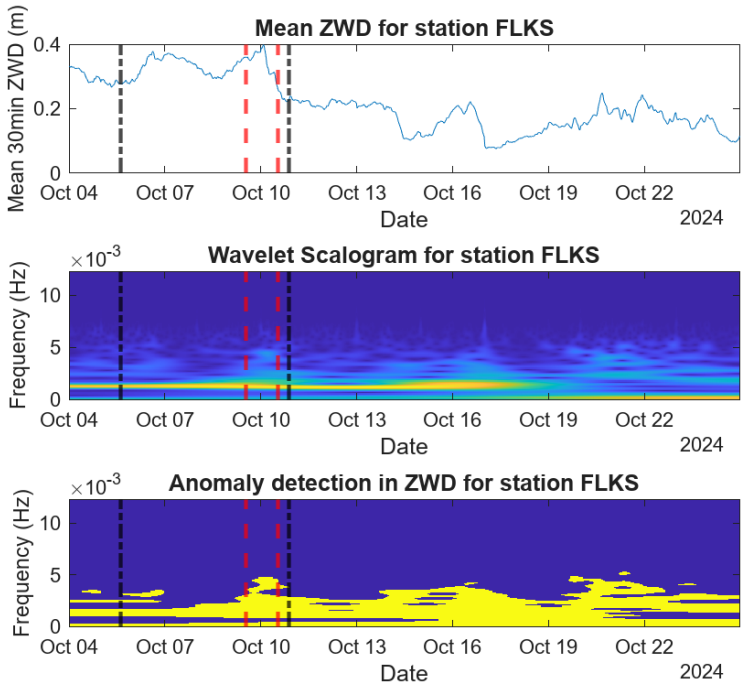

Figure A.5: *ZWD, Wavelet Scalogram, and anomaly detection results for station FLKS during Hurricane Milton.*

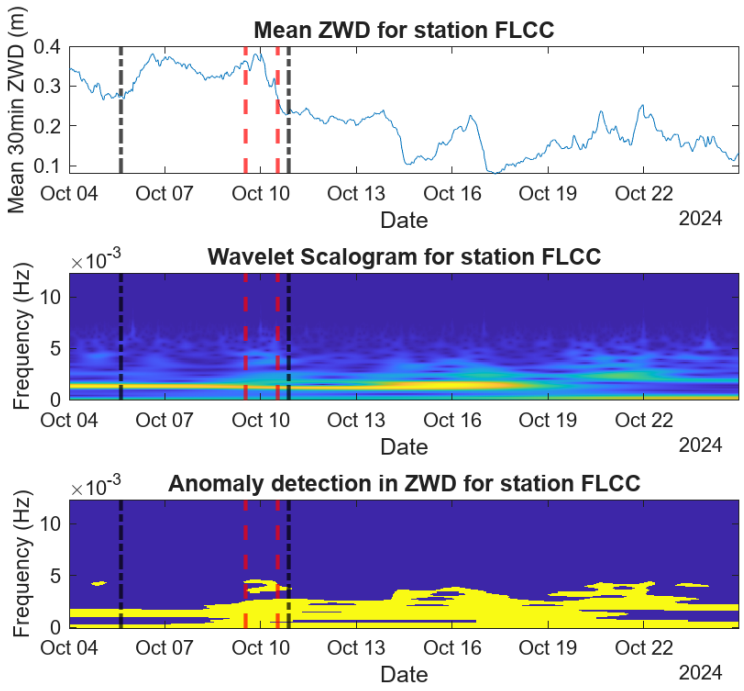

Figure A.6: *ZWD, Wavelet Scalogram, and anomaly detection results for station FLCC during Hurricane Milton.*

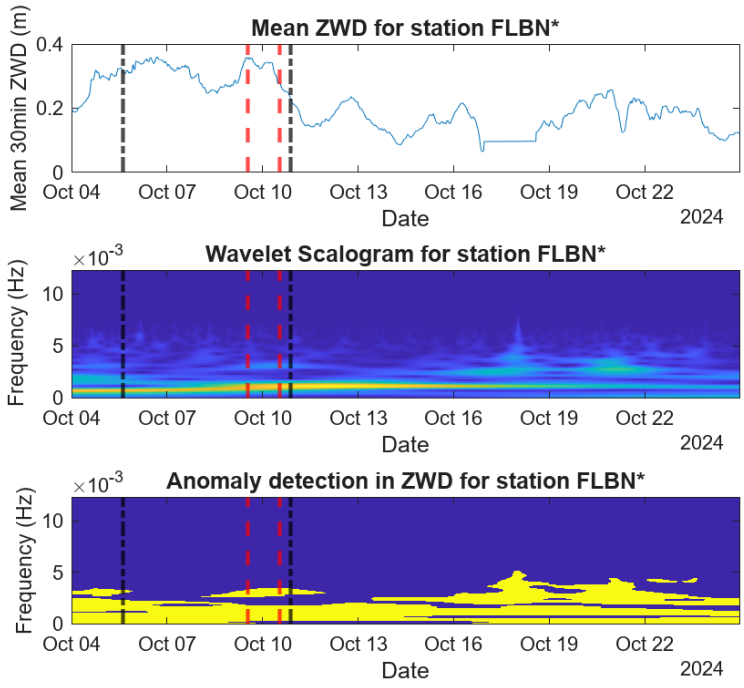

Figure A.7: *ZWD, Wavelet Scalogram, and anomaly detection results for station FLBN during Hurricane Milton.*

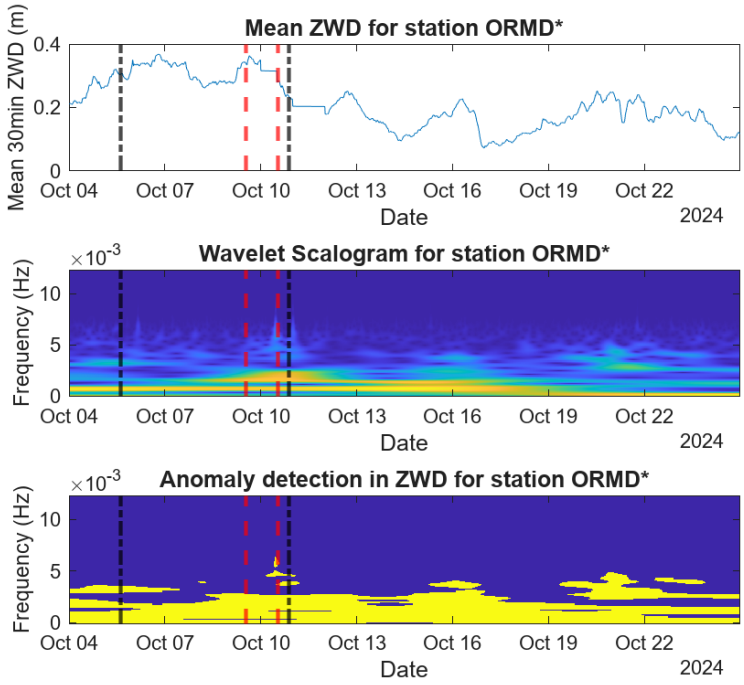

Figure A.8: *ZWD, Wavelet Scalogram, and anomaly detection results for station ORMD during Hurricane Milton.*

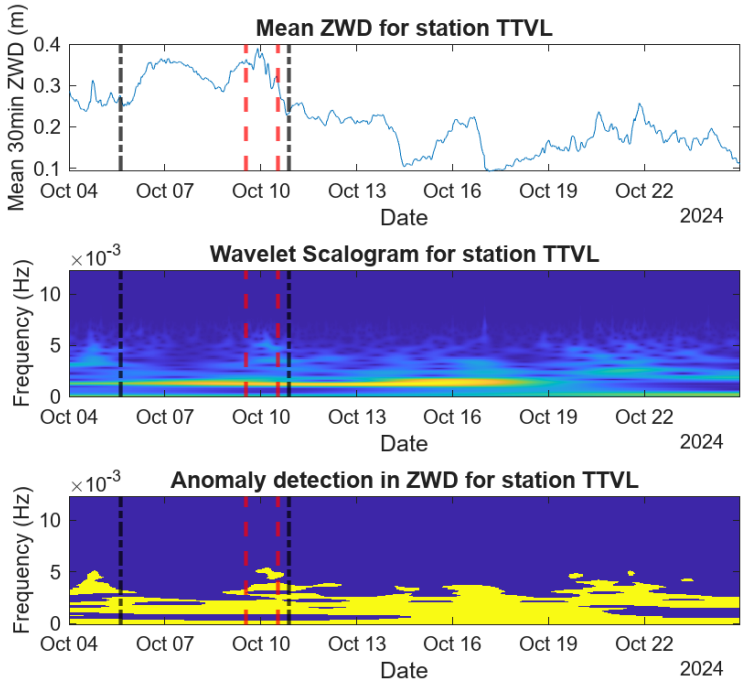

Figure A.9: *ZWD, Wavelet Scalogram, and anomaly detection results for station TTVL during Hurricane Milton.*

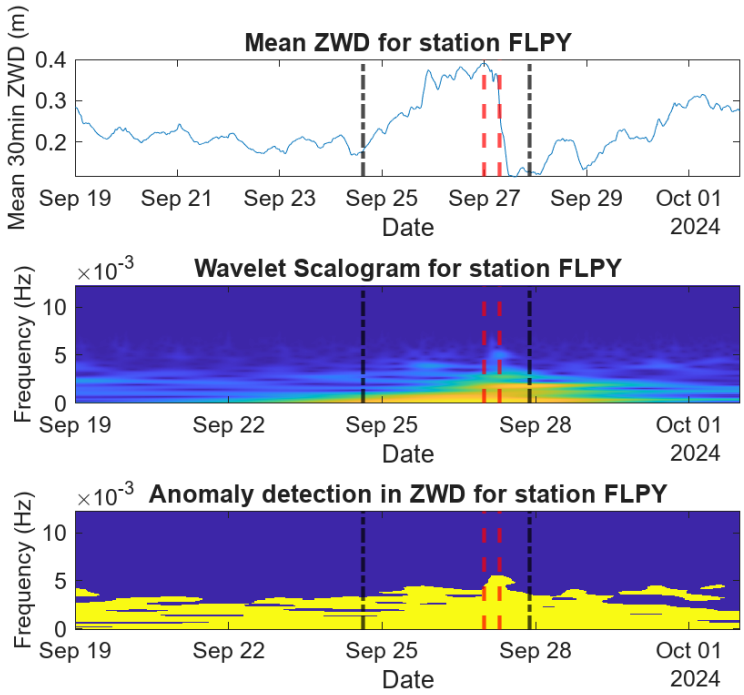

Figure A.10: *ZWD, Wavelet Scalogram, and anomaly detection results for station FLPY during Hurricane Helene.*

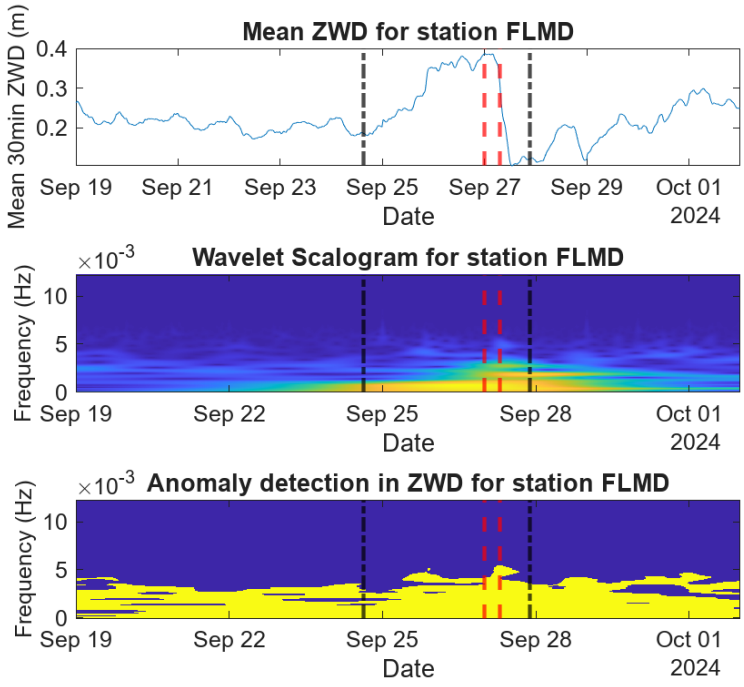

Figure A.11: *ZWD, Wavelet Scalogram, and anomaly detection results for station FLMD during Hurricane Helene.*

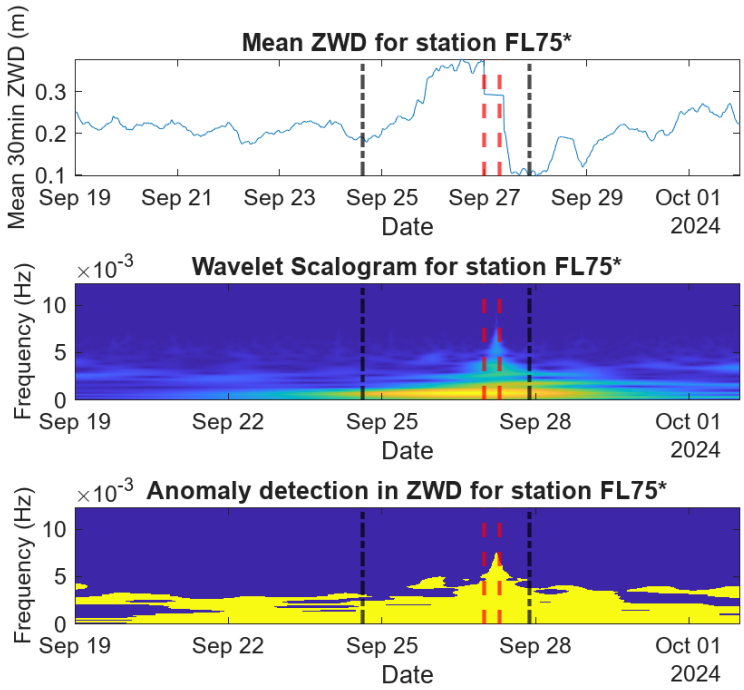

Figure A.12: *ZWD, Wavelet Scalogram, and anomaly detection results for station FL75 during Hurricane Helene.*

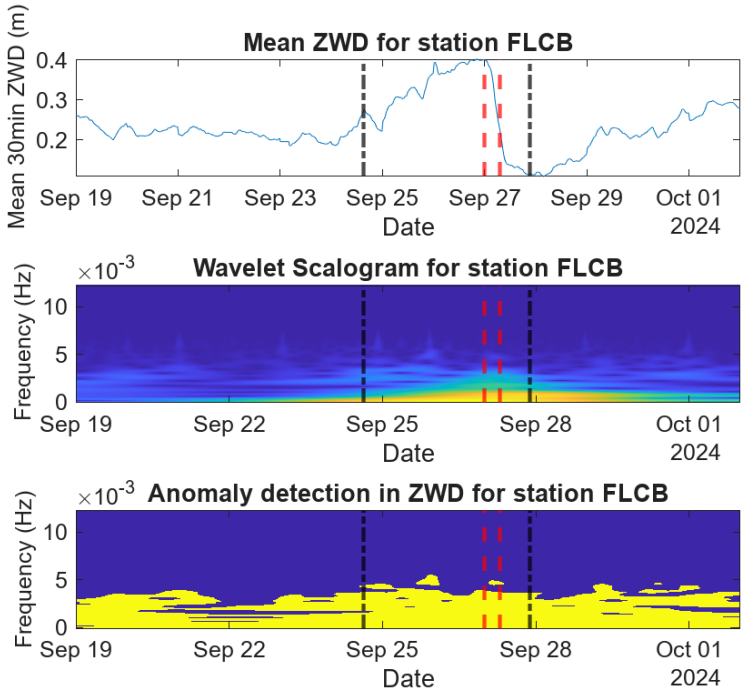

Figure A.13: *ZWD, Wavelet Scalogram, and anomaly detection results for station FLCB during Hurricane Helene.*

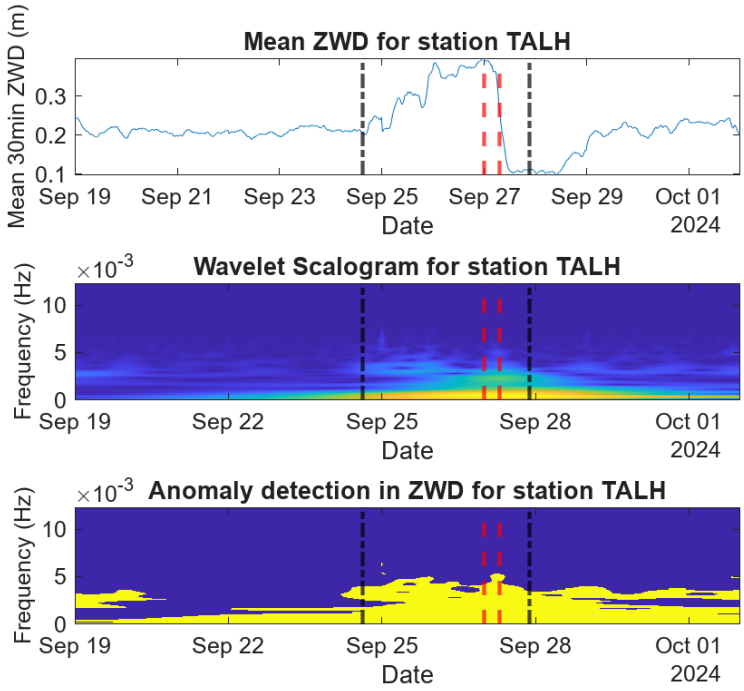

Figure A.14: *ZWD, Wavelet Scalogram, and anomaly detection results for station TALH during Hurricane Helene.*

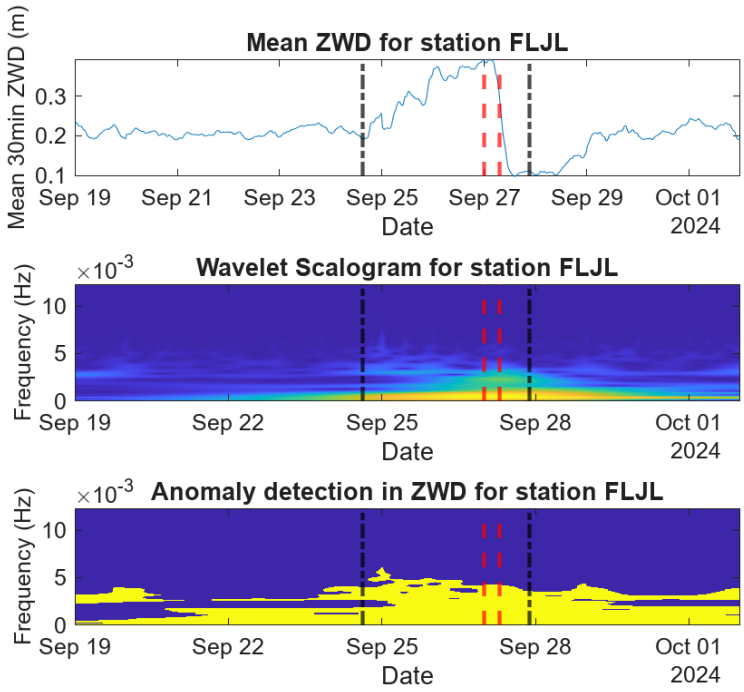

Figure A.15: *ZWD, Wavelet Scalogram, and anomaly detection results for station FLJL during Hurricane Helene.*

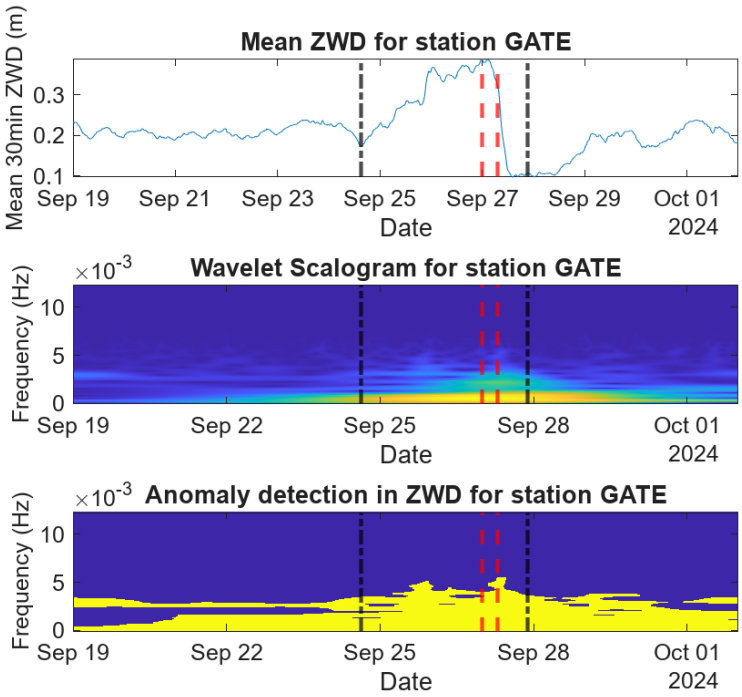

Figure A.16: *ZWD, Wavelet Scalogram, and anomaly detection results for station GATE during Hurricane Helene.*

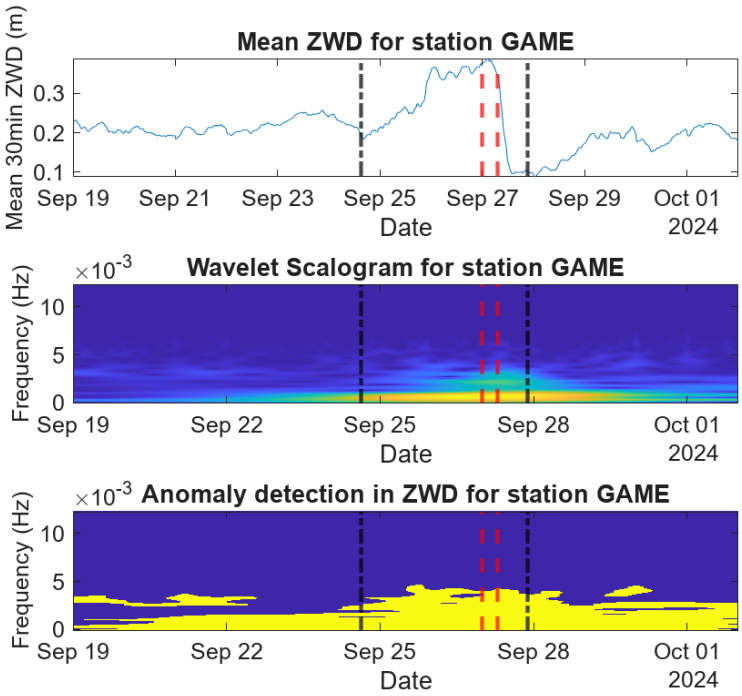

Figure A.17: *ZWD, Wavelet Scalogram, and anomaly detection results for station GAME during Hurricane Helene.*

B

Land subsidence Figures

This appendix presents detailed time series of the land subsidence based on height data relative to the median, the corresponding wavelet scalogram, and the results from anomaly detection applied to the scalogram, measured at different stations during Tropical Storms Milton and Helene. The figures show the complete station datasets used in this study, which were excluded from the main report due to space limitations but provide valuable information supporting the certainty of several conclusions made. The final figures present water level data and height data from the nearest permanent GNSS station, each shown relative to its respective median value.

Each figure follows the same format, with height data, the corresponding wavelet scalogram, and the anomaly detection results. Red lines indicate when the storm's core entered and exited Florida, while the black lines show the storm's active period. An asterisk (*) displayed after the station name indicates that the corresponding permanent station is affected by significant data faults.

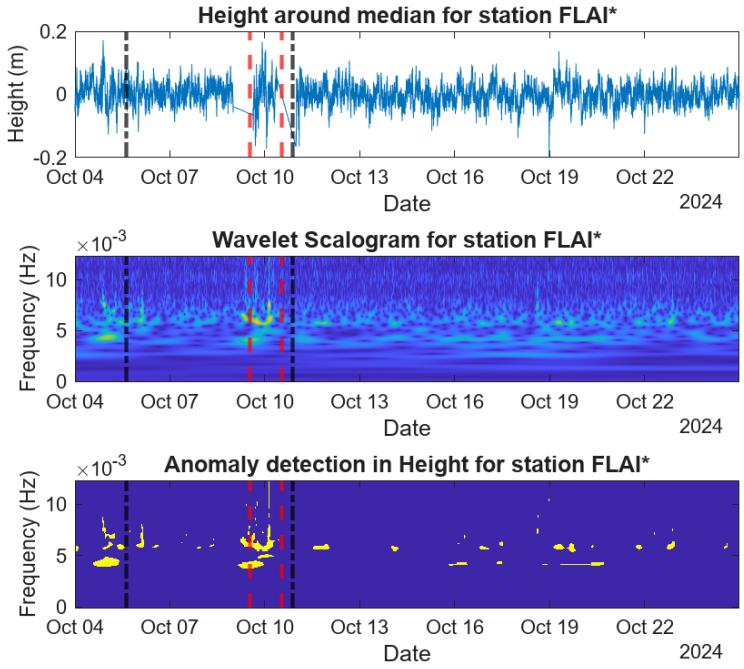

Figure B.1: *Height relative to the median, Wavelet Scalogram, and anomaly detection results for station FLAI during Hurricane Milton.*

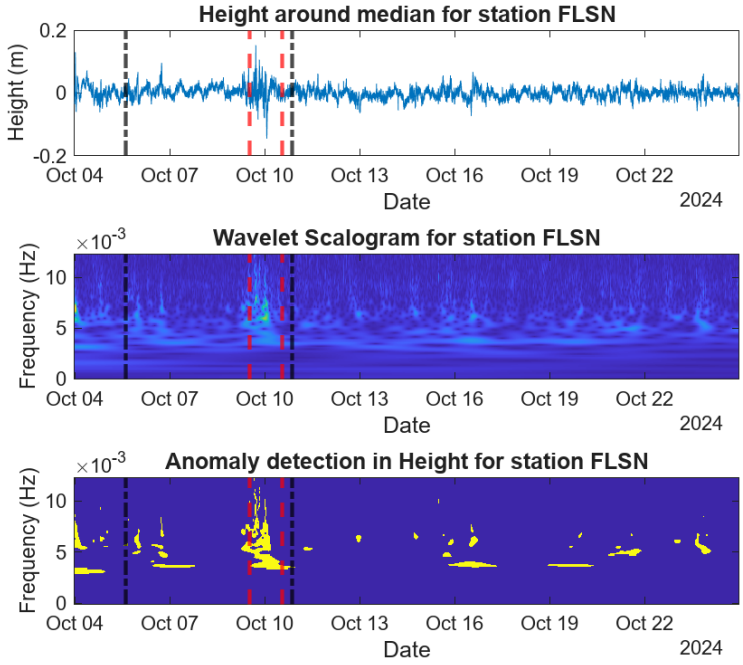

Figure B.2: *Height relative to the median, Wavelet Scalogram, and anomaly detection results for station FLSN during Hurricane Milton.*

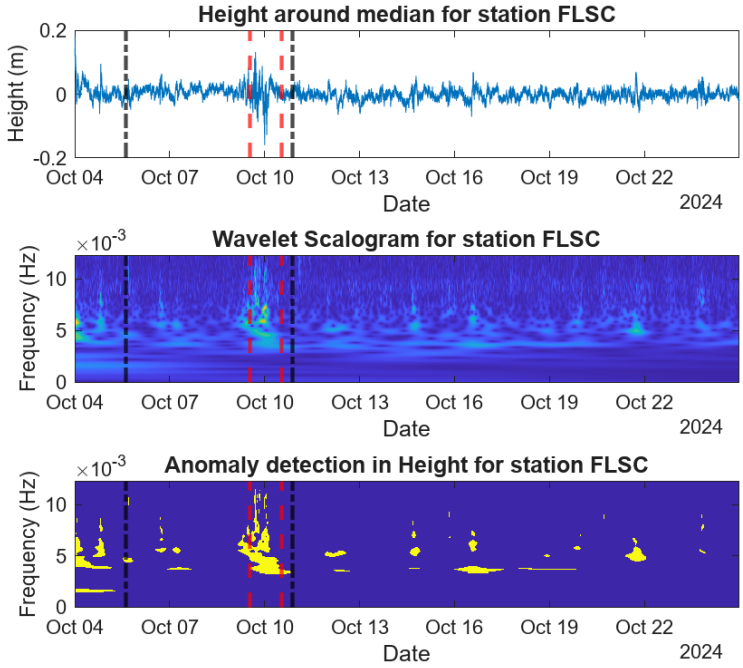

Figure B.3: *Height relative to the median, Wavelet Scalogram, and anomaly detection results for station FLSC during Hurricane Milton.*

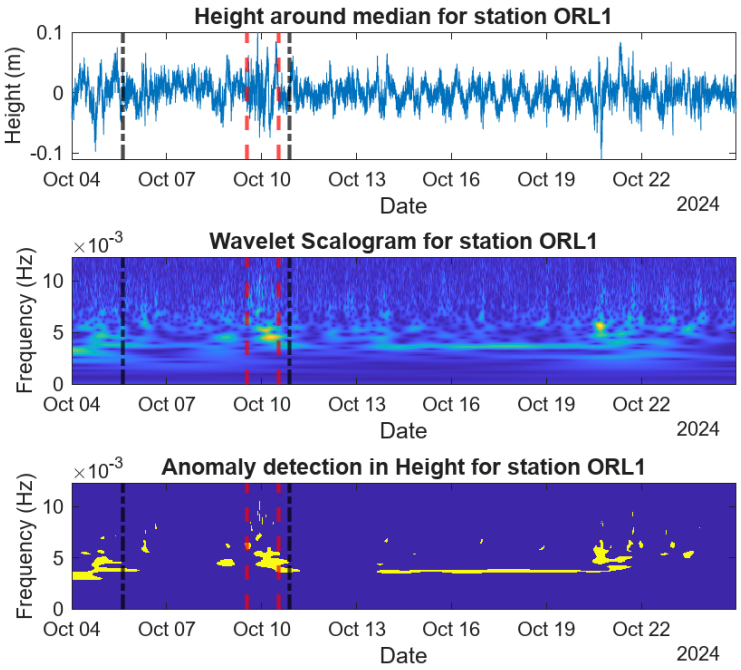

Figure B.4: *Height relative to the median, Wavelet Scalogram, and anomaly detection results for station ORL1 during Hurricane Milton.*

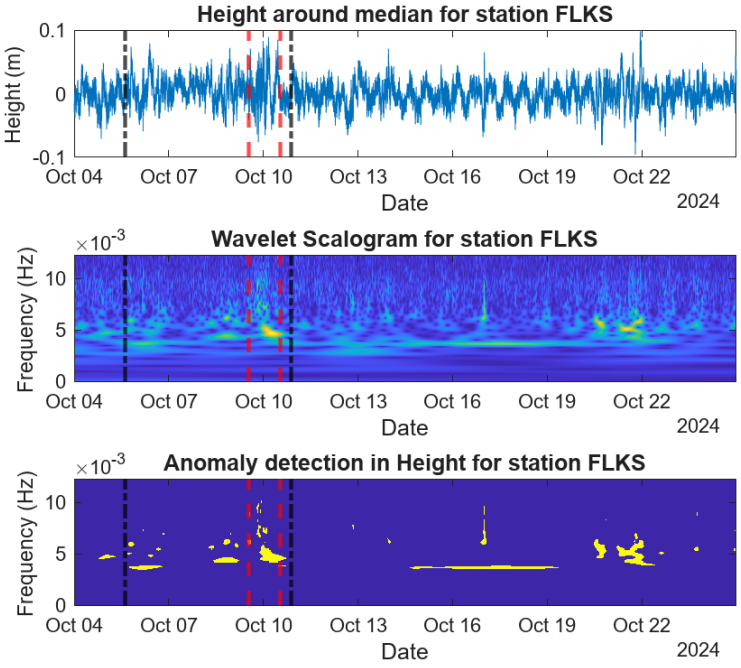

Figure B.5: *Height relative to the median, Wavelet Scalogram, and anomaly detection results for station FLKS during Hurricane Milton.*

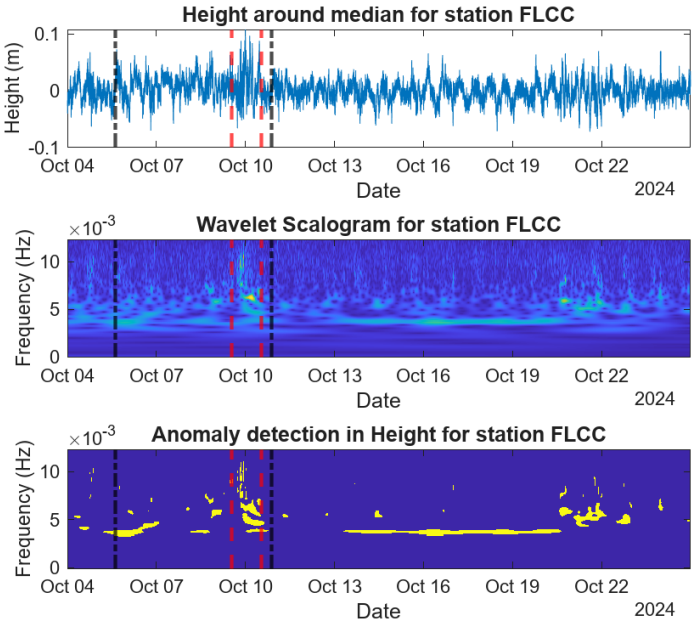

Figure B.6: *Height relative to the median, Wavelet Scalogram, and anomaly detection results for station FLCC during Hurricane Milton.*

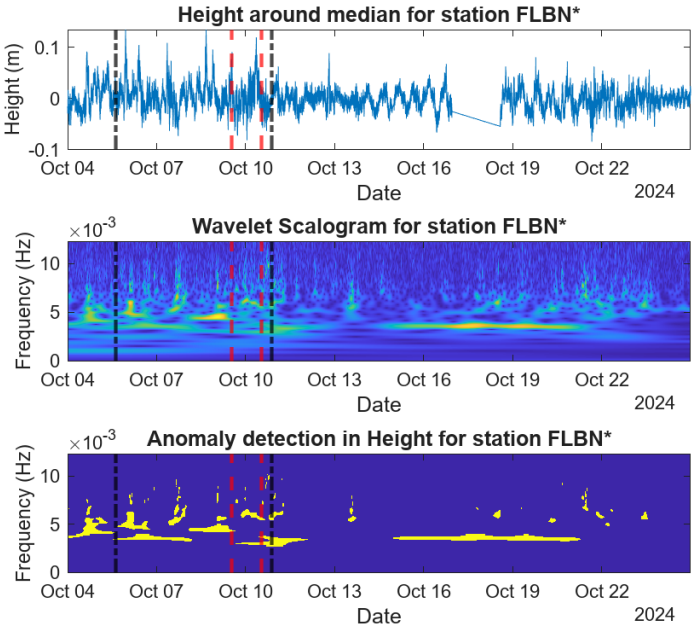

Figure B.7: *Height relative to the median, Wavelet Scalogram, and anomaly detection results for station FLBN during Hurricane Milton.*

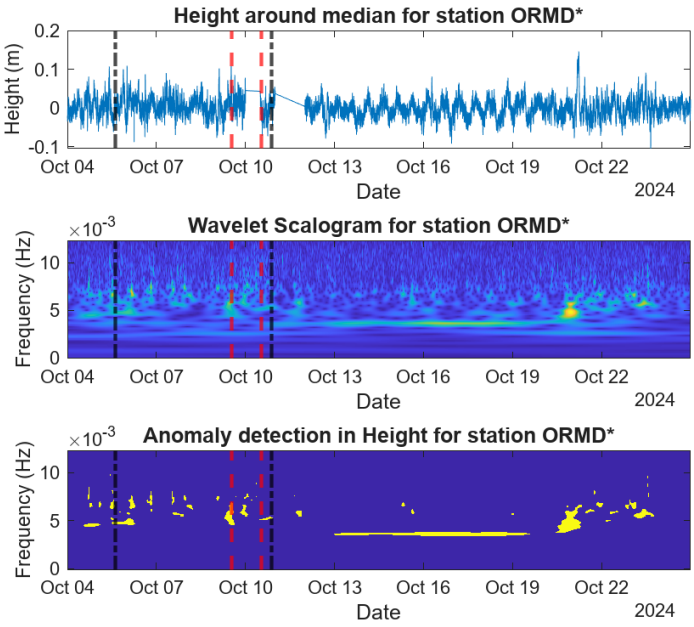

Figure B.8: *Height relative to the median, Wavelet Scalogram, and anomaly detection results for station ORMD during Hurricane Milton.*

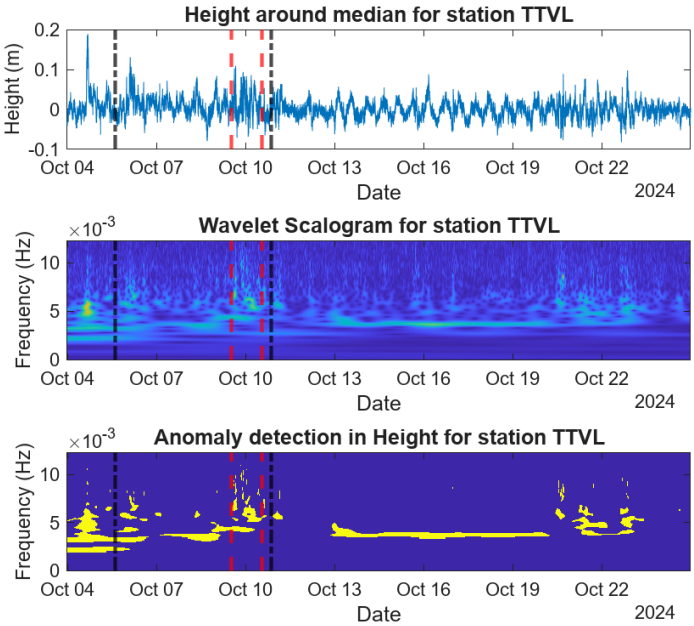

Figure B.9: *Height relative to the median, Wavelet Scalogram, and anomaly detection results for station TTVL during Hurricane Milton.*

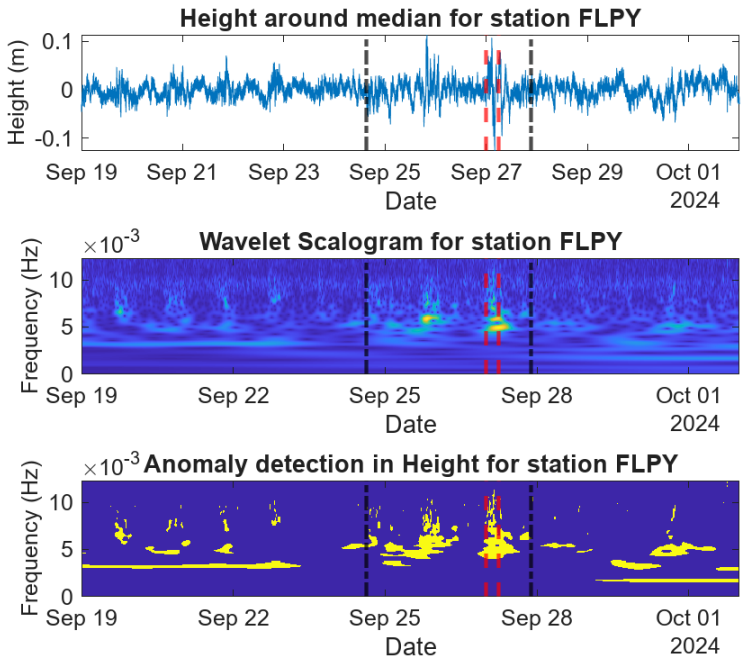

Figure B.10: *Height relative to the median, Wavelet Scalogram, and anomaly detection results for station FLPY during Hurricane Helene.*

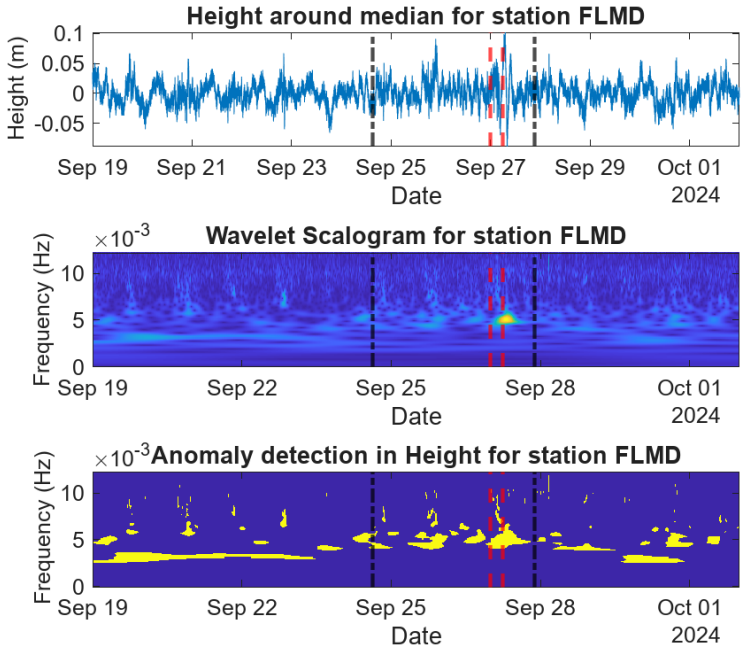

Figure B.11: *Height relative to the median, Wavelet Scalogram, and anomaly detection results for station FLMD during Hurricane Helene.*

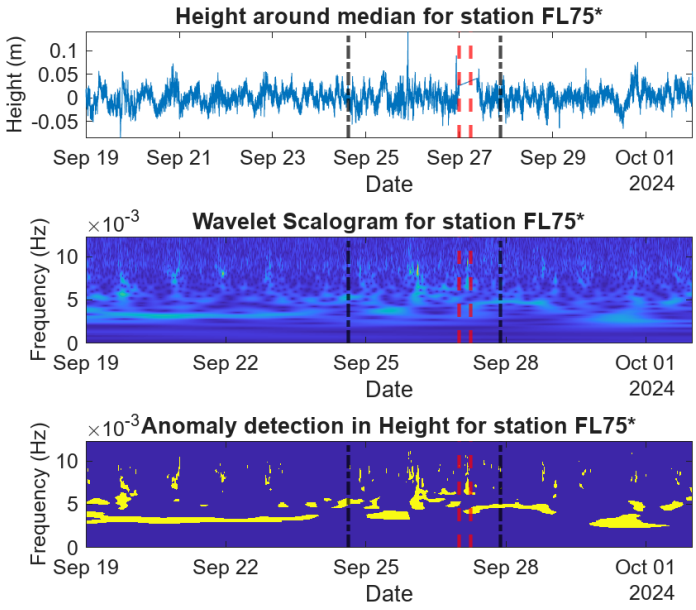

Figure B.12: *Height relative to the median, Wavelet Scalogram, and anomaly detection results for station FL75 during Hurricane Helene.*

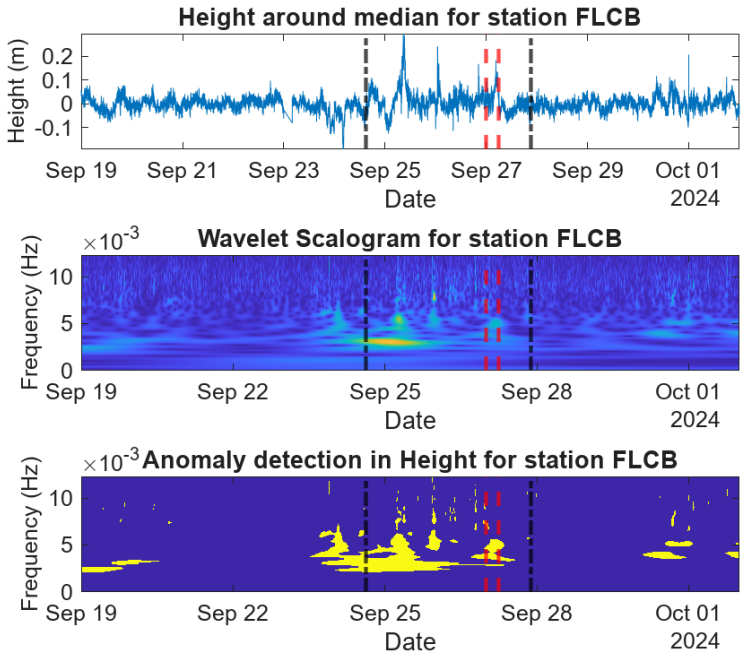

Figure B.13: *Height relative to the median, Wavelet Scalogram, and anomaly detection results for station FLCB during Hurricane Helene.*

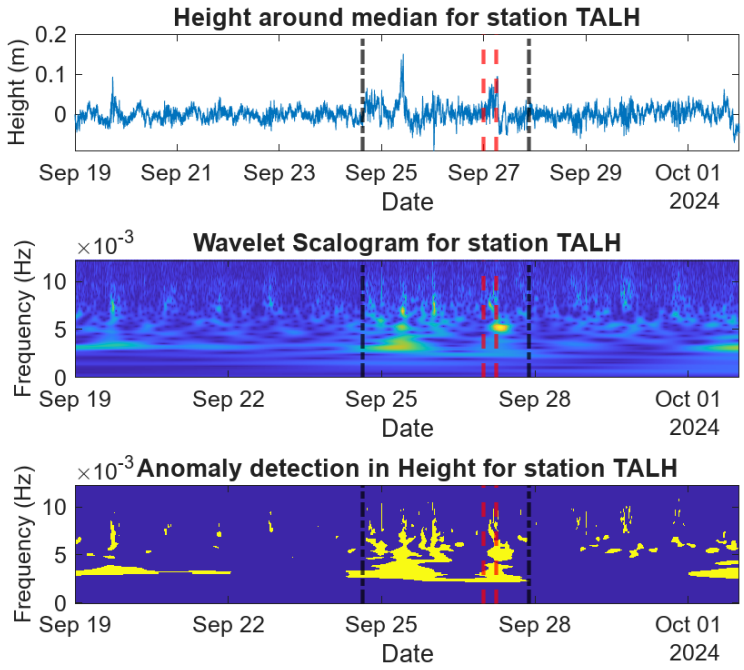

Figure B.14: *Height relative to the median, Wavelet Scalogram, and anomaly detection results for station TALH during Hurricane Helene.*

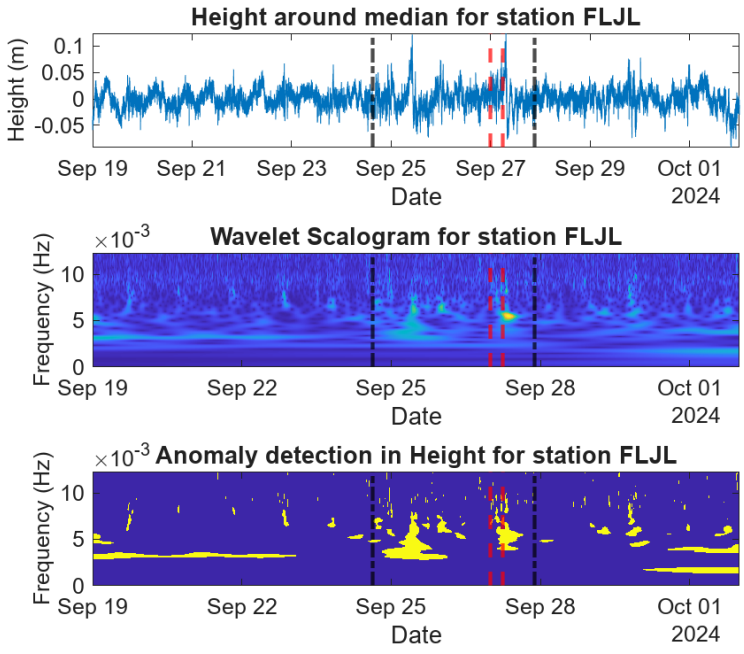

Figure B.15: *Height relative to the median, Wavelet Scalogram, and anomaly detection results for station FLJL during Hurricane Helene.*

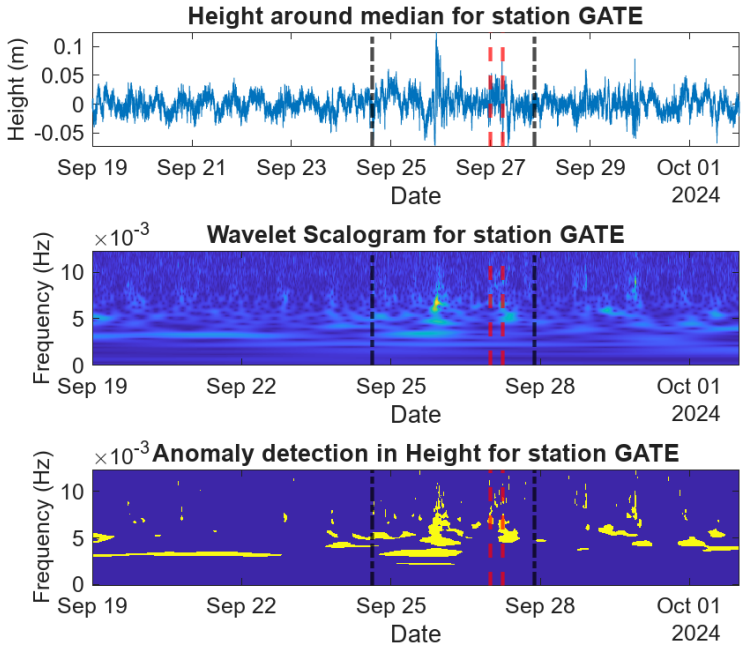

Figure B.16: *Height relative to the median, Wavelet Scalogram, and anomaly detection results for station GATE during Hurricane Helene.*

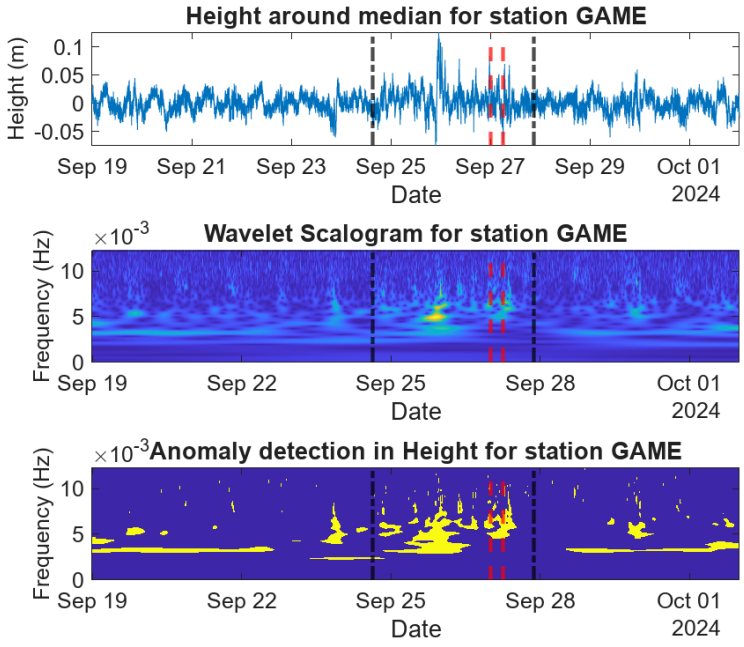

Figure B.17: *Height relative to the median, Wavelet Scalogram, and anomaly detection results for station GAME during Hurricane Helene.*

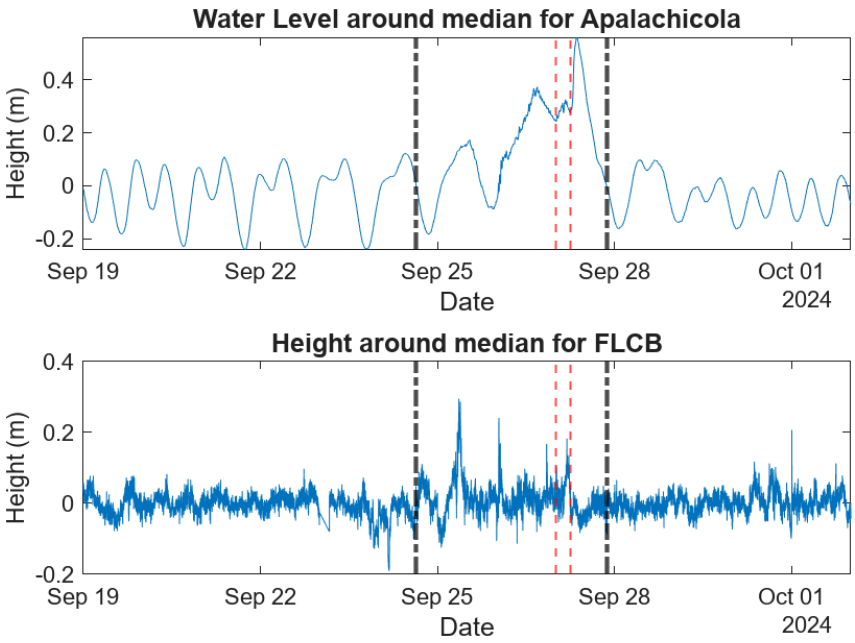

Figure B.18: *Water Level relative to the median at Apalachicola and the Height relative to the median at FLCB during Hurricane Helene.*

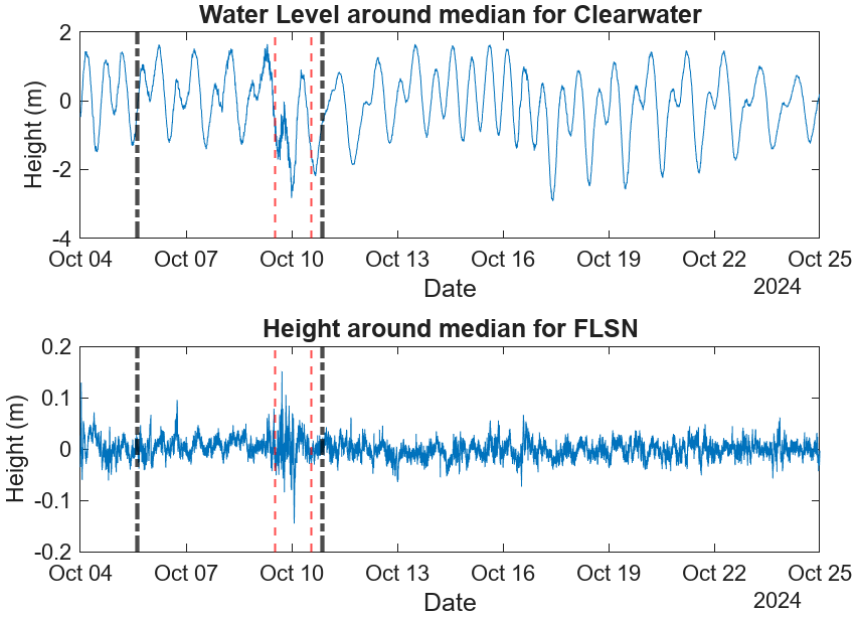

Figure B.19: *Water Level relative to the median at Clearwater Beach and the Height relative to the median at FLSN during Hurricane Milton.*

C

Matlab Scripts

C.1 Zenith Wet Delay for Milton

```
clc
clear
close all

% Show figures on/off
set(0, 'DefaultFigureVisible', 'on');

% Load all data & add position and name
% FLAI 4-24/10
GNSS_data{1} = readtable('Data\FLAI_2024278_298.dat');
GNSS_data{1}{:,10} = 'FLAI*';
GNSS_data{1}{:,11} = 27.449731;      % Latitude
GNSS_data{1}{:,12} = -82.690230;     % Longitude
% FLSN 4-24/10
GNSS_data{2} = readtable('Data\FLSN_2024278_298.dat');
GNSS_data{2}{:,10} = 'FLSN';
GNSS_data{2}{:,11} = 27.333611;      % Latitude
GNSS_data{2}{:,12} = -82.438323;     % Longitude
% FLSC 4-24/10
GNSS_data{3} = readtable('Data\FLSC_2024278_298.dat');
GNSS_data{3}{:,10} = 'FLSC';
GNSS_data{3}{:,11} = 27.217272;      % Latitude
GNSS_data{3}{:,12} = -82.404745;     % Longitude
% ORL1 4-24/10
GNSS_data{4} = readtable('Data\ORL1_2024278_298.dat');
GNSS_data{4}{:,10} = 'ORL1';
GNSS_data{4}{:,11} = 28.434562;     % Latitude
GNSS_data{4}{:,12} = -81.382467;    % Longitude
% FLKS 4-24/10
GNSS_data{5} = readtable('Data\FLKS_2024278_298.dat');
GNSS_data{5}{:,10} = 'FLKS';
GNSS_data{5}{:,11} = 28.295611;     % Latitude
GNSS_data{5}{:,12} = -81.436352;    % Longitude
% FLCC 4-24/10
```

```
GNSS_data{6} = readtable('Data\FLCC_2024278_298.dat');
GNSS_data{6}{:,10} = 'FLCC';
GNSS_data{6}{:,11} = 28.094482;     % Latitude
GNSS_data{6}{:,12} = -81.274206;    % Longitude
% FLBN 4-24/10
GNSS_data{7} = readtable('Data\FLBN_2024278_298.dat');
GNSS_data{7}{:,10} = 'FLBN*';
GNSS_data{7}{:,11} = 29.594142;     % Latitude
GNSS_data{7}{:,12} = -81.287096;    % Longitude
% ORMD 4-24/10
GNSS_data{8} = readtable('Data\ORMD_2024278_298.dat');
GNSS_data{8}{:,10} = 'ORMD*';
GNSS_data{8}{:,11} = 29.298186;     % Latitude
GNSS_data{8}{:,12} = -81.108892;    % Longitude
% TTVL 4-24/10
GNSS_data{9} = readtable('Data\TTVL_2024278_298.dat');
GNSS_data{9}{:,10} = 'TTVL';
GNSS_data{9}{:,11} = 28.505709;     % Latitude
GNSS_data{9}{:,12} = -80.803381;    % Longitude

% FLSN STO 4-24/10
GNSS_data{10} = readtable('Data\FLSN_STO_2024278_298.dat'
   );
GNSS_data{10}{:,10} = 'FLSN (STO)';

% FLSN HTC 4-24/10
GNSS_data_htc{1} = readtable('Data\FLSN_HTC_2024278_298.
   dat');


% Initialize for faster compile
numTables = length(GNSS_data);
yData_ZWD_tot = cell(1, numTables);

numTables_htc = length(GNSS_data_htc);

mean_move = cell(1, numTables);

wt = cell(1, numTables);
time = cell(1, numTables);
anomaly_mask = cell(1, numTables);

yData_htc_E_W = cell(1, numTables_htc);
yData_htc_N_S = cell(1, numTables_htc);
yData_htc_tot = cell(1, numTables_htc);
time_htc = cell(1, numTables_htc);
```

```
filtered1 = cell(numTables-1, numTables-1);
filtered2 = cell(numTables-1, numTables-1);

lags = cell(numTables-1, numTables-1);
c = cell(numTables-1, numTables-1);
lagDiff_all = cell(numTables-1, numTables-1);
distance_stations_all = cell(numTables-1, numTables-1);


speed_kmh_all = cell(numTables-1, numTables-1);
speed_ms_all = cell(numTables-1, numTables-1);

% Sampling frequency (Hz), since 30s sampling
fs = 1/30;

% Extract data
for i = 1:numTables
    % ZWD total is the ini + cor
    yData_ZWD_tot{i} = GNSS_data{i}{:,8} + GNSS_data{i
       }{:,9};

    % Set all date columns into one (for x-axis plot)
    time{i} = datetime(GNSS_data{i}{:,1}, GNSS_data{i
       }{:,2}, GNSS_data{i}{:,3}, GNSS_data{i}{:,4},
       GNSS_data{i}{:,5}, GNSS_data{i}{:,6});

    % Makes a mean value from the closest 60 values, 30
       before and 29 after
    mean_move{i} = movmean(yData_ZWD_tot{i}, 60);

    % Wavelet-transform with Morlet ('amor')
    [wt{i}, f] = cwt(mean_move{i}, 'amor', fs);

    % Threshold based median, where median is decided
       under "good" weather
    threshold = 12 * median(abs(wt{i}(:)));

    % Only saves the data above threshold
    anomaly_mask{i} = abs(wt{i}) > threshold;
end

% Extract the data for HTC
for j = 1:numTables_htc
    % HTC E-W is the HTGS-ini + cor
```

```
    yData_htc_E_W{j} = GNSS_data_htc{j}{:,15} +
       GNSS_data_htc{j}{:,16};

    % HTC N-S is the HTGC-ini + cor
    yData_htc_N_S{j} = GNSS_data_htc{j}{:,13} +
       GNSS_data_htc{j}{:,14};

    % HTC squared tot.
    yData_htc_tot{j} = sqrt(yData_htc_E_W{j}.^2 +
       yData_htc_N_S{j}.^2);

    % Set all date columns into one (for x-axis plot)
    time_htc{j} = datetime(GNSS_data_htc{j}{:,1},
       GNSS_data_htc{j}{:,2}, GNSS_data_htc{j}{:,3},
       GNSS_data_htc{j}{:,4}, GNSS_data_htc{j}{:,5},
       GNSS_data_htc{j}{:,6});
end

% Calculate the mean difference between PWC and STO (%)
diff_sto_perc = abs((mean_move{10} - mean_move{2}) ./
   mean_move{2}) * 100;
mean_diff_sto_perc = mean(diff_sto_perc);
mean_diff_max_sto_perc =  max(diff_sto_perc);

diff = abs((mean_move{10}) - (mean_move{2}));
diff_mean = mean(diff);
diff_max = max(diff);

% Calculate student t for 99 % conf.interval

% Standard Error
SEM = std(mean_move{10})/sqrt(length(mean_move{10}));
% T-Score
ts = tinv([0.005  0.995],length(mean_move{10})-1);
% Confidence Intervals
CI = mean(mean_move{10}) + ts*SEM;

% Standard Error
SEM2 = std(mean_move{2})/sqrt(length(mean_move{2}));
% T-Score
ts2 = tinv([0.005  0.995],length(mean_move{2})-1);
% Confidence Intervals
CI2 = mean(mean_move{2}) + ts2*SEM2;

CI_strength = abs(diff_mean / abs(CI(1) - CI(2)));   %
   Check how small/big CI is compared to diff_mean
```

```
% Calculate the normal distribution (Z), 2.576 for 99 %
   conf.interval
z1 = mean(mean_move{2}) + (2.576 * std(mean_move{2} /
   sqrt(length(mean_move{2}))));
z2 = mean(mean_move{2}) - (2.576 * std(mean_move{2} /
   sqrt(length(mean_move{2}))));

z1_2 = mean(mean_move{10}) + (2.576 * std(mean_move{10} /
    sqrt(length(mean_move{10}))));
z2_2 = mean(mean_move{10}) - (2.576 * std(mean_move{10} /
    sqrt(length(mean_move{10}))));

% Calculate amount of data above CI
above_CI = diff(diff > (abs(z1 - z2))/2);

% Print results in console
disp(['Mean difference between ', GNSS_data{10}{1,10}, '
   Mean and ', GNSS_data{2}{1,10}, ' Mean : ', num2str(
   diff_mean)]);
disp(['Mean difference between ', GNSS_data{10}{1,10}, '
   Mean and ', GNSS_data{2}{1,10}, ' Mean : ', num2str(
   mean_diff_sto_perc), ' %']);
disp(' ');
disp(['Max difference between ', GNSS_data{10}{1,10}, '
   Mean and ', GNSS_data{2}{1,10}, ' Mean : ', num2str(
   diff_max)]);
disp(['Max difference between ', GNSS_data{10}{1,10}, '
   Mean and ', GNSS_data{2}{1,10}, ' Mean : ', num2str(
   mean_diff_max_sto_perc), ' %']);
disp(' ');
disp(['99 % Confidence Interval (student t) for ',
   GNSS_data{10}{1,10}, ' Mean : ', num2str(CI(1)), ' and
    ', num2str(CI(2)), ' = ', num2str(abs(CI(1)-CI(2))),
   ' or +- ', num2str(abs(CI(1)-CI(2))/2)]);
disp(['99 % Confidence Interval (student t) for ',
   GNSS_data{2}{1,10}, ' Mean : ', num2str(CI2(1)), ' and
    ', num2str(CI2(2)), ' = ', num2str(abs(CI2(1)-CI2(2))
   ), ' or +- ', num2str(abs(CI2(1)-CI2(2))/2)]);
disp(' ');
disp(['99 % Confidence Interval (Z) for ', GNSS_data
   {10}{1,10}, ' Mean : ', num2str(z1_2), ' and ',
   num2str(z2_2), ' = ', num2str(abs(z1_2 - z2_2)), ' or
   +- ', num2str(abs(z1_2 - z2_2)/2)]);
disp(['99 % Confidence Interval (Z) for ', GNSS_data
   {2}{1,10}, ' Mean : ', num2str(z1), ' and ', num2str(
```

```
    z2), ' = ', num2str(abs(z1 - z2)), ' or +- ', num2str(
    abs(z1 - z2)/2)]);
disp(' ');
disp(['Amount of data above CI : ', num2str(length(
    above_CI)), ' or ', num2str(length(above_CI)/length(
    mean_move{2})*100), ' %']);
disp(' ');
disp(' ');

% Calculate the time delay & print to console
% The numTables-1 comes from that the last one is the one
    used for STO test
for i = 1:numTables-1
    % Loop to only cover each station pair once
    for j = i+1:numTables-1
        % Detrend (which removes the best straight-fit
            line)
        [c{i, j}, lags{i, j}] = xcorr(detrend(mean_move{i
            }), detrend(mean_move{j}));
        [~, maxIndex] = max(c{i, j});
        lagDiff = lags{i, j}(maxIndex);
        lagDiff_all{i, j} = lagDiff;
        disp(['Time Delay between stations ', GNSS_data{i
            }{1,10}, ' and ', GNSS_data{j}{1,10}, ' : ',
            num2str(lagDiff/2), ' minutes']);

        % Distance between stations
        [dist, az] = distance(GNSS_data{i}{1,11},
            GNSS_data{i}{1,12}, GNSS_data{j}{1,11},
            GNSS_data{j}{1,12});
        distance_stations = deg2km(dist, 'earth');
        distance_stations_all{i ,j} = distance_stations;
        disp(['Distance between stations ', GNSS_data{i
            }{1,10}, ' and ', GNSS_data{j}{1,10}, ' : ',
            num2str(distance_stations), ' km']);

        % Speed
        speed_kmh_all{i, j} = distance_stations / (
            lagDiff / 120);
        speed_ms_all{i, j} = (distance_stations * 1000) /
            (lagDiff * 30);
        disp(['Speed between stations ', GNSS_data{i
            }{1,10}, ' and ', GNSS_data{j}{1,10}, ' : ',
            num2str(speed_ms_all{i, j}), ' m/s or ',
            num2str(speed_kmh_all{i, j}), ' km/h']);
```

```
        disp(' ');
    end
end


% Loop over all stations and plot CWT, threshold and org.
    data
for i = 1:length(mean_move)
    figure;
    set(gcf, 'Units', 'centimeters', 'Position', [15, 8,
       16, 14])
    hold on;

    % Plot time series mean
    subplot(3,1,1)
    axis xy;
    plot(time{i}, mean_move{i})
    xlabel('Date');
    ylabel('Mean 30min ZWD (m)');
    title(['Mean ZWD for station ' GNSS_data{i}{1,10}]);
    xlim([time{i}(1), time{i}(length(time{i}))]);
    xline(datetime(2024,10,09,13,00,00), '--red', '
       LineWidth', 2);
    xline(datetime(2024,10,10,13,10,00), '--red', '
       LineWidth', 2);
    xline(datetime(2024,10,05,15,00,00), '-.black', '
       LineWidth', 2);
    xline(datetime(2024,10,10,21,00,00), '-.black', '
       LineWidth', 2);

    % Plot scalogram
    subplot(3,1,2)
    imagesc(time{i}, f, abs(wt{i}));
    axis xy;
    xlabel('Date');
    ylabel('Frequency (Hz)');
    title(['Wavelet Scalogram for station ' GNSS_data{i
       }{1,10}]);
    xline(datetime(2024,10,09,13,00,00), '--red', '
       LineWidth', 2);
    xline(datetime(2024,10,10,13,10,00), '--red', '
       LineWidth', 2);
    xline(datetime(2024,10,05,15,00,00), '-.black', '
       LineWidth', 2);
    xline(datetime(2024,10,10,21,00,00), '-.black', '
       LineWidth', 2);
```

```
    % Plot anomalies in wavelet
    subplot(3,1,3)
    imagesc(time{i}, f, anomaly_mask{i});
    axis xy;
    xlabel('Date');
    ylabel('Frequency (Hz)');
    title(['Anomaly detection in ZWD for station '
       GNSS_data{i}{1,10}]);
    xline(datetime(2024,10,09,13,00,00), '--red', '
       LineWidth', 2);
    xline(datetime(2024,10,10,13,10,00), '--red', '
       LineWidth', 2);
    xline(datetime(2024,10,05,15,00,00), '-.black', '
       LineWidth', 2);
    xline(datetime(2024,10,10,21,00,00), '-.black', '
       LineWidth', 2);

    hold off;
end


% Plot for all western stations
figure;
hold on
xlabel('Date')
ylabel('ZWD (m)')
title('Milton, Western Florida')

plot(time{1},mean_move{1})
plot(time{2},mean_move{2})
plot(time{3},mean_move{3})
xline(datetime(2024,10,09,13,00,00), '--red', 'LineWidth'
   , 2);
xline(datetime(2024,10,10,13,10,00), '--red', 'LineWidth'
   , 2);
xline(datetime(2024,10,05,15,00,00), '-.black', '
   LineWidth', 2);
xline(datetime(2024,10,10,21,00,00), '-.black', '
   LineWidth', 2);
legend('FLAI', 'FLSN', 'FLSC')
hold off

% Plot for all central stations
figure;
hold on
```

```
xlabel('Date')
ylabel('ZWD (m)')
title('Milton, Central Florida')

plot(time{4},mean_move{4})
plot(time{5},mean_move{5})
plot(time{6},mean_move{6})
xline(datetime(2024,10,09,13,00,00), '--red', 'LineWidth'
    , 2);
xline(datetime(2024,10,10,13,10,00), '--red', 'LineWidth'
    , 2);
xline(datetime(2024,10,05,15,00,00), '-.black', '
    LineWidth', 2);
xline(datetime(2024,10,10,21,00,00), '-.black', '
    LineWidth', 2);
legend('ORL1', 'FLKS', 'FLCC')
hold off

% Plot for all eastern stations
figure;
hold on
xlabel('Date')
ylabel('ZWD (m)')
title('Milton, Eastern Florida')

plot(time{7},mean_move{7})
plot(time{8},mean_move{8})
plot(time{9},mean_move{9})
xline(datetime(2024,10,09,13,00,00), '--red', 'LineWidth'
    , 2);
xline(datetime(2024,10,10,13,10,00), '--red', 'LineWidth'
    , 2);
xline(datetime(2024,10,05,15,00,00), '-.black', '
    LineWidth', 2);
xline(datetime(2024,10,10,21,00,00), '-.black', '
    LineWidth', 2);
legend('FLBN', 'ORMD', 'TTVL')
hold off

% Plot for all data
figure;
hold on
xlabel('Date')
ylabel('ZWD (m)')
title('ZWD Milton, Florida')
```

```
plot(time{1},mean_move{1}, 'Color', '#EDB120')
plot(time{2},mean_move{2}, 'Color', '#EDB120')
plot(time{3},mean_move{3}, 'Color', '#EDB120')
plot(time{4},mean_move{4}, 'Color', '#D95319')
plot(time{5},mean_move{5}, 'Color', '#D95319')
plot(time{6},mean_move{6}, 'Color', '#D95319')
plot(time{7},mean_move{7}, 'Color', '#4DBEEE')
plot(time{8},mean_move{8}, 'Color', '#4DBEEE')
plot(time{9},mean_move{9}, 'Color', '#4DBEEE')
xline(datetime(2024,10,09,13,00,00), '--red', 'LineWidth'
    , 2);
xline(datetime(2024,10,10,13,10,00), '--red', 'LineWidth'
    , 2);
xline(datetime(2024,10,05,15,00,00), '-.black', '
    LineWidth', 2);
xline(datetime(2024,10,10,21,00,00), '-.black', '
    LineWidth', 2);
legend('FLAI', 'FLSN', 'FLSC', 'ORL1', 'FLKS', 'FLCC', '
    FLBN', 'ORMD', 'TTVL')
hold off

% Plot the initial test of ZWD (not mean)
figure;
hold on
xlabel('Date')
ylabel('ZWD (m)')
title('ZWD for station FLSN')

plot(time{2},yData_ZWD_tot{2})
xline(datetime(2024,10,09,13,00,00), '--red', 'LineWidth'
    , 2);
xline(datetime(2024,10,10,13,10,00), '--red', 'LineWidth'
    , 2);
xline(datetime(2024,10,05,15,00,00), '-.black', '
    LineWidth', 2);
xline(datetime(2024,10,10,21,00,00), '-.black', '
    LineWidth', 2);
hold off

 % Plot the initial test of ZWD & Mean
figure;
hold on
xlabel('Date')
ylabel('ZWD (m)')
title('ZWD for station FLSN')
```

```
plot(time{2},yData_ZWD_tot{2})
plot(time{2},mean_move{2})
xline(datetime(2024,10,09,13,00,00), '--red', 'LineWidth'
    , 2);
xline(datetime(2024,10,10,13,10,00), '--red', 'LineWidth'
    , 2);
xline(datetime(2024,10,05,15,00,00), '-.black', '
    LineWidth', 2);
xline(datetime(2024,10,10,21,00,00), '-.black', '
    LineWidth', 2);
legend('Original Data', '30min Mean Data')
hold off

% Plot the CWT and Threshold
figure;
hold on;
subplot(2,1,1)
imagesc(time{2}, f, abs(wt{2}));
axis xy;
xlabel('Date');
ylabel('Frequency (Hz)');
title(['Wavelet Scalogram for station ' GNSS_data
    {2}{1,10}]);
xlim([time{2}(1), time{2}(length(time{2}))]);
xline(datetime(2024,10,09,13,00,00), '--red', 'LineWidth'
    , 2);
xline(datetime(2024,10,10,13,10,00), '--red', 'LineWidth'
    , 2);
xline(datetime(2024,10,05,15,00,00), '-.black', '
    LineWidth', 2);
xline(datetime(2024,10,10,21,00,00), '-.black', '
    LineWidth', 2);
subplot(2,1,2)
imagesc(time{2}, f, anomaly_mask{2});
axis xy;
xlabel('Date');
ylabel('Frequency (Hz)');
title(['Anomaly detection in ZWD for station ' GNSS_data
    {2}{1,10}]);
xline(datetime(2024,10,09,13,00,00), '--red', 'LineWidth'
    , 2);
xline(datetime(2024,10,10,13,10,00), '--red', 'LineWidth'
    , 2);
xline(datetime(2024,10,05,15,00,00), '-.black', '
    LineWidth', 2);
```

```
xline(datetime(2024,10,10,21,00,00), '-.black', '
   LineWidth', 2);
hold off;


% Plot the lags for FLSC-TTVL, FLSC-FLKS, FLKS-TTVL
% Plot the visual lags for station
figure;
stem(lags{3, 9}, c{3, 9})
[~, linearIndex] = max(c{3,9}(:));
xMax = lags{3,9}(linearIndex);
xline(0, '--red', 'LineWidth', 2);
xline(xMax, '--black', 'LineWidth', 2);
text(xMax, 0, [num2str(xMax)]);
title(['ZWD for station ' GNSS_data{3}{1,10} ' and '
   GNSS_data{9}{1,10}]);

% Plot the visual lags for station
figure;
stem(lags{3, 5}, c{3, 5})
[~, linearIndex] = max(c{3,5}(:));
xMax = lags{3,5}(linearIndex);
xline(0, '--red', 'LineWidth', 2);
xline(xMax, '--black', 'LineWidth', 2);
text(xMax, 0, [num2str(xMax)]);
title(['ZWD for station ' GNSS_data{3}{1,10} ' and '
   GNSS_data{5}{1,10}]);

% Plot the visual lags for station
figure;
stem(lags{5, 9}, c{5, 9})
[maxValue, linearIndex] = max(c{5,9}(:));
xMax = lags{5,9}(linearIndex);
xline(0, '--red', 'LineWidth', 2);
xline(xMax, '--black', 'LineWidth', 2);
text(xMax, 0, [num2str(xMax)]);
title(['ZWD for station ' GNSS_data{5}{1,10} ' and '
   GNSS_data{9}{1,10}]);


% Plot the detrend'ed data
figure;
hold on;
plot(filtered1{2, 9})
plot(filtered2{2, 9})
plot(mean_move{2})
```

```
plot(mean_move{9})
plot(detrend(mean_move{2}));
plot(detrend(mean_move{9}));
title(['ZWD for station ' GNSS_data{2}{1,10} ' and '
   GNSS_data{9}{1,10}]);
hold off;


% Plot the difference between the different datasets, for
    representation if
% STO is worth over PWC 5min, to do on all data
figure;
hold on
xlabel('Date')
ylabel('ZWD (m)')
title('ZWD for station FLSN')

plot(time{2},yData_ZWD_tot{2})
plot(time{2},mean_move{2})
plot(time{10},yData_ZWD_tot{10})
plot(time{10},mean_move{10})
legend('FLSN PWC 5min', 'FLSN PWC 5min Mean', 'FLSN STO',
    'FLSN STO Mean')
hold off;

% Plot HTC
figure;
hold on
xlabel('Date')
ylabel('HTC (m)')
title('HTC for station FLSN, 120 min interval')
plot(time_htc{1},yData_htc_E_W{1})
plot(time_htc{1},yData_htc_N_S{1})
plot(time_htc{1},yData_htc_tot{1})

xline(datetime(2024,10,09,13,00,00), '--red', 'LineWidth'
   , 2);
xline(datetime(2024,10,10,13,10,00), '--red', 'LineWidth'
   , 2);
xline(datetime(2024,10,05,15,00,00), '-.black', '
   LineWidth', 2);
xline(datetime(2024,10,10,21,00,00), '-.black', '
   LineWidth', 2);
yline(0, '-.black', 'LineWidth', 2);
legend('E-W HTC', 'N-S HTC', 'TOT HTC')
hold off;
```

C.2 Zenith Wet Delay for Helene

```
clc
clear
close all

% Show figures on/off
set(0, 'DefaultFigureVisible', 'on');

% Load all data & add position and name
% -- Segment 1 --
% FLPY 19/9-1/10
GNSS_data{1} = readtable('Data\FLPY_2024263_275.dat');
GNSS_data{1}{:,10} = 'FLPY';
GNSS_data{1}{:,11} = 30.094282;      % Latitude
GNSS_data{1}{:,12} = -83.572900;     % Longitude
% FLMD 19/9-1/10
GNSS_data{2} = readtable('Data\FLMD_2024263_275.dat');
GNSS_data{2}{:,10} = 'FLMD';
GNSS_data{2}{:,11} = 30.374022;      % Latitude
GNSS_data{2}{:,12} = -83.275478;     % Longitude
% FL75 19/9-1/10
GNSS_data{3} = readtable('Data\FL75_2024263_275.dat');
GNSS_data{3}{:,10} = 'FL75*';
GNSS_data{3}{:,11} = 30.612525;      % Latitude
GNSS_data{3}{:,12} = -83.146681;     % Longitude

% -- Segment 2 --
% FLCB 19/9-1/10
GNSS_data{4} = readtable('Data\FLCB_2024263_275.dat');
GNSS_data{4}{:,10} = 'FLCB';
GNSS_data{4}{:,11} = 29.842600;      % Latitude
GNSS_data{4}{:,12} = -84.695148;     % Longitude
% TALH 19/9-1/10
GNSS_data{5} = readtable('Data\TALH_2024263_275.dat');
GNSS_data{5}{:,10} = 'TALH';
GNSS_data{5}{:,11} = 30.396523;      % Latitude
GNSS_data{5}{:,12} = -84.355843;     % Longitude
% FLJL 19/9-1/10
GNSS_data{6} = readtable('Data\FLJL_2024263_275.dat');
GNSS_data{6}{:,10} = 'FLJL';
GNSS_data{6}{:,11} = 30.579702;      % Latitude
GNSS_data{6}{:,12} = -84.266277;     % Longitude
% GATE 19/9-1/10
GNSS_data{7} = readtable('Data\GATE_2024263_275.dat');
GNSS_data{7}{:,10} = 'GATE';
```

```
GNSS_data{7}{:,11} = 30.833576;      % Latitude
GNSS_data{7}{:,12} = -83.982649;     % Longitude
% GAME 19/9-1/10
GNSS_data{8} = readtable('Data\GAME_2024263_275.dat');
GNSS_data{8}{:,10} = 'GAME';
GNSS_data{8}{:,11} = 31.182252;      % Latitude
GNSS_data{8}{:,12} = -83.786949;     % Longitude


% Initialize for faster compile
numTables = length(GNSS_data);
yData_ZWD_tot = cell(1, numTables);

mean_move = cell(1, numTables);

wt = cell(1, numTables);
time = cell(1, numTables);
anomaly_mask = cell(1, numTables);

lags = cell(numTables-1, numTables-1);
c = cell(numTables-1, numTables-1);
lagDiff_all = cell(numTables-1, numTables-1);
distance_stations_all = cell(numTables-1, numTables-1);

speed_kmh_all = cell(numTables-1, numTables-1);
speed_ms_all = cell(numTables-1, numTables-1);

% Sampling frequency (Hz), since 30s sampling
fs = 1/30;

% Extract data
for i = 1:numTables
    % ZWD total is the ini + cor
    yData_ZWD_tot{i} = GNSS_data{i}{:,8} + GNSS_data{i
       }{:,9};

    % Set all date columns into one (for x-axis plot)
    time{i} = datetime(GNSS_data{i}{:,1}, GNSS_data{i
       }{:,2}, GNSS_data{i}{:,3}, GNSS_data{i}{:,4},
       GNSS_data{i}{:,5}, GNSS_data{i}{:,6});

    % Makes a mean value from the closest 60 values, 30
       before and 29 after
    mean_move{i} = movmean(yData_ZWD_tot{i}, 60);

    % Wavelet-transform with Morlet ('amor')
```

```
    [wt{i}, f] = cwt(mean_move{i}, 'amor', fs);

    % Threshold based median, where median is decided
       under "good" weather
    threshold = 12 * median(abs(wt{i}(:)));

    % Only saves the data above threshold
    anomaly_mask{i} = abs(wt{i}) > threshold;
end

% Calculate the time delay & print to console
% The numTables-1 comes from that the last one is the one
    used for STO test
for i = 1:numTables
    % Loop to only cover each station pair once
    for j = i+1:numTables
        % Detrend (which removes the best straight-fit
           line)
        [c{i, j}, lags{i, j}] = xcorr(detrend(mean_move{i
           }), detrend(mean_move{j}));
        [~, maxIndex] = max(c{i, j});
        lagDiff = lags{i, j}(maxIndex);
        lagDiff_all{i, j} = lagDiff;
        disp(['Time Delay between stations ', GNSS_data{i
           }{1,10}, ' and ', GNSS_data{j}{1,10}, ' : ',
           num2str(lagDiff/2), ' minutes']);

        % Distance between stations
        [dist, az] = distance(GNSS_data{i}{1,11},
           GNSS_data{i}{1,12}, GNSS_data{j}{1,11},
           GNSS_data{j}{1,12});
        distance_stations = deg2km(dist, 'earth');
        distance_stations_all{i ,j} = distance_stations;
        disp(['Distance between stations ', GNSS_data{i
           }{1,10}, ' and ', GNSS_data{j}{1,10}, ' : ',
           num2str(distance_stations), ' km']);

        % Speed
        speed_kmh_all{i, j} = distance_stations / (
           lagDiff / 120);
        speed_ms_all{i, j} = (distance_stations * 1000) /
            (lagDiff * 30);
        disp(['Speed between stations ', GNSS_data{i
           }{1,10}, ' and ', GNSS_data{j}{1,10}, ' : ',
           num2str(speed_ms_all{i, j}), ' m/s or ',
           num2str(speed_kmh_all{i, j}), ' km/h']);
```

```
        disp(' ');
    end
end


% Loop over all stations and plot CWT, threshold and org.
    data
for i = 1:length(mean_move)
    figure;
    set(gcf, 'Units', 'centimeters', 'Position', [15, 8,
       16, 14])
    hold on;

    % Plot time series mean
    subplot(3,1,1)
    axis xy;
    plot(time{i}, mean_move{i})
    xlabel('Date');
    ylabel('Mean 30min ZWD (m)');
    title(['Mean ZWD for station ' GNSS_data{i}{1,10}]);
    xlim([time{i}(1), time{i}(length(time{i}))]);
    xline(datetime(2024,09,27,00,00,00), '--red', '
       LineWidth', 2);
    xline(datetime(2024,09,27,07,00,00), '--red', '
       LineWidth', 2);
    xline(datetime(2024,09,24,15,00,00), '-.black', '
       LineWidth', 2);
    xline(datetime(2024,09,27,21,00,00), '-.black', '
       LineWidth', 2);


    % Plot scalogram
    subplot(3,1,2)
    imagesc(time{i}, f, abs(wt{i}));
    axis xy;
    xlabel('Date');
    ylabel('Frequency (Hz)');
    title(['Wavelet Scalogram for station ' GNSS_data{i
       }{1,10}]);
    xline(datetime(2024,09,27,00,00,00), '--red', '
       LineWidth', 2);
    xline(datetime(2024,09,27,07,00,00), '--red', '
       LineWidth', 2);
    xline(datetime(2024,09,24,15,00,00), '-.black', '
       LineWidth', 2);
```

```
    xline(datetime(2024,09,27,21,00,00), '-.black', '
       LineWidth', 2);



    % Plot anomalies in wavelet
    subplot(3,1,3)
    imagesc(time{i}, f, anomaly_mask{i});
    axis xy;
    xlabel('Date');
    ylabel('Frequency (Hz)');
    title(['Anomaly detection in ZWD for station '
       GNSS_data{i}{1,10}]);
    xline(datetime(2024,09,27,00,00,00), '--red', '
       LineWidth', 2);
    xline(datetime(2024,09,27,07,00,00), '--red', '
       LineWidth', 2);
    xline(datetime(2024,09,24,15,00,00), '-.black', '
       LineWidth', 2);
    xline(datetime(2024,09,27,21,00,00), '-.black', '
       LineWidth', 2);

    hold off;
end

% Plot for first segment
figure;
hold on
xlabel('Date')
ylabel('ZWD (m)')
title('ZWD Helene, Florida')

plot(time{1},mean_move{1}, 'Color', '#EDB120')
plot(time{2},mean_move{2}, 'Color', '#D95319')
plot(time{3},mean_move{3}, 'Color', '#4DBEEE')
xline(datetime(2024,09,27,00,00,00), '--red', 'LineWidth'
   , 2);
xline(datetime(2024,09,27,07,00,00), '--red', 'LineWidth'
   , 2);
xline(datetime(2024,09,24,15,00,00), '-.black', '
   LineWidth', 2);
xline(datetime(2024,09,27,21,00,00), '-.black', '
   LineWidth', 2);
legend('FLPY', 'FLMD', 'FL75')
hold off
```

```
% Plot for second segment
figure;
hold on
xlabel('Date')
ylabel('ZWD (m)')
title('ZWD Helene, Florida')

plot(time{4},mean_move{4})
plot(time{5},mean_move{5})
plot(time{6},mean_move{6})
plot(time{7},mean_move{7})
plot(time{8},mean_move{8})
xline(datetime(2024,09,27,00,00,00), '--red', 'LineWidth'
    , 2);
xline(datetime(2024,09,27,07,00,00), '--red', 'LineWidth'
    , 2);
xline(datetime(2024,09,24,15,00,00), '-.black', '
   LineWidth', 2);
xline(datetime(2024,09,27,21,00,00), '-.black', '
   LineWidth', 2);
legend(GNSS_data{4}{1,10}, GNSS_data{5}{1,10}, GNSS_data
   {6}{1,10}, GNSS_data{7}{1,10}, GNSS_data{8}{1,10})
hold off

% Plot the initial test of ZWD (not mean)
figure;
hold on
xlabel('Date')
ylabel('ZWD (m)')
title('ZWD for station FLMD')

plot(time{2},yData_ZWD_tot{2})
xline(datetime(2024,09,27,00,00,00), '--red', 'LineWidth'
    , 2);
xline(datetime(2024,09,27,07,00,00), '--red', 'LineWidth'
    , 2);
xline(datetime(2024,09,24,15,00,00), '-.black', '
   LineWidth', 2);
xline(datetime(2024,09,27,21,00,00), '-.black', '
   LineWidth', 2);
hold off

% Plot the initial test of ZWD & Mean
figure;
hold on
xlabel('Date')
```

```
ylabel('ZWD (m)')
title('ZWD for station FLMD')

plot(time{2},yData_ZWD_tot{2})
plot(time{2},mean_move{2})
xline(datetime(2024,09,27,00,00,00), '--red', 'LineWidth'
    , 2);
xline(datetime(2024,09,27,07,00,00), '--red', 'LineWidth'
    , 2);
xline(datetime(2024,09,24,15,00,00), '-.black', '
    LineWidth', 2);
xline(datetime(2024,09,27,21,00,00), '-.black', '
    LineWidth', 2);
legend('Original Data', '30min Mean Data')
hold off

% Plot the CWT and Threshold
figure;
hold on;

subplot(2,1,1)
imagesc(time{2}, f, abs(wt{2})); % Amplitude of wavelet
axis xy;
xlabel('Date');
ylabel('Frequency (Hz)');
title(['Wavelet Scalogram for station ' GNSS_data
    {2}{1,10}]);
xlim([time{2}(1), time{2}(length(time{2}))]);
xline(datetime(2024,09,27,00,00,00), '--red', 'LineWidth'
    , 2);
xline(datetime(2024,09,27,07,00,00), '--red', 'LineWidth'
    , 2);
xline(datetime(2024,09,24,15,00,00), '-.black', '
    LineWidth', 2);
xline(datetime(2024,09,27,21,00,00), '-.black', '
    LineWidth', 2);

subplot(2,1,2)
imagesc(time{2}, f, anomaly_mask{2});
axis xy;
xlabel('Date');
ylabel('Frequency (Hz)');
title(['Anomaly detection in ZWD for station ' GNSS_data
    {2}{1,10}]);
xline(datetime(2024,09,27,00,00,00), '--red', 'LineWidth'
    , 2);
```

```
xline(datetime(2024,09,27,07,00,00), '--red', 'LineWidth'
    , 2);
xline(datetime(2024,09,24,15,00,00), '-.black', '
    LineWidth', 2);
xline(datetime(2024,09,27,21,00,00), '-.black', '
    LineWidth', 2);
hold off;
```

C.3 Land subsidence for Milton

```
clc
clear
close all

% Show figures on/off
set(0, 'DefaultFigureVisible', 'on');

% Load all data & add position and name
% FLAI 4-24/10
GNSS_data{1} = readtable('Data\FLAI_Height_2024278_298.
    dat');
GNSS_data{1}{:,17} = 'FLAI*';
GNSS_data{1}{:,18} = 27.449731;      % Latitude
GNSS_data{1}{:,19} = -82.690230;     % Longitude
% FLSN 4-24/10
GNSS_data{2} = readtable('Data\FLSN_Height_2024278_298.
    dat');
GNSS_data{2}{:,17} = 'FLSN';
GNSS_data{2}{:,18} = 27.333611;      % Latitude
GNSS_data{2}{:,19} = -82.438323;     % Longitude
% FLSC 4-24/10
GNSS_data{3} = readtable('Data\FLSC_Height_2024278_298.
    dat');
GNSS_data{3}{:,17} = 'FLSC';
GNSS_data{3}{:,18} = 27.217272;      % Latitude
GNSS_data{3}{:,19} = -82.404745;     % Longitude
% ORL1 4-24/10
GNSS_data{4} = readtable('Data\ORL1_Height_2024278_298.
    dat');
GNSS_data{4}{:,17} = 'ORL1';
GNSS_data{4}{:,18} = 28.434562;      % Latitude
GNSS_data{4}{:,19} = -81.382467;     % Longitude
% FLKS 4-24/10
GNSS_data{5} = readtable('Data\FLKS_Height_2024278_298.
    dat');
GNSS_data{5}{:,17} = 'FLKS';
```

```
GNSS_data{5}{:,18} = 28.295611;      % Latitude
GNSS_data{5}{:,19} = -81.436352;     % Longitude
% FLCC 4-24/10
GNSS_data{6} = readtable('Data\FLCC_Height_2024278_298.
   dat');
GNSS_data{6}{:,17} = 'FLCC';
GNSS_data{6}{:,18} = 28.094482;      % Latitude
GNSS_data{6}{:,19} = -81.274206;     % Longitude
% FLBN 4-24/10
GNSS_data{7} = readtable('Data\FLBN_Height_2024278_298.
   dat');
GNSS_data{7}{:,17} = 'FLBN*';
GNSS_data{7}{:,18} = 29.594142;      % Latitude
GNSS_data{7}{:,19} = -81.287096;     % Longitude
% ORMD 4-24/10
GNSS_data{8} = readtable('Data\ORMD_Height_2024278_298.
   dat');
GNSS_data{8}{:,17} = 'ORMD*';
GNSS_data{8}{:,18} = 29.298186;      % Latitude
GNSS_data{8}{:,19} = -81.108892;     % Longitude
% TTVL 4-24/10
GNSS_data{9} = readtable('Data\TTVL_Height_2024278_298.
   dat');
GNSS_data{9}{:,17} = 'TTVL';
GNSS_data{9}{:,18} = 28.505709;      % Latitude
GNSS_data{9}{:,19} = -80.803381;     % Longitude

% Tide Level StPetersburg 4-24/10
Tide_Level{1} = readtable('Data\
   Milton_Water_Level_StPetersburg.dat');
% Tide Level Clearwater Beach 4-24/10
Tide_Level{2} = readtable('Data\
   Milton_Water_Level_Clearwater.dat');
% Tide Level Port Manatee 4-24/10
Tide_Level{3} = readtable('Data\
   Milton_Water_Level_Port_Manatee.dat');

% For MJD time
start_date = datetime(1858, 11, 17);

% Initialize for faster compile
numTables = length(GNSS_data);
numTables2 = length(Tide_Level);
xData_date = cell(1, numTables);

yData_Height = cell(1, numTables);
```

```
mean_move = cell(1, numTables);

wt = cell(1, numTables);
time = cell(1, numTables);
anomaly_mask = cell(1, numTables);

yData_around_median = cell(1, numTables2);
timeVector = cell(1, numTables2);

% Sampling frequency (Hz), since 30s sampling
fs = 1/30;

% Extract data
for i = 1:numTables
    % Get date from MJD
    xData_date{i} = datetime(start_date + days(GNSS_data{
       i}{:,1}), 'InputFormat', 'dd-MMM-yyyy');

    % Sets the data around the median of each dataset
    yData_Height{i} = GNSS_data{i}{:,8} - median(
       GNSS_data{i}{:,8});

    % Set all date columns into one (for x-axis plot)
    time{i} = xData_date{i} + seconds(GNSS_data{i}{:,2});

    % Makes a mean value from the closest 60 values, 30
       before and 29 after
    mean_move{i} = movmean(yData_Height{i}, 60);

    % Wavelet-transform with Morlet ('amor')
    [wt{i}, f] = cwt(GNSS_data{i}{:,8}, 'amor', fs);

    % Threshold based median
    threshold = 4.5 * median(abs(wt{i}(:)));
    anomaly_mask{i} = abs(wt{i}) > threshold;
end



% Loop over all stations and plot
for i = 1:length(yData_Height)
    figure;
    set(gcf, 'Units', 'centimeters', 'Position', [15, 8,
       16, 14])
    hold on;
```

```
% Plot time series
subplot(3,1,1)
axis xy;
plot(time{i}, yData_Height{i})
xlabel('Date');
ylabel('Height (m)');
title(['Height around median for station ' GNSS_data{
    i}{1,17}]);
xlim([time{i}(1), time{i}(length(time{i}))]);
xline(datetime(2024,10,09,13,00,00), '--red', '
    LineWidth', 2);
xline(datetime(2024,10,10,13,10,00), '--red', '
    LineWidth', 2);
xline(datetime(2024,10,05,15,00,00), '-.black', '
    LineWidth', 2);
xline(datetime(2024,10,10,21,00,00), '-.black', '
    LineWidth', 2);

% Plot scalogram
subplot(3,1,2)
imagesc(time{i}, f, abs(wt{i}));
axis xy;
xlabel('Date');
ylabel('Frequency (Hz)');
title(['Wavelet Scalogram for station ' GNSS_data{i
    }{1,17}]);
xline(datetime(2024,10,09,13,00,00), '--red', '
    LineWidth', 2);
xline(datetime(2024,10,10,13,10,00), '--red', '
    LineWidth', 2);
xline(datetime(2024,10,05,15,00,00), '-.black', '
    LineWidth', 2);
xline(datetime(2024,10,10,21,00,00), '-.black', '
    LineWidth', 2);

% Plot anomalies in wavelet
subplot(3,1,3)
imagesc(time{i}, f, anomaly_mask{i});
axis xy;
xlabel('Date');
ylabel('Frequency (Hz)');
title(['Anomaly detection in Height for station '
    GNSS_data{i}{1,17}]);
xline(datetime(2024,10,09,13,00,00), '--red', '
    LineWidth', 2);
xline(datetime(2024,10,10,13,10,00), '--red', '
```

```
        LineWidth', 2);
    xline(datetime(2024,10,05,15,00,00), '-.black', '
        LineWidth', 2);
    xline(datetime(2024,10,10,21,00,00), '-.black', '
        LineWidth', 2);

    hold off;
end


% Plot of the CWT
figure;
set(gcf, 'Units', 'centimeters', 'Position', [15, 8, 16,
    10])
hold on;
imagesc(time{2}, f, abs(wt{2}));
axis xy;
xlabel('Date');
ylabel('Frequency (Hz)');
title(['Wavelet Scalogram for station ' GNSS_data
    {2}{1,17}]);
xlim([time{2}(1), time{2}(length(time{2}))]);
ylim([0, 12*10^-3]);
xline(datetime(2024,10,09,13,00,00), '--red', 'LineWidth'
    , 2);
xline(datetime(2024,10,10,13,10,00), '--red', 'LineWidth'
    , 2);
xline(datetime(2024,10,05,15,00,00), '-.black', '
    LineWidth', 2);
xline(datetime(2024,10,10,21,00,00), '-.black', '
    LineWidth', 2);
hold off;

% Plot of threshold of the cwt
figure;
set(gcf, 'Units', 'centimeters', 'Position', [15, 8, 16,
    10])
hold on;
imagesc(time{2}, f, anomaly_mask{2});
axis xy;
xlabel('Date');
ylabel('Frequency (Hz)');
title(['Anomaly detection in Height for station '
    GNSS_data{2}{1,17}]);
xlim([time{2}(1), time{2}(length(time{2}))]);
ylim([0, 12*10^-3]);
```

```
xline(datetime(2024,10,09,13,00,00), '--red', 'LineWidth'
    , 2);
xline(datetime(2024,10,10,13,10,00), '--red', 'LineWidth'
    , 2);
xline(datetime(2024,10,05,15,00,00), '-.black', '
   LineWidth', 2);
xline(datetime(2024,10,10,21,00,00), '-.black', '
   LineWidth', 2);
hold off;

% Plot the initial test of land subsidence
figure;
set(gcf, 'Units', 'centimeters', 'Position', [15, 8, 16,
   10])
hold on
xlabel('Date')
ylabel('Height (m)')
title('Height around median for station FLSN')

plot(time{2},yData_Height{2})
xline(datetime(2024,10,09,13,00,00), '--red', 'LineWidth'
    , 2);
xline(datetime(2024,10,10,13,10,00), '--red', 'LineWidth'
    , 2);
xline(datetime(2024,10,05,15,00,00), '-.black', '
   LineWidth', 2);
xline(datetime(2024,10,10,21,00,00), '-.black', '
   LineWidth', 2);
hold off

% Tide Level
for i = 1:numTables2
    opts = detectImportOptions('Data\
       Milton_Water_Level_StPetersburg.dat', 'Delimiter',
        ',');
    opts.SelectedVariableNames = opts.VariableNames(1:2);
    data = readtable('Data\
       Milton_Water_Level_StPetersburg.dat', opts);
    dateStrings = strcat(data.Var1, {' '}, data.Var2);
    timeVector{i} = datetime(dateStrings, 'InputFormat',
       'yyyy/MM/dd HH:mm');
    yData = table2array(Tide_Level{i}(:,5));
    yData_around_median{i} = yData - median(yData);

end
```

```
% Plot the Tide Level
figure;
set(gcf, 'Units', 'centimeters', 'Position', [15, 8, 16,
    11])
hold on

subplot(2,1,1)
plot(timeVector{2}, yData_around_median{2})
xlabel('Date')
ylabel('Height (m)')
title('Water Level around median for Clearwater')
xline(datetime(2024,10,09,13,00,00), '--red', 'LineWidth'
    , 1);
xline(datetime(2024,10,10,13,10,00), '--red', 'LineWidth'
    , 1);
xline(datetime(2024,10,05,15,00,00), '-.black', '
    LineWidth', 2);
xline(datetime(2024,10,10,21,00,00), '-.black', '
    LineWidth', 2);

subplot(2,1,2)
plot(time{2}, yData_Height{2})
xlabel('Date')
ylabel('Height (m)')
title('Height around median for FLSN')
xline(datetime(2024,10,09,13,00,00), '--red', 'LineWidth'
    , 1);
xline(datetime(2024,10,10,13,10,00), '--red', 'LineWidth'
    , 1);
xline(datetime(2024,10,05,15,00,00), '-.black', '
    LineWidth', 2);
xline(datetime(2024,10,10,21,00,00), '-.black', '
    LineWidth', 2);

hold off;

% -- Plots of initial observations (all 3 regions and one
    complete) --

% Plot the weastern height around median
figure;
hold on
xlabel('Date')
ylabel('Height around median (m)')
title('Land Subsidence, Milton, Western Florida')
```

```
plot(time{1},yData_Height{1})
plot(time{2},yData_Height{2})
plot(time{3},yData_Height{3})
legend('FLAI','FLSN','FLSC')
hold off

% Plot the central height around median
figure;
hold on
xlabel('Date')
ylabel('Height around median (m)')
title('Land Subsidence, Milton, Central Florida')

plot(time{4},yData_Height{4})
plot(time{5},yData_Height{5})
plot(time{6},yData_Height{6})
legend('ORL1', 'FLKS', 'FLCC')
hold off

% Plot the eastern height around median
figure;
hold on
xlabel('Date')
ylabel('Height around median (m)')
title('Land Subsidence, Milton, Eastern Florida')

plot(time{7},yData_Height{7})
plot(time{8},yData_Height{8})
plot(time{9},yData_Height{9})
legend('FLBN', 'ORMD', 'TTVL')
hold off

% Plot for all stations
figure;
hold on
xlabel('Date')
ylabel('Height around median (m)')
title('Land Subsidence, Milton, Florida')

plot(time{1},yData_Height{1}, 'red')
plot(time{2},yData_Height{2}, 'red')
plot(time{3},yData_Height{3}, 'red')
plot(time{4},yData_Height{4}, 'blue')
plot(time{5},yData_Height{5}, 'blue')
plot(time{6},yData_Height{6}, 'blue')
plot(time{7},yData_Height{7}, 'black')
```

```
plot(time{8},yData_Height{8}, 'black')
plot(time{9},yData_Height{9}, 'black')
legend('FLAI', 'FLSN', 'FLSC', 'ORL1', 'FLKS', 'FLCC', '
   FLBN', 'ORMD', 'TTVL')
hold off
```

C.4 Land subsidence for Helene

```
clc
clear
close all

% Show figures on/off
set(0, 'DefaultFigureVisible', 'on');

% Load all data & add position and name
% -- Segment 1 --
% FLPY 19/9-1/10
GNSS_data{1} = readtable('Data\FLPY_Height_2024263_275.
   dat');
GNSS_data{1}{:,17} = 'FLPY';
GNSS_data{1}{:,18} = 30.094282;      % Latitude
GNSS_data{1}{:,19} = -83.572900;     % Longitude
% FLMD 19/9-1/10
GNSS_data{2} = readtable('Data\FLMD_Height_2024263_275.
   dat');
GNSS_data{2}{:,17} = 'FLMD';
GNSS_data{2}{:,18} = 30.374022;      % Latitude
GNSS_data{2}{:,19} = -83.275478;     % Longitude
% FL75 19/9-1/10
GNSS_data{3} = readtable('Data\FL75_Height_2024263_275.
   dat');
GNSS_data{3}{:,17} = 'FL75*';
GNSS_data{3}{:,18} = 30.612525;      % Latitude
GNSS_data{3}{:,19} = -83.146681;     % Longitude

% -- Segment 2 --
% FLCB 19/9-1/10
GNSS_data{4} = readtable('Data\FLCB_Height_2024263_275.
   dat');
GNSS_data{4}{:,17} = 'FLCB';
GNSS_data{4}{:,18} = 29.842600;      % Latitude
GNSS_data{4}{:,19} = -84.695148;     % Longitude
% TALH 19/9-1/10
GNSS_data{5} = readtable('Data\TALH_Height_2024263_275.
   dat');
```

```
GNSS_data{5}{:,17} = 'TALH';
GNSS_data{5}{:,18} = 30.396523;      % Latitude
GNSS_data{5}{:,19} = -84.355843;     % Longitude
% FLJL 19/9-1/10
GNSS_data{6} = readtable('Data\FLJL_Height_2024263_275.
   dat');
GNSS_data{6}{:,17} = 'FLJL';
GNSS_data{6}{:,18} = 30.579702;      % Latitude
GNSS_data{6}{:,19} = -84.266277;     % Longitude
% GATE 19/9-1/10
GNSS_data{7} = readtable('Data\GATE_Height_2024263_275.
   dat');
GNSS_data{7}{:,17} = 'GATE';
GNSS_data{7}{:,18} = 30.833576;      % Latitude
GNSS_data{7}{:,19} = -83.982649;     % Longitude
% GAME 19/9-1/10
GNSS_data{8} = readtable('Data\GAME_Height_2024263_275.
   dat');
GNSS_data{8}{:,17} = 'GAME';
GNSS_data{8}{:,18} = 31.182252;      % Latitude
GNSS_data{8}{:,19} = -83.786949;     % Longitude

% Tide Level 19/9-1/10
Tide_Level{1} = readtable('Data\
   Helene_Water_Level_Apalachicola.dat');

% For MJD time
start_date = datetime(1858, 11, 17);

% Initialize for faster compile
numTables = length(GNSS_data);
numTables2 = length(Tide_Level);
xData_date = cell(1, numTables);

yData_Height = cell(1, numTables);
mean_move = cell(1, numTables);

wt = cell(1, numTables);
time = cell(1, numTables);
anomaly_mask = cell(1, numTables);

timeVector = cell(1, numTables2);
yData_around_median = cell(1, numTables2);

% Sampling frequency (Hz), since 30s sampling
fs = 1/30;
```

```
% Extract data
for i = 1:numTables
    % Get date from MJD
    xData_date{i} = datetime(start_date + days(GNSS_data{
       i}{:,1}), 'InputFormat', 'dd-MMM-yyyy');

    % Sets the data around the median of each dataset
    yData_Height{i} = GNSS_data{i}{:,8} - median(
       GNSS_data{i}{:,8});

    % Set all date columns into one (for x-axis plot)
    time{i} = xData_date{i} + seconds(GNSS_data{i}{:,2});

    % Makes a mean value from the closest 60 values, 30
       before and 29 after
    mean_move{i} = movmean(yData_Height{i}, 60);

    % Wavelet-transform with Morlet ('amor')
    [wt{i}, f] = cwt(yData_Height{i}, 'amor', fs);

    % Threshold based median
    threshold = 3 * median(abs(wt{i}(:)));
    anomaly_mask{i} = abs(wt{i}) > threshold;
end


% Loop over all stations and plot
for i = 1:length(yData_Height)
    figure;
    set(gcf, 'Units', 'centimeters', 'Position', [15, 8,
       16, 14])
    hold on;

    % Plot time series
    subplot(3,1,1)
    axis xy;
    plot(time{i}, yData_Height{i})
    xlabel('Date');
    ylabel('Height (m)');
    title(['Height around median for station ' GNSS_data{
       i}{1,17}]);
    xlim([time{i}(1), time{i}(length(time{i}))]);
    xline(datetime(2024,09,27,00,00,00), '--red', '
       LineWidth', 2);
    xline(datetime(2024,09,27,06,00,00), '--red', '
```

```
        LineWidth', 2);
    xline(datetime(2024,09,24,15,00,00), '-.black', '
        LineWidth', 2);
    xline(datetime(2024,09,27,21,00,00), '-.black', '
        LineWidth', 2);

    % Plot scalogram
    subplot(3,1,2)
    imagesc(time{i}, f, abs(wt{i}));
    axis xy;
    xlabel('Date');
    ylabel('Frequency (Hz)');
    title(['Wavelet Scalogram for station ' GNSS_data{i
        }{1,17}]);
    xline(datetime(2024,09,27,00,00,00), '--red', '
        LineWidth', 2);
    xline(datetime(2024,09,27,06,00,00), '--red', '
        LineWidth', 2);
    xline(datetime(2024,09,24,15,00,00), '-.black', '
        LineWidth', 2);
    xline(datetime(2024,09,27,21,00,00), '-.black', '
        LineWidth', 2);

    % Plot anomalies in wavelet
    subplot(3,1,3)
    imagesc(time{i}, f, anomaly_mask{i});
    axis xy;
    xlabel('Date');
    ylabel('Frequency (Hz)');
    title(['Anomaly detection in Height for station '
        GNSS_data{i}{1,17}]);
    xline(datetime(2024,09,27,00,00,00), '--red', '
        LineWidth', 2);
    xline(datetime(2024,09,27,06,00,00), '--red', '
        LineWidth', 2);
    xline(datetime(2024,09,24,15,00,00), '-.black', '
        LineWidth', 2);
    xline(datetime(2024,09,27,21,00,00), '-.black', '
        LineWidth', 2);

    hold off;
end


% Plot of the CWT
figure;
```

```
set(gcf, 'Units', 'centimeters', 'Position', [15, 8, 16,
    10])
hold on;
imagesc(time{2}, f, abs(wt{2}));
axis xy;
xlabel('Date');
ylabel('Frequency (Hz)');
title(['Wavelet Scalogram for station ' GNSS_data
    {2}{1,17}]);
xlim([time{2}(1), time{2}(length(time{2}))]);
ylim([0, 12*10^-3]);
xline(datetime(2024,09,27,00,00,00), '--red', 'LineWidth'
    , 2);
xline(datetime(2024,09,27,06,00,00), '--red', 'LineWidth'
    , 2);
xline(datetime(2024,09,24,15,00,00), '-.black', '
    LineWidth', 2);
xline(datetime(2024,09,27,21,00,00), '-.black', '
    LineWidth', 2);
hold off;

% Plot of threshold of the cwt
figure;
set(gcf, 'Units', 'centimeters', 'Position', [15, 8, 16,
    10])
hold on;
imagesc(time{2}, f, anomaly_mask{2});
axis xy;
xlabel('Date');
ylabel('Frequency (Hz)');
title(['Anomaly detection in Height for station '
    GNSS_data{2}{1,17}]);
xlim([time{2}(1), time{2}(length(time{2}))]);
ylim([0, 12*10^-3]);
xline(datetime(2024,09,27,00,00,00), '--red', 'LineWidth'
    , 2);
xline(datetime(2024,09,27,06,00,00), '--red', 'LineWidth'
    , 2);
xline(datetime(2024,09,24,15,00,00), '-.black', '
    LineWidth', 2);
xline(datetime(2024,09,27,21,00,00), '-.black', '
    LineWidth', 2);
hold off;

% Plot the initial test of land subsidence
figure;
```

```
set(gcf, 'Units', 'centimeters', 'Position', [15, 8, 16,
   10])
hold on
xlabel('Date')
ylabel('Height (m)')
title(['Height around median for station ' GNSS_data
   {2}{1,17}]);

plot(time{2},yData_Height{2})
xline(datetime(2024,09,27,00,00,00), '--red', 'LineWidth'
   , 2);
xline(datetime(2024,09,27,06,00,00), '--red', 'LineWidth'
   , 2);
xline(datetime(2024,09,24,15,00,00), '-.black', '
   LineWidth', 2);
xline(datetime(2024,09,27,21,00,00), '-.black', '
   LineWidth', 2);
hold off

% Tide Level
for i = 1:numTables2
    opts = detectImportOptions('Data\
       Helene_Water_Level_Apalachicola.dat', 'Delimiter',
        ',');
    opts.SelectedVariableNames = opts.VariableNames(1:2);
    data = readtable('Data\
       Helene_Water_Level_Apalachicola.dat', opts);
    dateStrings = strcat(data.Var1, {' '}, data.Var2);
    timeVector{i} = datetime(dateStrings, 'InputFormat',
       'yyyy/MM/dd HH:mm');
    yData = table2array(Tide_Level{i}(:,5));
    yData_around_median{i} = yData - median(yData);

end

% Plot the Tide Level
figure;
set(gcf, 'Units', 'centimeters', 'Position', [15, 8, 16,
   11])
hold on

subplot(2,1,1)
plot(timeVector{1}, yData_around_median{1} / 2)
xlabel('Date')
ylabel('Height (m)')
title('Water Level around median for Apalachicola')
```

```
xline(datetime(2024,09,27,00,00,00), '--red', 'LineWidth'
    , 1);
xline(datetime(2024,09,27,06,00,00), '--red', 'LineWidth'
    , 1);
xline(datetime(2024,09,24,15,00,00), '-.black', '
    LineWidth', 2);
xline(datetime(2024,09,27,21,00,00), '-.black', '
    LineWidth', 2);

subplot(2,1,2)
plot(time{4}, yData_Height{4})
xlabel('Date')
ylabel('Height (m)')
title('Height around median for FLCB')
xline(datetime(2024,09,27,00,00,00), '--red', 'LineWidth'
    , 1);
xline(datetime(2024,09,27,06,00,00), '--red', 'LineWidth'
    , 1);
xline(datetime(2024,09,24,15,00,00), '-.black', '
    LineWidth', 2);
xline(datetime(2024,09,27,21,00,00), '-.black', '
    LineWidth', 2);

hold off
```

C.5 Map of base stations

```
clc
clear
close all

% --- Milton ---
% Locations for the GPS data
locations_milton = [
    27.449731, -82.690230; % FLAI
    27.333611, -82.438323; % FLSN
    27.217272, -82.404745; % FLSC
    28.434562, -81.382467; % ORL1
    28.295611, -81.436352; % FLKS
    28.094482, -81.274206; % FLCC
    29.594142, -81.287096; % FLBN
    29.298186, -81.108892; % ORMD
    28.505709, -80.803381; % TTVL

    27 + 58.7/60, -(82 + 49.9/60) % Water Level
       Clearwater Beach
```

```
];

% Labels for the locations
labels_milton = {
    'FLAI'
    'FLSN'
    'FLSC'
    'ORL1'
    'FLKS'
    'FLCC'
    'FLBN'
    'ORMD'
    'TTVL'

    'WL Clearwater'
};

% --- Helene ---
% Locations for the GPS data
locations_helene = [
    30.094282, -83.572900; % FLPY
    30.374022, -83.275478; % FLMD
    30.612525, -83.146681; % FL75

    29.842600, -84.695148; % FLCB
    30.396523, -84.355843; % TALH
    30.579702, -84.266277; % FLJL
    30.833576, -83.982649; % GATE
    31.182252, -83.786949; % GAME

    29 + 43.5/60, -(84 + 58.8/60) % Water Level
       Apalachicola
];

% Labels for the locations
labels_helene = {
    'FLPY'
    'FLMD'
    'FL75'

    'FLCB'
    'TALH'
    'FLJL'
    'GATE'
    'GAME'
```

```
    'WL Apalachicola'
};

% Positioning of the background satellite images from
   NOAA / NESDIS
A_milton = flipud(imread('
   Milton_2024284_0330_2kX2k_cropped.jpg'));
latlim_milton = [25.00, 30.84];
lonlim_milton = [-85.00, -80.00];
R_milton = georefcells(latlim_milton, lonlim_milton, size
   (A_milton));

A_helene = flipud(imread('
   Helene_2024271_0450_2kX2k_cropped.jpg'));
latlim_helene = [26.31, 33.49];
lonlim_helene = [-86.51, -80.00];
R_helene = georefcells(latlim_helene, lonlim_helene, size
   (A_helene));

% Milton Figure
figure
set(gcf, 'Units', 'centimeters', 'Position', [15, 8, 17,
   16])

hold on;
axesm('mercator','MapLatLimit',latlim_milton,'MapLonLimit
   ',lonlim_milton)
setm(gca, 'MLabelLocation', 5, 'PLabelLocation', 5, '
   MLabelParallel', 'south', 'PLabelMeridian', 'west')
geoshow(A_milton, R_milton)

% Plot all locations and labels
for i = 1:size(locations_milton, 1)
    geoshow(locations_milton(i,1), locations_milton(i,2),
        'DisplayType', 'point', 'Marker', 'o', '
       MarkerSize', 8, 'MarkerEdgeColor', 'black', '
       MarkerFaceColor', 'white');
    textm(locations_milton(i,1) - 0.01, locations_milton(
       i,2) + 0.09, labels_milton(i), 'Color', 'k', '
       FontSize', 12);
end

% Fixes grids for lat/lon & better positioning of image
gridm on
mlabel on
plabel on
```

```
framem on
tightmap

hold off;

% Helene Figure
figure
set(gcf, 'Units', 'centimeters', 'Position', [15, 8, 17,
   16])

hold on;
axesm('mercator','MapLatLimit',latlim_helene,'MapLonLimit
   ',lonlim_helene)
setm(gca, 'MLabelLocation', 5, 'PLabelLocation', 5, '
   MLabelParallel', 'south', 'PLabelMeridian', 'west')
geoshow(A_helene, R_helene)

% Plot all locations and labels
for i = 1:size(locations_helene, 1)
    geoshow(locations_helene(i,1), locations_helene(i,2),
        'DisplayType', 'point', 'Marker', 'o', '
       MarkerSize', 8, 'MarkerEdgeColor', 'black', '
       MarkerFaceColor', 'white');
    textm(locations_helene(i,1) - 0.01, locations_helene(
       i,2) + 0.09, labels_helene(i), 'Color', 'k', '
       FontSize', 12);
end

% Fixes grids for lat/lon & better positioning of image
gridm on
mlabel on
plabel on
framem on
tightmap

hold off;

% -- Image used for front page --
% Positioning of the background satellite images from
   NOAA / NESDIS
A_front = flipud(imread('test_picture_M_H_cropped_2.jpg')
   );
latlim_front = [23.5897, 32.3700];
lonlim_front = [-87.3932, -79.1453];
R_front = georefcells(latlim_front, lonlim_front, size(
   A_front));
```

```
% Front Figure
figure
set(gcf, 'Units', 'centimeters', 'Position', [15, 8, 17,
   16])

hold on;
axesm('mercator', 'MapLatLimit', latlim_front, '
   MapLonLimit', lonlim_front)
setm(gca, 'MLabelLocation', 5, 'PLabelLocation', 5, '
   MLabelParallel', 'south', 'PLabelMeridian', 'west')
geoshow(A_front, R_front)

% Plot locations for Helene & Milton
for i = 1:size(locations_helene, 1)
    geoshow(locations_helene(i,1), locations_helene(i,2),
        'DisplayType', 'point', 'Marker', 'o', '
       MarkerSize', 8, 'MarkerEdgeColor', 'black', '
       MarkerFaceColor', 'white');
end
for i = 1:size(locations_milton, 1)
    geoshow(locations_milton(i,1), locations_milton(i,2),
        'DisplayType', 'point', 'Marker', 'o', '
       MarkerSize', 8, 'MarkerEdgeColor', 'black', '
       MarkerFaceColor', 'white');
end

% Fixes grids for lat/lon & better positioning of image
gridm on
mlabel on
plabel on
framem on
tightmap

hold off;
```

DEPARTMENT OF SPACE, EARTH AND ENVIRONMENT
CHALMERS UNIVERSITY OF TECHNOLOGY
Gothenburg, Sweden
www.chalmers.se

CHALMERS